**UNIVERSIDADE DE LISBOA**
**FACULDADE DE CIÊNCIAS**

# Regulation of glucose uptake in mammalian cells by protein phosphorylation networks

"*Documento definitivo*"

**Doutoramento em Biologia**
Especialidade de Biologia de Sistemas

Andreia Filipa Almeida Henriques

Tese orientada por:
Doutor Peter Jordan
Doutor Luka Clarke

Documento especialmente elaborado para a obtenção do grau de doutor

2019

**UNIVERSIDADE DE LISBOA**
**FACULDADE DE CIÊNCIAS**

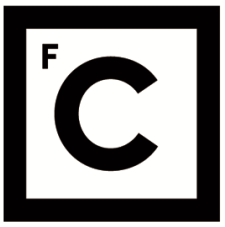

Ciências
ULisboa

# Regulation of glucose uptake in mammalian cells by protein phosphorylation networks

**Doutoramento em Biologia**
Especialidade de Biologia de Sistemas

Andreia Filipa Almeida Henriques

Tese orientada por:
Doutor Peter Jordan
Doutor Luka Clarke

Júri:

Presidente:

- Doutor Rui Manuel Santos Malhó, Professor Catedrático e Presidente do Departamento de Biologia Vegetal da Faculdade de Ciências da Universidade de Lisboa

Vogais:

- Doutora Jacinta de Fátima Rosário Serpa, Professora Auxiliar da Faculdade de Ciências Médicas da Universidade Nova de Lisboa;
- Doutora Ana Arminda Lopes Preto Almeida, Professora Auxiliar do Departamento Biologia da Universidade do Minho;
- Doutor Peter Jordan, Investigador Principal do Instituto Nacional de Saúde Dr. Ricardo Jorge – INSA, Orientador;
- Doutora Paula Duque Magalhães Santos, Investigadora Principal do Instituto Gulbenkian da Ciência – IGC.

Documento especialmente elaborado para a obtenção do grau de doutor

Bolsa de doutoramento financiada pela Fundação para a Ciência e a Tecnologia
(SFRH/BD/106080/2015)

2019

Andreia Filipa Almeida Henriques foi bolseira de doutoramento no âmbito do Programa doutoral BioSys em Sistemas Biológicos, Genómica Funcional & Integrativa (FCT/PD/00065/2012) da Faculdade de Ciências da Universidade de Lisboa. Esta dissertação teve financiamento pela Fundação para a Ciência e Tecnologia do Ministério da Ciência, Tecnologia e Ensino Superior: bolsa SFRH/BD/106080/2015, pelo projeto PTDC/SAU-MET/117236/2010 e pelo BioISI - Biosystems & Integrative Sciences Institute, Faculty of Sciences, University of Lisboa (UID/MULTI/04046/2019).


De acordo com o disposto no artigo 24º do Regulamento de Estudos de Pós-Graduação da Universidade de Lisboa, Despacho nº 7024/2017, publicado no Diário da República – 2ª Série – nº 155 – 11 de Agosto de 2017, foram utilizados nesta dissertação secções incluídas nos seguintes artigos:

Henriques A.F.A., Barros P., Carvalho A.S, Azkargorta M., Elortza F., Matthiesen R. Matos P., Jordan P. (2019) Ser 565 in TBC1D1 and Ser 704 in TBC1D4 phosphorylation modulate cell surface expression of GLUT1 (submitted for publication).

Gonçalves V.*, Henriques A.F.A.*, Matos P., Jordan P. Ibuprofen inhibits formation of a WNK1-GSK3β complex involved in SRPK1-dependent alternative splicing of RAC1B in colorectal tumor cells (submitted for publication).

*autores com contribuição equivalente

No cumprimento do disposto da referida deliberação, o autor esclarece serem da sua responsabilidade, exceto quando referido o contrário, a execução das experiências que permitiram a elaboração dos resultados apresentados, assim como, a interpretação e discussão dos mesmos. Os resultados obtidos por outros autores foram incluídos com a autorização dos mesmos para facilitar a compreensão dos trabalhos e estão assinalados nas respetivas figuras.

*“When things go wrong as they sometimes will,*

*When the road you're trudging seems all up hill,*

*(...) When care is pressing you down a bit,*

*Rest if you must, but don't you quit.*

*(...) Don't give up though the pace seems slow,*

*You may succeed with another blow.*

*Success is failure turned inside out,*

*The silver tint of the clouds of doubt,*

*And you never can tell just how close you are,*

*It may be near when it seems so far;*

*So stick to the fight when you're hardest hit*

*It's when things seem worst that you must not quit.”*

John Greenleaf Whittier

(1807 - 1892)

# Table of contents

# Agradecimentos

Chegou esta bela fase em que agradecemos a todos os que nos permitiram chegar aqui, e se eu tenho o que agradecer! Não entendia muito bem o drama por que todos passavam para terminar esta tarefa (já entendi) e principalmente não esperava alguns dos percalços no caminho, mas certamente não chegaria aqui sem todos vós e todos tiveram um papel determinante ainda que possam não ter reparado.

Em primeiro lugar quero agradecer ao meu orientador Doutor Peter Jordan, o mais paciente e ponderado chefe. Obrigada pela oportunidade, por tudo o que me ensinou, pela amizade e carinho com que sempre me tratou, por todo o tempo investido em mim e no meu trabalho e acima de tudo por ter juntado um grupo que se tornou uma segunda casa para mim.

Quero agradecer também ao Doutor Luka Clarke, co-orientador deste trabalho pela disponibilidade que sempre demonstrou e pela ajuda nesta fase final.

Institucionalmente quero deixar o meu agradecimento ao Instituto Nacional de Saúde Dr. Ricardo Jorge (INSA) e ao BioISI por terem proporcionado as condições para que este projeto tivesse sido levado a cabo.

Agradeço também a todos os colegas do Departamento de Genética Humana, representado pela Dra Glória, de alguma forma muitos ajudaram a que este trabalho fosse executado pela experiência, interesse ou apoio. Particularmente, quero agradecer ao Dr. José Furtado, "Senhor Zé dos meios" como sempre chamei, por me ter tratado sempre da melhor forma, por ter sempre mostrado preocupação e cuidado e por ser um exemplo de dedicação. Não posso também deixar de referir os colegas do laboratório do Metabolismo do RNA, desde os mais antigos aos mais recentes elementos foram sempre uma fonte de apoio e ótimos colegas. Rafaela, Paulo e Rafael a vós em particular o meu obrigada.

Ao Paulo Matos quero agradecer o precioso acompanhamento e apoio, sem dúvida foi essencial e determinante. Foi ótimo poder aprender com alguém que parece dominar todos os temas, desde *signaling* a temas do quotidiano e claro, as sagas do entretenimento! Obrigada por todo o apoio, pela ajuda em tudo principalmente no microscópio.

Ao Doutor Rune Matthiesen e Doutora Ana Carvalho agradeço a colaboração na preparação das amostras de espectrometria de massa e ao Doutor Francisco Pinto

agradeço pela análise bioinformática dos dados para determinação dos níveis de confiança.

Onconetes, minhas queridas, todas diferentes, todas especiais. Agradeço toda a amizade e companheirismo. Todas me ensinaram alguma coisa, Vânia, Patrícia, Joaninha, Márcia, Ana e Cláudia, as verdadeiras princesas lindas. E claro, todas as meninas que por lá passaram nos seus estágios e a quem mostrei os dentes quando estavam na "minha" bancada. À Patrícia, agradeço em especial a generosidade que sempre mostrou, e sobretudo na revisão deste documento.

Aos meus colegas do Biosys 2*nd Ed.*, agradeço ao Nuno e à Joana Silva, pela amizade, carinho e atenção. A Joana a melhor ex-*flat* colega que podia ter tido foi uma grande amiga desde o início desta jornada.

Amigos de sempre e mais recentes, todos sempre estiveram lá para mim, são os maiores. Obrigada em especial à Joana, Bia, Bota, Beatriz e Mário.

E finalmente, os mais importantes, os que estão sempre lá, em todas as ocasiões, os que nunca me deixaram ficar mal. Os meus pais, mano e avó. O núcleo duro de uma família a quem devo tudo. Foi difícil, mas chegamos aqui.

À minha mãe agradeço por ter lutado. E por durante a luta ter tido sempre os filhos no pensamento. Continua a cuidar de nós todos os dias ✯!

# Abbreviations

| | |
|---|---|
| 2DG | 2-deoxyglucose |
| 2DG6P | 2-deoxyglucose-6-phosphate |
| 6PDG | 6-phosphodeoxygluconate |
| Ac | Acetylation |
| AKT | RAC-alpha serine/threonine-protein kinase or PKB |
| ATP | Adenosine triphosphate |
| AU | Arbitrary units |
| CBD | Calmodulin- binding domain |
| CCS | Combined confidence score |
| CD | Collecting duct |
| CFTR | Cystic fibrosis transmembrane conductance regulator |
| CRC | Colorectal cancer |
| C-terminal | Carboxyl-terminal |
| D | Aspartate residue |
| DAPI | 4,6-diamidino-2-phenylindole |
| DCT | Distal convoluted tubule |
| DMEM | Dulbecco’s modified minimal essential medium |
| EGF | Epidermal growth factor |
| EGFR | Epidermal growth factor receptor |
| ePK | Eukaryotic protein kinase |
| EMT | Epithelial-mesenchymal transition |
| ENaC | Epithelial sodium channel |
| ERK | Extracellular signal-regulated kinase |
| ESSs | Exonic splicing enhancers |
| ESSs | Exonic splicing silencers |

| | |
|---|---|
| FBS | Fetal bovine serum |
| FLAG | Tag peptide sequence of DYKDDDDK |
| FHHt | Familial hyperkalemic hypertension |
| G6PDH | Glucose-6-phosphate dehydrogenase |
| GFP | Green fluorescent protein |
| GLUT | Glucose transporter |
| GO | Gene ontology |
| GS | Glycogen synthase |
| GSK3 | Glycogen synthase kinase 3 |
| GST | Glutathione S-transferase |
| GSV | Glucose transporter storage vesicle |
| HEK293 | Human embryonic kidney cells |
| HIS | Polyhistidine-tag |
| IAA | Iodoacetamide |
| ISE | Intronic splicing enhancers |
| ISS | Intronic splicing silencers |
| IP | Immunoprecipitation |
| K | Lysine residue |
| KCC | $K^+$-$Cl^-$ cotransporter |
| KD | Kinase-dead |
| kDa | Kilodaltons |
| KS-WNK1 | Kidney-specificWNK1 |
| L-WNK1 | Long-WNK1 |
| MAPK | Mitogen-activated protein kinase |
| Me | Methylation |
| Myc | Epitope tag derived from the c-myc gene product |

| | |
|---|---|
| MS | Mass spectrometry |
| NCC | $Na^+$-$Cl^-$ cotransporter |
| NKCC | $Na^+$-$K^+$-$Cl^-$ cotransporter |
| NSCLC | Non-small cell lung cancer |
| N-terminal | Amino-terminal |
| OSR1 | Oxidative stress-responsive kinase 1 |
| P | Phosphorylation |
| PAS | Phospho-AKT substrate |
| PBS | Phosphate-buffered saline |
| PBS-T | PBS + 0.01% Tween |
| PCS | Protein confidence score |
| PDK1 | Phosphoinositide-dependent kinase 1 |
| PH | Pleckstrin homology |
| PI3K | Phosphatidylinositol-3-kinase |
| PIP3 | Phosphatidylinositol (3,4,5) trisphosphate |
| PK | Protein kinase |
| PKB | Protein kinase B |
| PM | Plasma membrane |
| PPI | Protein-protein interactions |
| PTB | Phospho-tyrosine-binding domain |
| PTM | Post-translational modification |
| PVDF | Polyvinylidene difluoride |
| R | Arginine residue |
| Rab-GAP | Rab GTPase-activating protein |
| ROI | Region of interest |
| ROMK | Renal outer medullary potassium channel |

| | |
|---|---|
| RLU | Relative light unit |
| Ser | Serine residue |
| SGK1 | Serum glucocorticoid-inducible protein kinase1 |
| siRNA | Small interfering RNA oligonucleotide |
| SH2 | Src-homology 2 |
| SHC1 | SHC-transforming protein 1 |
| SPAK | STE20/SPS1-related proline-alanine-rich kinase |
| SR | Serine/arginine-rich |
| SRPK1 | SR protein kinase 1 |
| SRSF1 | Serine/arginine-rich splicing factor 1 |
| S565A | Serine substitution at position 565 to alanine |
| S565D | Serine substitution at position 565 to aspartate |
| S704A | Serine substitution at position 704 to alanine |
| S704D | Serine substitution at position 704 to aspartate |
| TBC1D1 | Tre-2/USP6, BUB2, Cdc16 domain family, member 1 |
| TBC1D4 | Tre-2/USP6, BUB2, Cdc16 domain family, member 4 |
| TBS | Tris-buffered saline |
| TfR | Transferrin receptor |
| Thr | Threonine residue |
| Tyr | Tyrosine residue |
| Tris | Tris(hydroxymethyl)aminomethane |
| T505A | Threonine substitution at position 505 to alanine |
| T505D | Threonine substitution at position 505 to aspartate |
| Ub | Ubiquitination |
| WB | Western blot |
| WNK | With no K (K=lysine) |

# Abstract

Glucose uptake is a key mechanism to maintain cell, tissue and body homeostasis. Among others, glucose transporter proteins (GLUTs) are responsible for glucose transport into the cell. Besides their expression level, the GLUT number present at the plasma membrane (PM) is regulated by signaling mechanisms. Previously, protein kinase WNK1 was found to phosphorylate TBC1D4, a Rab-GAP involved in membrane traffic regulation, and to regulate the surface expression of the constitutive glucose transporter GLUT1.

In this work the phosphorylation of either TBC1D4 or its paralogue TBC1D1 was studied as a key step in regulatory cascades modulating glucose uptake. First, we showed that downregulation of WNK1 through RNA interference translates in a 2-fold decrease in PM GLUT1 expression and a 60% decrease in glucose uptake. Then, we compared by mass spectrometry (MS) the *in vitro* phosphorylation of TBC1D1 and 4 by AKT1, WNK1 and SGK1 and 3. We identified two novel WNK1-specific phosphorylation sites at TBC1D1-Ser565 and TBC1D4-Ser704 and showed that transfection of their phosphomimetic or unphosphorylatable mutants affected cell surface abundance of GLUT1.

To define new biological pathways regulated by WNK1, we determined the interactome of WNK1 by MS. Interestingly, the bioinformatic and gene ontology analysis pointed to a previously unrecognized function related to mRNA processing. Our studies identified a novel function of WNK1 in alternative splicing using RAC1B in colorectal HT29 cells as a model. In particular, WNK1 acts as a scaffolding protein through complex formation with GSK3β. This complex protects GSK3β from an inhibitory phosphorylation at Ser9. The active GSK3β allows the translocation of kinase SRPK1 and splicing factor SRSF1 to the nucleus, which is important for RAC1B generation. Considering that RAC1B is known to be essential for cell survival and malignant progression, the results establish a new link between WNK kinases and tumorigenesis.

Altogether, this work reinforced a role for WNK1 in cell metabolism and uncovered a new function in regulation of alternative splicing, two events that can contribute to tumor development. The data may provide new targets for pharmacological modulation of RAC1B expression and cellular metabolism, with potential impact for the treatment of cancer and type 2 diabetes.

**Keywords:**

cell metabolism; WNK1; protein phosphorylation; protein interaction; tumorigenesis

# Resumo

A regulação da entrada de glucose para o interior da célula é um mecanismo chave no que respeita à manutenção da homeostase celular e do corpo como um todo. Esta regulação passa pela localização dos canais transportadores de glucose (GLUT) que, entre outros canais, são os principais responsáveis pela entrada de glucose. Além dos níveis de expressão dos transportadores GLUT, a sua inserção na membrana plasmática (PM) é regulada por mecanismos de sinalização que determinam a translocação de vesículas intracelulares contendo estes transportadores.

O mecanismo regulatório da localização do transportador GLUT4 melhor caracterizado é o da resposta à insulina. Este envolve a ativação do recetor de insulina e a cascata de sinalização das cinases PI3K/AKT, levando à inativação da proteína reguladora do tráfego membranar TBC1D4 (do inglês: *Tre-2/USP6, BUB2, Cdc16 domain family member 4*), que assim permite a ativação de GTPases da família Rab (Rab-GAP) que promovem a translocação de vesículas e o aumento da expressão de GLUT4 na membrana.

A fosforilação de TBC1D4, bem como da proteína paráloga TBC1D1, é um passo chave para a regulação da localização dos canais GLUT na membrana. Trabalhos anteriores do laboratório de acolhimento revelaram que a proteína cinase WNK1 [do inglês: *with no K (K=lysine) 1*] modula a localização do transportador GLUT1 na membrana plasmática. WNK1 tem a capacidade de fosforilar a TBC1D4, inibindo a sua atividade RAB-GAP o que permite a translocação de vesiculas de transportadores GLUT1 para a membrana plasmática através da ativação da proteína Rab8A.

O objetivo desta tese foi identificar novos locais de fosforilação nas proteínas reguladoras da localização de GLUT1, TBC1D1 e TBC1D4. Comparámos por espetrometria de massa os locais de fosforilação em TBC1D1 e TBC1D4 reguladas *in vitro* pelas cinases AKT, WNK1, SGK1 e SGK3. Encontrámos dois novos locais de fosforilação regulados pela cinase WNK1, uma serina na posição 565 (Ser565) em TBC1D1 e uma serina na posição 704 (Ser704) em TBC1D4.

Ao expressar mutantes dos resíduos Ser565 em TBC1D1 e Ser704 em TBC1D4 foi possível concluir que a fosforilação destes locais regula a prevalência de GLUT1 à superfície das células. O mutante que mimetiza o estado não fosforilado causou, em

ambos os casos (Ser565 em TBC1D1 e Ser704 em TBC1D4) uma redução significativa da quantidade de GLUT1 na membrana plasmática. Esta diminuição foi comparável ao nível observado nas células aquando da depleção da cinase WNK1. Concordantemente, a transfeção dos mutantes que mimetizam o estado fosforilado dos locais mostrou, em ambos os casos, que estes causam uma manutenção da quantidade de transportador de glucose GLUT1 na membrana, apesar da depleção da proteína cinase WNK1 que induz a perda de expressão de GLUT1 à superfície. Demonstrou-se então, que locais especificamente fosforilados pela cinase WNK1 nas proteínas TBC1D regulam o metabolismo de glucose, modulando a quantidade de canais transportadores de glucose GLUT1 presentes à superfície das células HEK293.

Na pesquisa de locais específicos encontrámos também o resíduo de treonina 505 (Thr505) em TBC1D1 fosforilado especificamente pela cinase SGK1 (do inglês: *serum glucocorticoid-inducible protein kinase 1*). Contudo, experimentalmente não se verificou uma relação direta entre a fosforilação do local e a quantidade de transportador GLUT1 presente na membrana plasmática. São então necessários mais estudos para entender de que forma esta fosforilação específica de TBC1D1 pode afetar a célula e quais os mecanismos moleculares envolvidos.

Seguidamente, tivémos como objetivo encontrar novas proteínas que interagem com WNK1, de forma a escrutinar novas vias de sinalização reguladas por esta proteína cinase. Para tal, isolámos e identificámos as proteínas que compõem os complexos macromoleculares associados à WNK1, recorrendo novamente a técnicas de espectrometria de massa. Os dados obtidos foram primeiro sujeitos a uma análise bioinformática do nível de confiança (CCS do inglês: *combined confidence score*) de forma a eliminar interações não específicas. A subsequente análise, por ontologia génica das proteínas candidatas indicou uma relação da cinase WNK1 com o processamento de RNA-mensageiro. De facto, a validação experimental dos candidatos confirmou a existência de um complexo proteico entre WNK1 e três proteínas cujas funções estão ligadas à regulação de *splicing* alternativo, em dois modelos celulares distintos (a linha celular estabelecida de células embrionárias de rim, HEK293 e a de cancro colorretal, HT29). Designadamente, as proteínas GSK3β (do inglês: *glycogen synthase kinase 3 beta*), SRPK1 (do inglês: *SRFS protein kinase 1*) e SRSF1 (do inglês: *serine/arginine-rich splicing factor 1*).

Dado que os alvos validados (GSK3β, SRPK1 e SRSF1) estão envolvidos na expressão de RAC1B, um produto do processamento alternativo de RNA mensageiro, testámos qual a influência da expressão da cinase WNK1 na expressão de RAC1B. Verificámos que a depleção de WNK1 em células HT29, um modelo de carcinoma colorretal, levou a uma significativa diminuição da expressão de RAC1B.

Tomando partido do conhecimento de que a droga anti-inflamatória Ibuprofeno (IBU) tem como um dos efeitos a diminuição da expressão de RAC1B em células HT29, fomos testar o envolvimento de WNK1 nesta diminuição. Os nossos resultados sugerem que a interação com WNK1 protege a cinase GSK3β de ser inativada, através de fosforilação da serina na posição 9 (Ser9). Verificámos que o tratamento com IBU altera a capacidade de interação entre as proteínas WNK1, GSK3β e SRPK1. Apurámos, ainda, que quer o tratamento com IBU, quer a depleção de WNK1, em células HT29 causam uma diminuição da expressão de RAC1B associada a um aumento da fosforilação de GSK3β na Ser9. Através de tratamento com IBU ou depleção de WNK1 seguidos de depleção da cinase AKT1 verificámos que a fosforilação de GSK3β na Ser9 é, pelo menos em parte, levada a cabo pela AKT1.

Quando no núcleo, SRSF1 promove a inclusão de um exão adicional normalmente excluído, o que leva à expressão de RAC1B. Fomos, então, testar de que forma os tratamentos IBU e depleção de WNK1 levariam a uma alteração na localização celular das proteínas SRPK1 e SRSF1. Por imunofluorescência, observámos que células tratadas com IBU em que a expressão de WNK1 foi silenciada, ocorre uma diminuição da intensidade do sinal nuclear correspondente a SRPK1 e SRSF1.

De forma a verificar se esta alteração de localização era dependente de GSK3β, repetimos os tratamentos IBU e depleção de WNK1 em células transfetadas com um mutante não fosforilável na Ser9 de GSK3β, proveniente da substituição de uma serina por um resíduo de alanina na posição 9 [GSK3β (S9A)]. Apurámos que as células transfetadas com o mutante GSK3β (S9A) são resistentes ao efeito do tratamento com IBU ou depleção de WNK1, levando a uma relocalização de SRPK1 e SRSF1 para o núcleo. Deste modo, verificámos que a forma ativa de GSK3β é determinante na localização nuclear de SRPK1 e SRSF1.

Por fim, e de forma a verificar se ambos os efeitos de WNK1 estavam relacionados, fomos comparar o efeito da depleção de WNK1 ou de RAC1B na capacidade de absorção de glucose em células HT29. Os nossos resultados indicam que

apenas a depleção de WNK1 causa uma diminuição significativa na absorção de glucose, ao mesmo tempo que causa uma diminuição da expressão de RAC1B. Por sua vez, o silenciamento da expressão de RAC1B parece não causar um efeito na absorção de glucose nas células tumorais. Estes resultados indicam que os dois efeitos de WNK1 estudados neste trabalho são independentes.

Em conclusão, os nossos resultados reforçam a importância de WNK1 no metabolismo de glucose e identificaram ainda uma nova via em que a cinase WNK1 regula processos de processamento alternativo de RNA. Ambos os efeitos podem ter um papel no desenvolvimento tumoral. Estes resultados podem providenciar novos alvos de modulação farmacológica da expressão de RAC1B ou do metabolismo de glucose com potencial impacto no combate de doenças como cancro e diabetes tipo 2.

**Palavras-chave:**

metabolismo celular; WNK1; fosforilação de proteínas; interação proteica; tumorigénese

# List of Figures

# List of Tables

# Chapter 1 General Introduction

## 1.1 Cell-environment interaction

The evolution of a cell membrane permitted life by creating and maintaining an internal environment within which genetic material exists and metabolic activities can take place without being mixed with the environment. With this compartmentalization the need to integrate information and respond to changes led to the evolution of tightly regulated systems capable of sensing, transmitting, storing, and interpreting information such that the regulatory machinery can endorse a coordinated and appropriate response (Schrum et al. 2010; Humphrey et al. 2015; Day et al. 2016). Most of these responses derive from post-translational modifications (PTMs). Over 200 protein PTMs have been described, including phosphorylation (P), ubiquitination (Ub), methylation (Me) and acetylation (Ac), that serve as elegant transducers of these signals. These protein modifications are rapid, reversible and associated with relatively small metabolic cost, and they profoundly modulate the function of the target protein. Phosphorylation is perhaps the most prevalent and best-studied PTM, and is closely involved in almost every cellular process (Cohen 2002).

## 1.2 Protein phosphorylation regulates signaling in multiple ways

A signaling pathway involves a group of molecules in a cell that work together to control one or more cell functions or processes (e.g. cell division). The signal is received by the first molecule in a pathway and transmitted in a cascade activating or inhibiting another molecule. This process is repeated until the last molecule is activated and the cell function is carried out.

Cells may integrate information from multiple signaling pathways to make decisions. The control of cellular phenotypes by networks of protein phosphorylation events, context-dependence of signaling, and signaling heterogeneity among cells are regulated by the complex interplay between kinases and phosphatases. Kinase-mediated signaling is a master regulator of cell signaling pathways involved in a high number of cellular processes, including cell proliferation, cell death (apoptosis, necroptosis, necrosis), metabolism, behavior and neurological function, development, and pathogen resistance (Pawson and Scott 2005; Day et al. 2016). Protein phosphorylation is a PTM which operates like a molecular switch mechanism, modulating diverse protein functions such as enzymatic activity, protein localization, interactions with other proteins,

conformational changes, protein turnover and even crosstalk with other PTMs (Figure 1.1) (Humphrey et al. 2015; Day et al. 2016). Examples of PTMs functioning as molecular switches modulating protein functions are presented in Table 1.1.

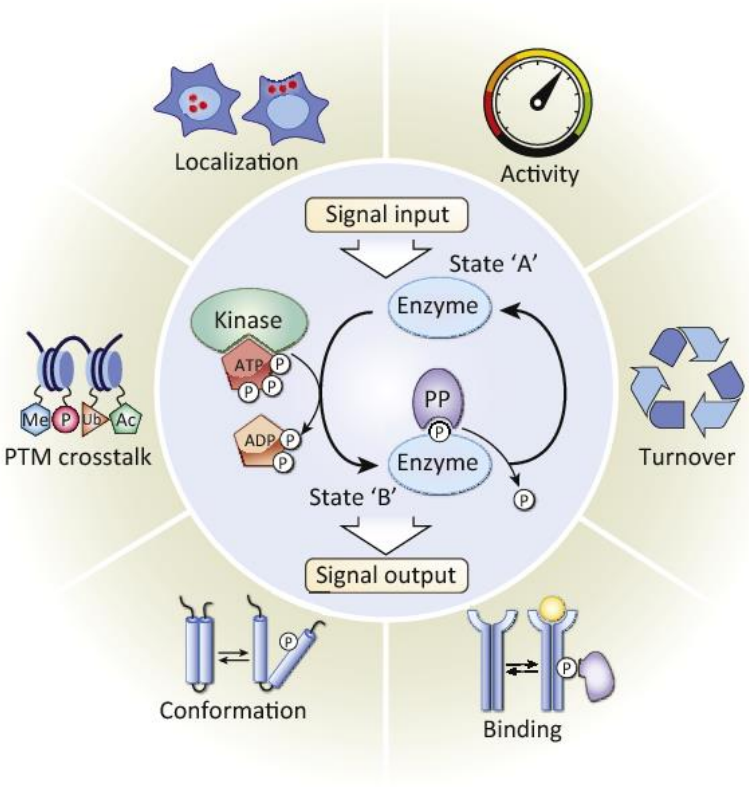


**Figure 1.1 – Protein phosphorylation as a molecular switch.** Protein phosphorylation is a post-translational modification (PTM) in which protein kinases reversibly transfer a phosphate from ATP (or other nucleoside phosphates) to selected amino acids, by esterification. Phosphorylation serves as a molecular switch mechanism, modulating diverse protein functions such as enzymatic activity, protein localization, interactions with other proteins, conformational changes, protein turnover and even crosstalk with other PTMs Ac, acetylation; Me, methylation, P, phosphorylation; Ub, ubiquitination. Image from Humphrey et al. 2015.

### 1.2.1 Protein kinases

In protein phosphorylation, protein kinases (PKs) reversibly transfer a phosphate from ATP (or other nucleoside phosphates) to selected amino acids, by esterification (Figure 1.1). Serine (Ser) and threonine (Thr) phosphorylation are the most common phosphorylation events whereas tyrosine represents less than 1% of the total esterified phosphate. PKs have conserved structural motifs including an activation loop, catalytic domain, and ATP binding domain (Day et al. 2016).

**Table 1.1 – Examples of phosphorylation as molecular switches.**

| EVENT | Example | Reference |
|---|---|---|
| **Activity** | Phosphorylation by AKT at Ser9 inhibits GSK3β activity. | (Cross et al. 1995) |
| **Protein localization** | Through protein complex formation and phosphorylation, kinase SRPK1 regulates translocation of the splicing factor SRSF1 to the nucleus. | (Koizumi et al. 1999) |
| **Protein interaction** | Phosphorylation of TBC1D4 by WNK1 increases the binding of TBC1D4 to regulatory 14-3-3 proteins and this reduces its interaction with the exocytic small GTPase Rab8A. | (Mendes et al. 2010) |
| **Conformational change** | AKT1 exists in an inactive conformation due to an autoinhibitory interaction between its pleckstrin homology (PH) and kinase domains. Phosphorylation of Ser473 by mTORC2 can activate AKT1 *via* a conformational change that relieves autoinhibition by the PH domain exposing the kinase domain. | (Chu et al. 2018) |
| **Protein turnover** | IKK-α can phosphorylate IκB, causing degradation of IκB and nuclear translocation of transcription factor NF-κB. | (Romashkova and Makarov 1999) |
| **PTM crosstalk** | Phosphorylation of tumor suppressor protein p53 interferes with its carboxy-terminal acetylation, increasing p53 protein stability and transcriptional activity. | (Sakaguchi et al. 1998) |

Kinases are regulated in a variety of ways, but a major regulatory mode is by phosphorylation, the same modification they catalyze. One critical regulatory phosphorylation event common to most kinases is activation-loop phosphorylation, which promotes an active kinase conformation and can occur from autophosphorylation, implying that they are also self-activating enzymes, or by other kinases (Beenstock et al. 2016). An example of the first is protein kinase B (PKB/AKT) activation by Phosphoinositide-dependent kinase-1 (PDK1) upon phosphoinositide 3-kinase (PI3K) recruitment in insulin signaling (Burgering and Coffer 1995; Alessi et al. 1997). An example for activation by autophosphorylation is serine 382 of WNK1 in the activation loop , required for the kinase activity (Xu et al. 2002). However, some phosphorylation events negatively regulate kinase activity, an example of it is the serine/threonine kinase GSK3β phosphorylation on Ser 9 to render it inactive (Stambolic and Woodgett 1994). Protein phosphorylation also creates binding sites for other proteins containing specific

recognition motifs and so regulates complex formation between proteins. Therefore, phosphorylation events regulate protein kinase activity in several layers, including protein localization, activation of constituent proteins, and protein trafficking (Day et al. 2016).

### 1.2.2 Phosphatases

Protein phosphatases, which hydrolyze phosphate esters from phosphorylated residues such as phosphotyrosine, phosphoserine or phosphothreonine are critical for normal cell signaling regulation. Eukaryotic protein phosphatases are structurally and functionally diverse enzymes represented by three distinct gene families according to the phosphorylated residue they can dephosphorylate. Biochemical functions have been well studied in phosphatases, however, the substrates of specific phosphatases remain largely unknown (Barford et al. 2002; Day et al. 2016). In Table 1.2 we find some examples of the importance of phosphatases regulating diverse signaling pathways.

**Table 1.2 – Examples of phosphatases as antagonists in signalling**

| EVENT | Example | Reference |
|---|---|---|
| **Glycogen synthesis** | Dephosphorylation catalyzed by PP-1 activates the enzime glycogen synthase (GS) promoting glycogen synthesis. | (Ragolia and Begum 1998) |
| **AKT inactivation** | PTEN negatively regulates intracellular levels of phosphatidylinositol (3,4,5) trisphosphate (PIP3) in cells and dephosphorylates AKT in vitro, negatively regulating the PI3K/AKT signaling pathway. | (Stambolic et al. 1998) |
| **SRSF1 dephosphorylation** | Dephosphorylation of RNA splicing factor SRSF1 by PP-1 is required for maturation of the spliceosome and other RNA processing events. | (Ma et al. 2010) |
| **NFAT activation** | Dephosphorylation by calcineurin on an N-terminal regulatory domain activates and promotes nuclear translocation of the transcription factor nuclear factor of activated T cells (NFAT). | (Loh et al. 1996) |
| **EGFR inhibition** | PTPN12, tyrosine phosphatase interacts with and inhibits the epithelial growth factor receptor (EGFR) signaling suppressing cell proliferation and thus acting as a tumor suppressor. | (Sun et al. 2011) |

## 1.3 Human kinome

The human kinome comprises over 500 distinct protein kinase genes that form one superfamily of proteins sharing the eukaryotic protein kinase (ePK) catalytic domain: a sequence composed of 250-300 amino acids which can be subdivided into twelve conserved subdomains containing highly conserved individual amino acids and motifs. Although no residue is universal, the subdomains are is preserved in all protein kinases, and the presence of a pattern of residue conservation has been used to determine the grouping of kinases into families (Hanks and Hunter 1995; Manning et al. 2002).

The superfamily is subdivided into seven major ePK families : TK (tyrosine kinases), AGC (containing PKA, PKG, PKC families), CAMK (calmodulin- dependent kinases), CMGC (comprising the CDK, MAPK, GSK, and CLK families), TKL (tyrosine kinase-like, phylogenetically close to the tyrosine kinases), STE (kinases that function in the MAPK kinase cascades that were first described through characterization of yeast *sterile* mutants) and CK1 (casein kinase 1 family and related enzymes) (Figure1.2). Apart from the major subfamilies, some kinases do not fit in any of the categories above and are considered as “other”. In addition, a group of kinases classified as atypical show low sequence similarity to the main kinase superfamily but were shown to possess catalytic activity (Manning et al. 2002; Hanks 2003).

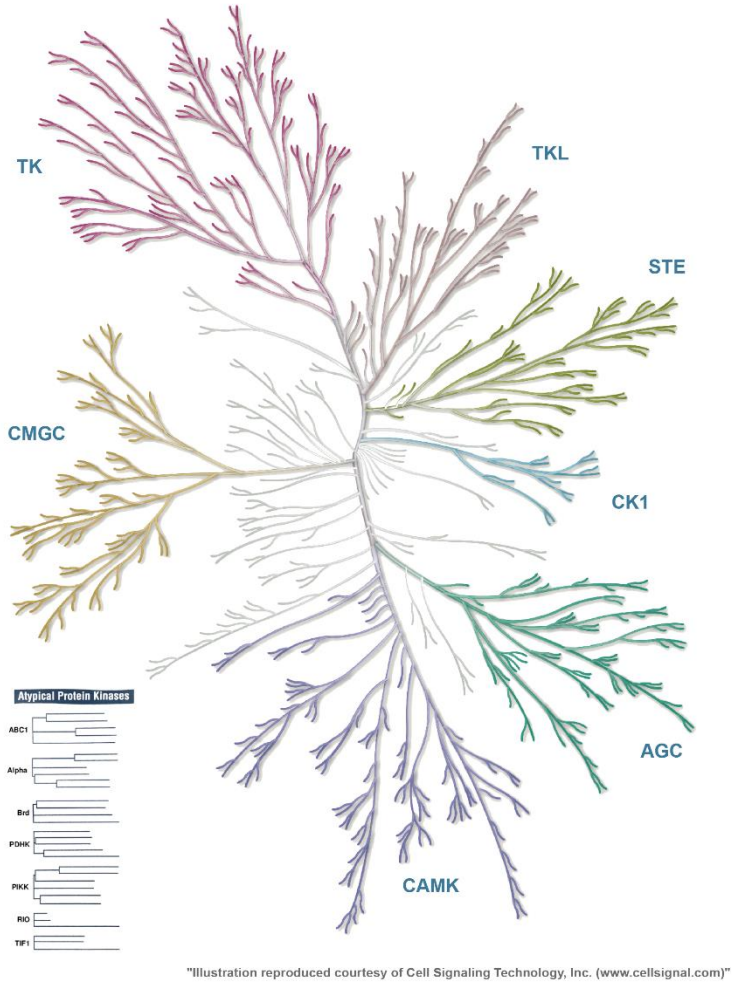


**Figure 1.2 – Phylogenetic tree representing the superfamily of protein kinases**. The superfamily is subdivided in seven major PK families: **TK** (tyrosine kinases), **AGC** (containing PKA, PKG, PKC families), **CAMK** (calmodulin-dependent kinases), **CMGC** (comprising the CDK, MAPK, GSK, and CLK families), **TKL** (tyrosine kinase-like), **STE** (first described through characterization of yeast *sterile* mutants), **CK1** (casein kinase 1 family and related enzymes). The group of kinases classified as **atypical** have low sequence similarity in the protein kinase domain comparatively to the main kinase superfamily (http://www.kinhub.org/kinmap/).

## 1.4 Tyrosine kinases

Tyrosine kinases form a distinct group inside the superfamily of protein kinases, whose members phosphorylate proteins on tyrosine residues, whereas enzymes in all other groups phosphorylate primarily serine and threonine residues. X-ray analysis revealed a structural difference that determines the substrate preference for tyrosine (Tyr) rather than for serine (Ser) or for threonine (Thr) (Hubbard et al. 1994).

Autoradiography measurements estimated Tyr phosphorylation to be less representative in terms of phosphorylation events when compared with Ser or Thr

phosphorylation (ratio Ser:Thr:Tyr – 90:10:0.05) (Hunter et al. 1980). Tyr phosphosites are frequently regulatory, most tyrosine kinases are activated under specific conditions, highly downregulated and the phosphotyrosine residues have a very short half-life, unless protected by binding domains which explains the low ratio of Tyr phosphorylation observed (Hunter 2009). Furthermore, phosphorylation by protein tyrosine kinases regulates cell-to-cell signals concerning growth, differentiation, adhesion, motility, and death. Although initially associated with signal transduction by growth factor and cytokine receptors at the plasma membrane through phosphorylation of transmembrane receptors, tyrosine kinases are now subdivided in two main groups, receptor and non-receptor tyrosine kinases (Robinson et al. 2000; Manning et al. 2002).

Receptor tyrosine kinases have an N-terminal extracellular domain, which can bind activating ligands, a single transmembrane domain, and a C-terminal cytoplasmic domain that includes the catalytic domain (e.g. epidermal growth factor receptor, EGFR). The group of non-receptor tyrosine kinases lacks a transmembrane domain, most are soluble intracellular proteins that regulate protein function in several cellular processes including cell cycle, transcription and synaptic transmission among others (e.g. spleen tyrosine kinase, SYK). Tyrosine phosphorylation acts by generating, exposing or masking docking sites for other adaptor proteins containing modular Src-homology 2 (SH2) and-or phosphotyrosine binding (PTB) domains. The binding of adaptor proteins promotes the interaction with downstream effectors and multi-protein complex formation, regulating their activity and cellular localization (Taylor et al. 1995; Manning et al. 2002; Pawson and Nash 2003).

## 1.5 Serine/threonine kinases

Serine/threonine kinases share some features with tyrosine kinases in terms of action, namely their ability to change their conformation, subcellular localization and changes in protein-protein interaction upon serine/threonine phosphorylation, shifting assembly of protein-protein complexes (Muslin et al. 1996; Yaffe and Elia 2001). Yaffe and colleagues (2001) showed that specific adaptors proteins, including 14-3-3 proteins, interact with phosphorylated targets similarly to the SH2-domain-mediated recognition of phosphotyrosine-containing motifs (Yaffe and Elia 2001).

The vast majority of cellular protein phosphorylation events reported in mass spectrometry (MS)-based studies occurs on serine and threonine residues (Sharma et al. 2014). Thus, serine/threonine kinases represent the majority of protein kinases and are distributed into several groups according to similarities in their kinase domain (e.g. AGC, CMGC and CAMK) (Manning et al. 2002).

### 1.5.1 AGC group

The AGC group includes kinases related to cAMP-dependent protein kinase 1 (PKA), cGMP-dependent protein kinase (PKG) and protein kinase C (PKC). Members of this group are conserved throughout several species and share aspects of their mechanisms of inhibition and activation (Arencibia et al. 2013; Leroux et al. 2018) AGC kinases are involved in diverse and important cellular functions, and mutations or dysregulation of kinases from this group contribute to the pathogenesis of many human diseases, including cancer and diabetes (Pearce et al. 2010).

The AKT serine/threonine kinase, also known as protein kinase B (PKB) is one of the members of AGC group and is a component of intracellular signaling pathways promoting cell survival (Datta et al. 1999) cell proliferation, apoptosis, transcription, cell migration (Brazil and Hemmings 2001) glucose metabolism (Thong et al. 2007; Zaid et al. 2008) and inflammatory processes (Tang et al. 2016). AKT is activated downstream of PI3K by being recruited to the membrane by the lipid phosphatidylinositol (3,4,5)-trisphosphate (PIP3), followed by phosphorylation at Thr 309 (activation segment) and Ser 474 (hydrophobic motif) (Yang et al. 2002) by kinase PDK1. AKT signal transduction occurs through downstream effectors such as mTOR, glycogen synthase kinase 3 beta (GSK3β), or forkhead box protein O1 (FOXO1). Overexpression or abnormal activation of AKT has been associated with increased cancer cell proliferation and survival in many cancers types, including ovarian, lung, and pancreatic cancers and has been studied as a target for cancer therapy (Song et al. 2019).

The SGK (serum and glucocorticoid-inducible kinase) family belong to the AGC group and consists of three distinct but highly homologous isoforms (SGK1, SGK2, and SGK3) that are encoded from three distinct genes localized on different chromosomes (Webster et al. 1993; Lang and Cohen 2001). SGKs share similarities with AKT, including great sequence homology, being activated in response to a variety of

extracellular stimuli (e.g. PI3K) and upon growth factor stimulation translocate to the nucleus (Brunet et al. 2002; Pearce et al. 2010). Moreover, SGK1 is involved in cell metabolism by modulating GLUT1 transporter membrane expression (Palmada et al. 2006). However, although they have some substrates in common, SGKs and AKT have different roles. SGK1 plays an important role in the regulation of processes such as cell survival, neuronal excitability, and renal sodium excretion. Additionally, SGK has pathophysiological significance upon dysregulated expression and activity in hypertension, cancer, obesity, neuronal diseases and diabetic nephropathy (Lang and Cohen 2001; Lang et al. 2006).

### 1.5.2 CMGC group

CMGC kinases are mostly serine/threonine kinases and include the CDK family (cyclin-dependent kinase), the MAPK family (mitogen-activated protein kinase), the GSK family (glycogen synthase kinase), the DYRK family (dual specificity tyrosine regulated kinase), and the dual specificity CLK family (CDC2-Like Kinase) (Hanks and Hunter 1995; Manning et al. 2002). Kinases in this group have impact in alternative splicing (Ngo et al. 2005; Qian et al. 2011; Zhou et al. 2012) and metabolism control regulation throughout several of the families represented in the group

GSK is a small family of kinases from the CMGC group. GSK3, initially described as one of the kinases that phosphorylates and inhibits glycogen synthase (GS), decreasing its affinity to allosteric activation by glucose-6-phosphate (Embi et al. 1980). GSK3 is a known regulator of glycogen metabolism, the Wnt signaling pathway, involved in protein synthesis and cell proliferation and differentiation (Doble and Woodgett 2003; Ciaraldi et al. 2010; Wu and Pan 2010). In humans, GSK3 exists as two isoforms, GSK3α and GSK3β, encoded by two distinct genes. The major structural differences include an N-terminal extension in GSK3α and variability in the C-terminal region. (Doble and Woodgett 2003). GSK3 is regulated by a variety of means including phosphorylation, protein complex formation, subcellular localization, priming-substrate specificity and regulation by proteolytic cleavage (Medina and Wandosell 2011). Inactivation of these kinases is associated with a specific serine residue phosphorylation, Ser21 and Ser9 in GSK3 α and β, respectively creating a pseudo substrate/autoinhibitory domain that mimics these primed phosphorylation sites (Cross et al. 1995; Frame et al. 2001). Insulin stimulation of cells leads to GSK3 inactivation upon PI3K activation and probably occurs

through AKT (Halse et al. 1999). GSK3β also regulates alternative splicing by phosphorylation of several splicing factors and regulators of RNA biosynthesis (Hernández et al. 2004; Liu and Klein 2018).

GSK3 acts as a key regulator of diverse processes, and when dysregulated, has been implicated in diseases such as diabetes, Alzheimer's disease, bipolar disorder and cancer (MacAulay and Woodgett 2008; Hernández et al. 2009; Luo 2009; Jope and Roh 2012).

SRPK (SR protein kinase) family is also part of the CMGC group and is composed of serine/threonine kinases that specifically phosphorylate serine residues in serine/arginine dipeptide motifs (arginine/serine (RS)-rich domains) and facilitate the nuclear import of the targets (Gui et al. 1994; Hanks and Hunter 1995). The presence of a domain interrupting the kinase catalytic site into two structural entities, "the spacer domain", is a distinctive feature of the SRPK family (Ding et al. 2006). SRPKs are mostly related with RNA processing due to their targets contain RS domains. Most of RS domain-containing proteins are serine/arginine-rich (SR) proteins that contain an RNA recognition motif and act as splicing factors when translocated to the nucleus. Moreover, SPRKs are involved in cell cycle progression, chromatin reorganization and in metabolic signaling (Giannakouros et al. 2011).

SRPK1, one of the members of the family regulates splicing by phosphorylating SR-rich proteins and plays an important role in constitutive and alternative pre-mRNA splicing (see 1.7.1) (Zhou et al. 2012; Zhou and Fu 2013).

### 1.5.3 "Other" group

The "other" kinase group consists of many diverse families, most of which are serine/threonine protein kinases. These conserved families differ in some highly conserved sequence features from any of the other kinase groups, and therefore are classified together in the irregular "other" group. (Hanks and Hunter 1995). One of the families in this group is the WNK1 family described in the following (see 1.6).

## 1.6 WNK family

The small family of WNK [with no K (K=lysine)] kinases includes proteins characterized by a substitution of a highly conserved lysine (hence their name) in the subdomain II of the catalytic domain by a cysteine. Although in most Ser/Thr kinases, the conserved lysine residue usually mediates ATP binding and the catalysis of phosphoryl transfer, WNKs use an alternative lysine from subdomain I which confers catalytic activity (Figure 1.3A) (Xu et al. 2000; Veríssimo and Jordan 2001; Kostich et al. 2002; Xu et al. 2002). This feature confers an alteration in the 3D structure of the kinase conferring a unique conformation in the activation loop which might help in the design of specific inhibitor molecules (Min et al. 2004).

Four members of the WNK kinase family have been identified in the human genome: WNK1, WNK2, WNK3 and WNK4, exhibiting about only 40% amino acid identity but containing the same structure and the conserved autoinhibitory domain and two coiled-coil domains (Figure 1.3B) (Veríssimo and Jordan 2001; Xu et al. 2002; Gamba 2005). WNKs are regulated by their autoinhibitory domain, which keeps them inactive until activated by yet poorly characterized signals. Autoinhibition of WNK1 is dependent on highly conserved phenylalanine residues (Phe522/524), since mutation of these residues to alanine eliminates the autoinhibition. One example of an activation signal is autophosphorylation at two serine residues (Ser378/382) in the kinase domain in response to osmotic stress conditions (Xu et al. 2002).

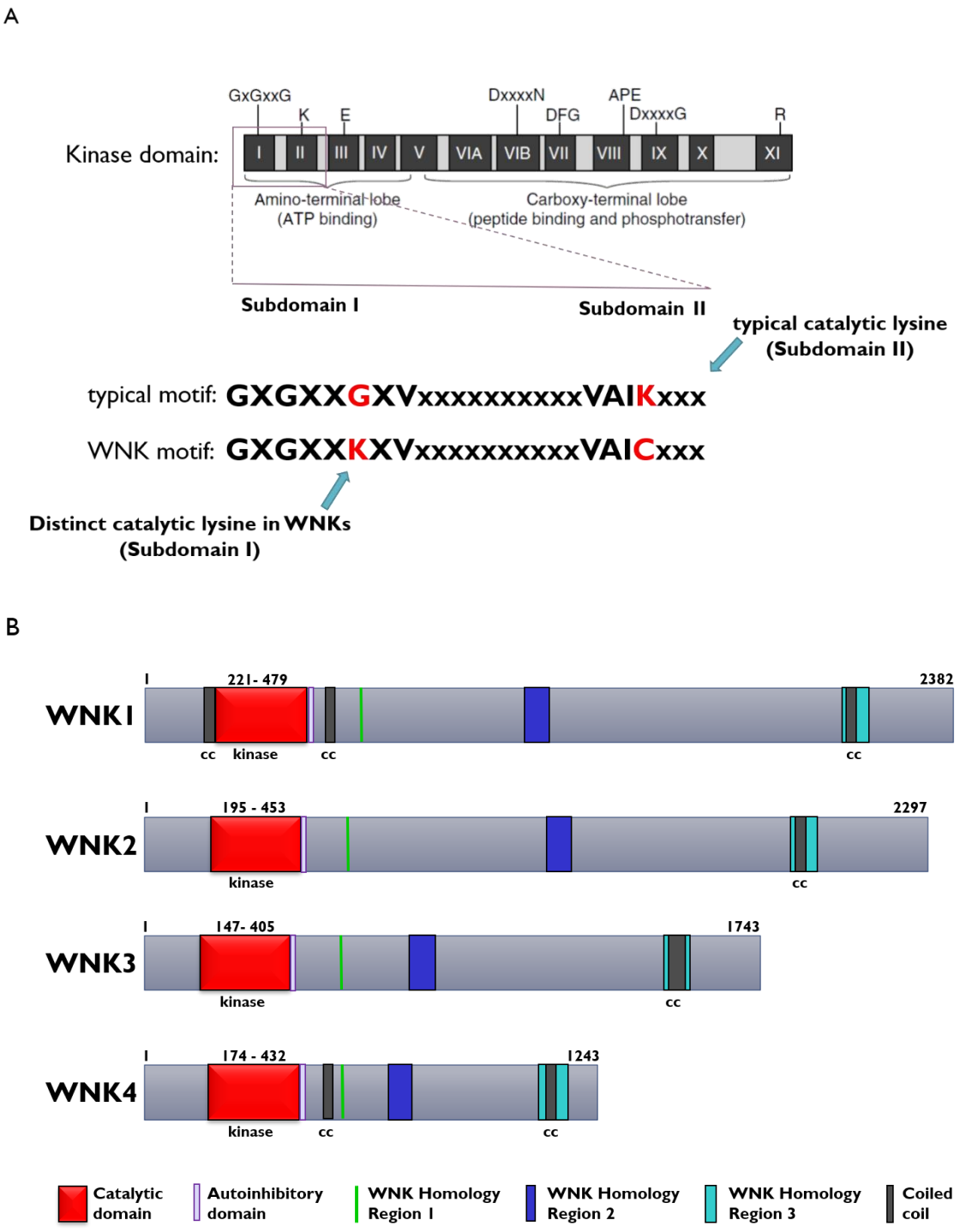


**Figure 1.3 – WNK protein kinases family.** (**A**) Comparison of the sequence in subdomains I and II of the catalytic domain between a typical protein kinase and the WNK kinases. A conserved lysine in subdomain II, which binds to ATP, is absent in WNK kinases and functionally substituted by another lysine located in subdomain I, as indicated. (**B**) Schematic representation of the four human WNK proteins. Catalytic, autoinhibitory and coiled-coil domains are shown as well as conserved regions of homology between WNK kinases (Xu et al. 2000; Gamba 2005; Moniz and Jordan 2010)

Shortly after the discovery of this family of kinases they were associated with regulation of ion transport in the kidney. Mutations in WNK1 and WNK4 cause the human monogenic disease familiar hyperkalemic hypertension (FHHt also known as pseudohypoaldosteronism type 2 or Gordon syndrome), a human disease characterized by excessive renal sodium and potassium retention (Wilson et al. 2001). Because this disease phenotype is associated with renal function and balance of $Na^+$, $Cl^-$ and $K^+$ electrolytes, the study of this signaling pathway revealed WNKs as important regulators of solute transport and arterial pressure.

WNK1, WNK3 and WNK4 act as multifunctional regulators of renal ion transport and use different mechanisms to control a variety of channels and transporters, responsible for ion reabsorption and excretion in different segments of the nephron, which are accountable for electrolyte and fluid balance maintenance. This ion transport regulation depends on the electrochemical gradient established by the ATP-dependent Na+/K+-ATPase in the different nephron structures (Gamba 2005; Kahle et al. 2008b). Both WNK1 and WNK4 are expressed in the distal convoluted tubule (DCT), connecting tubule (CNT) and collecting duct (CD) of the nephron, suggesting that WNKs are part of a signaling pathway that modulates renal solute transport (Figure 1.4).

### 1.6.1 WNK1

WNK1 is the most studied member of this subfamily and was the first to be identified in a search for new MAP kinases (Xu et al. 2000; Veríssimo and Jordan 2001). The human WNK1 gene is located on chromosome 12, and its transcription is regulated by three alternative promoters, generating several WNK1 isoforms with a tissue-specific distribution. The two most important isoforms are long WNK1 (L-WNK1) and kidney-specific or KS-WNK1. L-WNK1 codes for a protein of 2382 amino acids that is ubiquitously expressed with highest levels in skeletal muscle, heart, and brain (Veríssimo and Jordan 2001). KS-WNK1 is a shorter transcript expressed from an internal promoter that lacks the kinase domain and is expressed exclusively in the kidney, more precisely in the DCT and CNT of the nephron (Delaloy et al. 2003; Vidal-Petiot et al. 2012).

The majority of studies conducted to date on WNK1 have focused on its role in ion transport regulation in the kidney (Kahle et al. 2008a), mainly through

phosphorylation of intermediate proteins controlling ion channels and cotransporters (see 1.6.5).

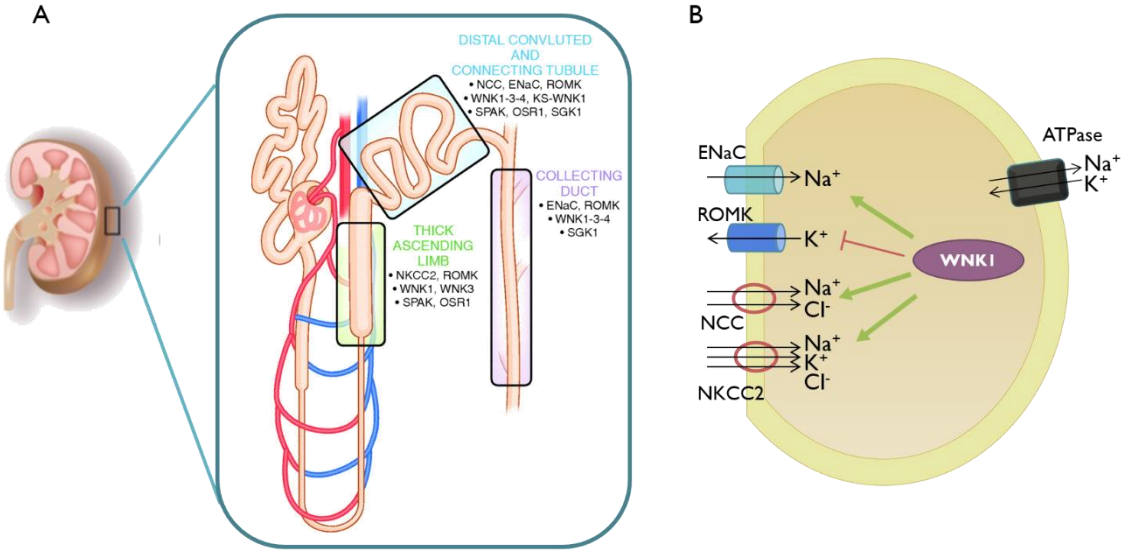


**Figure 1.4 – Differential expression of WNK family members and ion transporters in the kidney.** (**A**) Differential expression pattern of major ion transport proteins and regulatory kinases in the distal nephron (adapted from: Hoorn et al. 2011). (**B**) Schematic representation of the role of WNK1 in the regulation of the indicated ion channels and cotransporters (ENaC: Epithelial sodium channel; ROMK: Renal outer medullary potassium channel; NKCC2: $Na^+$-$K^+$-$Cl^-$ cotransporter 2; ATPase ATP-dependent Na+/K+-ATPase)

### 1.6.2 WNK2

WNK2 is the least studied member of the WNK subfamily. In humans the WNK2 gene is present at chromosome 9, position q22.31 (Veríssimo and Jordan 2001), encoding a 2297 amino acid protein. The WNK2 expression profile is unique among the WNK kinases because it is almost exclusively expressed in the brain, heart muscle, small intestine and colon, with no detectable expression in kidney (Moniz et al. 2007). The expression is predominant in developing and mature brain neurons and associated with regional and temporal differential expression during brain development (Rinehart et al. 2011). The expression of WNK2 has a tumor suppressor role in gliomas (Moniz et al. 2007) and is further described in section 1.8.

### 1.6.3 WNK3

The human gene for WNK3 is located on chromosome X position p11.22 and encodes a 1743 amino acid protein expressed in secreting epithelial tissues, with higher expression in brain and kidney. Unlike WNK1 and WNK4, WNK3 can be found in all nephron segments with the protein being localized in the tight junctions (Rinehart et al. 2005). Similar to WNK2, WNK3 brain expression is regional and temporally regulated during embryonic development. WNK3 has been shown to function as an ion transport regulator, and it also plays a role in the increase of cell survival by interacting with procaspase-3 and delaying apoptosis (Veríssimo et al. 2006). WNK3 kinase promotes the entry of chloride into the cell during cell volume regulation, by activating $Na^+$-$K^+$-$Cl^-$ cotransporter 1 (NKCC1) and 2 (NKCC2) and $Na^+$-$Cl^-$ cotransporters (NCC) and simultaneously preventing chloride exit from the cell by inhibiting all four $K^+$-$Cl^-$ cotransporters (KCC) (Kahle et al. 2005a; Rinehart et al. 2005; de los Heros et al. 2006).

### 1.6.4 WNK4

The human WNK4 gene is located on chromosome 17 and encodes for a 1243 amino acid protein expressed predominantly in the kidney. It is also expressed in secretory epithelia from brain, colon, pancreas, biliary ducts, and epididymis. In the kidney its expression is restricted to the DCT and CD, distal nephron segments known to be crucial in the homeostasis of electrolytes (Wilson et al. 2001; Veríssimo and Jordan 2001; Kahle et al. 2005b).

WNK4 regulates the balance between NaCl reabsorption and $K^+$ secretion by inhibiting and activating several types of ion channels, like activating $Cl^-$ channel, cystic fibrosis transmembrane conductance regulator (CFTR) and inhibiting epithelial sodium channel (ENaC) (Ring et al. 2007; Mendes et al. 2011). WNK4 also regulates several cotransporters like NCC, NKCC1 (Hadchouel et al. 2016) and appears to be the predominant regulator of NCC in the DCT, being particularly sensitive to changes in chloride concentration (Terker et al. 2016). Interestingly the effect of WNK4 on NCC is inconsistent, with in vitro and in vivo studies indicating that WNK4 could be either an inhibitor or an activator of this cotransporter (Bazúa-Valenti et al. 2014; Shekarabi et al. 2017). As previously mentioned, mutations in WNK4 cause the human monogenic disease FHHt.

### 1.6.5 Ion transport regulation by WNK1

Based on the disease phenotype resulting from WNK kinase mutations, it is clear that WNKs play important roles in regulating ion channels and transporters. Some examples of WNK1 ion transport regulation are resumed in Figure 1.4B.

It has been shown that WNK1 inhibited renal outer medullary potassium channel 1 (ROMK1). This inhibition is exerted by the L-WNK1, which stimulates the endocytosis of the channel synergistic with, but not dependent, on WNK4. Moreover, KS-WNK1 is highly expressed in the kidney and reverses the inhibition of ROMK1 caused by L-WNK1 (Lazrak et al. 2006). WNK1 also regulates ENaC through activation of SGK1 (Xu et al. 2005a).

WNK1 is a powerful upstream activator of the cotransporter NCC by phosphorylating and activating two homologous kinases, STE20/SPS1-related proline-alanine-rich kinase (SPAK) and oxidative-stress-responsive kinase (OSR1). These, in turn, directly phosphorylate NCC on two threonine residues in the amino terminal cytoplasmic domain activating the cotransporter. The regulation of this process is antagonized by WNK4 (Chávez-Canales et al. 2014). WNK1 is also a positive regulator of the cotransporter (NKCC2) in a SPAK and OSR1-dependent pathway activated in hypotonic low-chloride conditions (Richardson et al. 2011). WNK1 can act as a chloride sensor since chloride binds to the WNK1 catalytic domain, thereby inhibiting autophosphorylation and kinase activity (Piala et al. 2014). The phosphorylation of NCC and NKCC2 through the WNK/SPAK/ORS1 pathway leads to increased solute transport, in part by increasing cotransporter retention in the PM (Rosenbaek et al. 2014) (Figure 1.4B).

### 1.6.6 Role of WNKs in cancer

Several studies have suggested a possible role for WNK kinases in cell growth, differentiation and apoptosis, processes linked to cancer upon dysregulation. For example, large-scale genomic studies that have analyzed the coding sequences of the 518 protein kinases in the human genome for somatic mutations in several types of cancers, including those of the kidney, breast, lung, and colon, have revealed missense, insertion, and other types of mutations in the genes encoding all WNK family members (Davies et al. 2005; Stephens et al. 2005; Sjöblom et al. 2006; Greenman et al. 2007). The functional

effects and the biological significance of these mutations for cancer phenotypes need further studies. However, there is evidence for a relationship between the WNKs and cell growth, differentiation, migration and apoptosis (Moniz and Jordan 2010).

WNKs share sequence homology with MAPKs, kinases linked to the transition from quiescent to proliferative state in epithelial cells and deregulated in approximately one-third of all human cancer (Moniz and Jordan 2010). WNKs directly affect MAPK signaling, for example WNK1 is required for EGF-dependent stimulation, acting by protein–protein interaction to activate extracellular signal-regulated kinase 5 (ERK5). Accordingly, WNK1 depletion in mouse neural progenitor cells suppressed activation of ERK5 and greatly reduced cell growth and migration (Xu et al. 2004; Sun et al. 2006).

Other studies demonstrate that WNK2 negatively regulates the EGF-induced proliferation pathway of MEK1/ERK1 in a RHOA-mediated crosstalk mechanism in cancer cells, functioning as an antiproliferative tumor suppressor (Moniz et al. 2007, 2008). WNK2 controls the activation of the small GTPase RHOA, which in a reciprocal way regulates activation of RAC1, controlling the dynamics of the actin cytoskeleton, important for cell migration and invasiveness (Moniz et al. 2008). WNK2 levels are significantly reduced in human glioma and meningioma due to epigenetic silencing of the WNK2 promoter and this correlated with increased tumor cell proliferation, migration, and motility (Moniz et al. 2013).

WNKs also regulate growth factor receptor turnover by affecting vesicular traffic and therefore modulate cellular signaling intensity. WNK1 and WNK4 have been shown to stimulate clathrin-dependent endocytosis of the ROMK1, thus inhibiting potassium secretion (Lazrak et al. 2006). In the same manner, WNK4 stimulates NCC internalization and lysosomal degradation (Subramanya et al. 2009) and a similar mechanism may be able to modulate the ratio of degradation of endocytosed growth factor receptors (Moniz and Jordan 2010).

Transforming growth factor - β (TGF-β) demonstrates both tumor suppressing and tumor promoting activities, although initial actions are often anti-proliferative, transmitting inhibitory growth signals in many cell types. WNKs interact with TGF-β signaling, namely, siRNA-mediated knockdown of WNK1 increased Smad2/3-dependent transcriptional responses suggesting that WNK1 inhibits Smad2 and TGF-β signaling (Lee et al. 2007). It is also known that TGF-β signaling is related to epithelial-mesenchymal transition (EMT), a process related to tumor invasion and metastasis

formation. WNK1 inhibition of Smad2 regulates transcription of factors involved in E-cadherin expression required for cell adhesion. WNK1 decreased expression or inactivating mutations could promote EMT of epithelial tumor cells (Kankanamalage et al. 2018).

Another example of WNK1 effect in EMT is the study of miR-93 in breast cancer cells. The expression of this miRNA decreased WNK1 expression leading to decreased cell migratory capability and invasive potential, as well as increased adhesion. (Shyamasundar et al. 2016).

Apart from the cell-cycle examples demonstrated so far, WNKs also shown a relationship with apoptosis regulation, namely WNK3, which has been shown to promote cell survival by acting as an adaptor or scaffold protein in the complex that controls procaspase-3 activation and thus inhibiting caspase-3, permitting cells to evade apoptosis (Veríssimo et al. 2006)

AKT phosphorylates WNK1 at Thr60 *in vivo* not affecting WNK1 kinase activity directly nor its cellular localization, suggesting it influences protein-protein interactions (Vitari et al. 2004). Also, there is an interplay between WNK1, AKT and SGK1 regulating glucose channels (further explored in 1.8), which provide a connection between the PI3K/AKT pathway and WNK1 that may influence cell migration, invasion and angiogenesis (Kankanamalage et al. 2018).

Thus, WNKs are involved in several cancer-associated signaling networks (Figure 1.5) such as MAPK cascades, PI3K-AKT and TGF-β and thus affect cell-cycle progression, metabolic tumor cell adaptation, evasion of apoptosis and metastasis (Moniz and Jordan 2010; Kankanamalage et al. 2018).

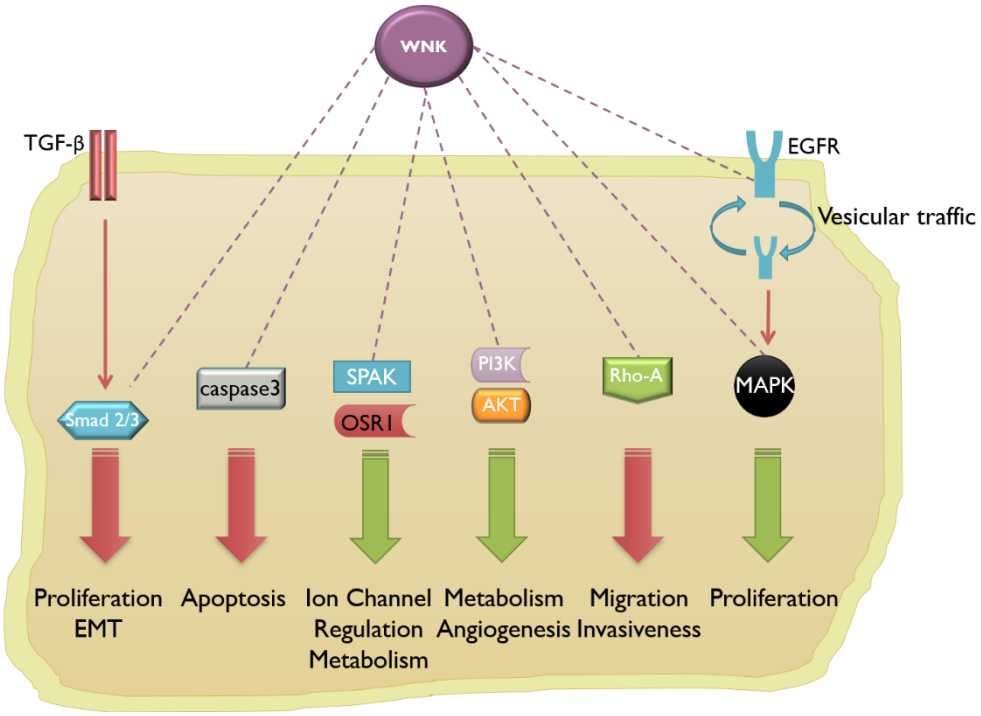


**Figure 1.5 –WNKs regulate several cancer-associated signaling networks.** Overview of the WNK pathway and its connection to major cancer-associated signaling pathways which affect cell-cycle progression, evasion of apoptosis, metabolic tumor regulation, migration and invasiveness. Green arrows represent activation, red arrows represent repression.

## 1.7 Protein kinases in the regulation of other cellular processes

In the human proteome up to 30% of proteins may be modified by kinase activity, and kinases are known to regulate the majority of cellular pathways, especially those involved in signal transduction (McCance and Huether 2014). Thus, signaling by protein phosphorylation is present in a wide range of cellular processes and we will focus on some examples in the following sections.

### 1.7.1 Kinases regulating gene expression and alternative splicing

In eukaryotes, the regulation of gene expression has multiple and complex levels of regulation which include multiple PTMs, such as phosphorylation, methylation and acetylation of proteins. Phosphorylation and hence, protein kinases play a role in several layers of gene expression regulation. First, activation of transcription through transcription factor phosphorylation followed by nuclear translocation and docking at promoter sequences is regulated by signaling pathways mediated by PK (Hunter and

Karin 1992). Second, after transcription, the mRNA sequence is target of a process of maturation and processing in which alternative splicing might occur. This process increases the complexity of the proteome encoded by higher eukaryotic genomes synthesizing different products from a single gene. The decision as to whether an exon is excluded or included involves RNA sequence elements and protein regulators in a multi-protein complex, the spliceosome. Depending on the position and function of the cis-regulatory elements, they are divided into four categories: exonic splicing enhancers (ESEs), exonic splicing silencers (ESSs), intronic splicing enhancers (ISEs) and intronic splicing silencers (ISSs). ESEs are usually bound by members of the SR protein family of splicing factors, which promote the insertion of a certain exon in the final product (Chen and Manley 2009).

SR proteins are regulated upstream by phosphorylation, which regulates their activity and localization (Gonçalves et al. 2018). An example of kinases regulating alternative splicing is SRPK1 during RAC1 pre-mRNA processing. Upon activation, SRPK1 leads to activation of SRSF1 (SR splicing factor 1, formerly designated as ASF/SF2). Through protein complex formation and phosphorylation, SRPK1 regulates SRSF1 translocation to the nucleus (Koizumi et al. 1999). Here, SRSF1 binds to and promotes inclusion of RAC1 exon 3b into the mature mRNA. The inclusion of the extra exon leads to the expression of alternative splicing variant RAC1B in colorectal cancer cells (Gonçalves et al. 2009, 2014), essential for cell cycle progression, cell survival (Matos and Jordan 2005, 2008; Matos et al. 2008) and tumor progression via senescence overcome (Henriques et al. 2015).

### 1.7.2 Kinases regulating glucose metabolism

Cell metabolism is complex and all the processes required for maintaining essential functions, from producing the structural elements of cellular structures to the energy production and storage, are tightly regulated. Kinases are involved throughout the regulation processes of cell metabolism, from the regulation of glucose uptake to the fine-tuning of energy storage processes (e.g. glycogen storage). In the following sections, we will describe in some detail the relevance of kinases regulating metabolism, namely GSK3 regulating glycogen and protein synthesis (see 1.7.2.1) and the PI3K/AKT axis regulating glucose uptake upon insulin receptor activation (see 1.7.2.2)

#### 1.7.2.1 Role of GSK3 in glucose metabolism

Insulin promotes the conversion of glucose to glycogen, a branched polymer of glucose that serves as energy and carbon repository in skeletal muscle and this involves stimulating glucose uptake and activating glycogen synthase (GS) (Roach 2002; Ferrer et al. 2003).

The activation by insulin of GS in the skeletal muscle (Figure 1.6) (Halse et al. 1999; McManus et al. 2005) requires GSK3β inactivation, by phosphorylation at Ser9, catalyzed by AKT (Cross et al. 1995). GSK3β inactivation allows GS dephosphorylation at a C-terminal cluster of serine residues (641, 645, 649 and 653) through the action of protein phosphatases, activating it and leading to glycogen synthesis (Cohen and Frame 2001).

#### 1.7.2.2 Role of insulin signaling in glucose metabolism

Control of circulating glucose is a key task for the homeostasis of the body. In normal physiology, glucose uptake from the blood is mainly regulated in two ways, insulin-regulated or stimulated by physical exercise in an insulin-independent absorption by muscle cells. The increased levels of circulating glucose in the blood after a meal induce the pancreas to release insulin so that glucose is rapidly absorbed by insulin-sensitive muscle and adipose tissues to lower the blood glucose level. These cell types rapidly respond to insulin with the translocation of glucose transporter storage vesicles (GSVs) from intracellular storage compartments to the PM, thereby delivering glucose transporters GLUT (Bogan 2012).

GLUT are glucose carriers that have 12 transmembrane helixes and provide bidirectional facilitated glucose transport through the PM (Hall 2015). These proteins use the concentration gradient of glucose across the cell membrane and therefore operate without energy consumption. There are at least 14 known members, encoded by the human genome as GLUT1 to GLUT14, the most important in terms of glucose homeostasis being GLUT1 - GLUT4 (Huang and Czech 2007; Thorens and Mueckler 2009; Hall 2015).

Regulation of GLUT localization is best established for GLUT4 in insulin responsive cells. These cell types rapidly respond to insulin with the translocation of GSVs, from intracellular storage compartments, to the PM, thereby delivering glucose

transporter GLUT4 (*SLC2A4*). In adipocytes, for example, this results in a 10-20 fold increase in glucose uptake mediated by GLUT4.

The underlying molecular mechanism (Figure 1.6) involves insulin binding to its receptor, stimulation of the PI3K pathway and activation of protein kinase AKT, which then phosphorylates the protein Tre-2/Bub2/Cdc16 (TBC) domain family member 4 [TBC1D4, also known as AKT substrate 160 kDa (AS160)] (Kane et al. 2002; Zaid et al. 2008; Sakamoto and Holman 2008). TBC1D4 contains a GTPase-activating domain for Rab proteins (Rab-GAP), a family of small GTPases required for membrane trafficking (Kane et al. 2002; Sano et al. 2003; Chen and Lippincott-Schwartz 2013). Experimental suppression of TBC1D4 leads to insulin-independent GLUT4 release to the PM (Eguez et al. 2005) and a functional GAP domain in TBC1D4 is required for insulin-stimulated GLUT4 translocation. In the absence of insulin signaling, the GAP domain of TBC1D4 keeps a critical Rab protein inactive, acting as a brake on Rab-GTPase activation. The GDP bound state prevents GLUT4 vesicle translocation until inhibitory phosphorylation of TBC1D4 occurs (Klip et al. 2014).

Recently, the closely related Rab-GAP TBC1D1 was also found to participate in the insulin-induced GLUT4 translocation (Roach et al. 2007; Taylor et al. 2008; Peck et al. 2009; An et al. 2010). TBC1D1 and TBC1D4 have high sequence homology and hold similar domain structures, including two PTB domains, a calmodulin- binding domain (CBD), the GAP domain and also share multiple phosphorylation sites (Cartee 2015). TBC1D1 and TBC1D4 are also part of an additional signaling mechanism regulated through physical exercise (Figure 1.6) and TBC1D1 was found to be the predominantly expressed GAP in the second crucial insulin-sensitive cell type, muscle cells. Physical exercise of muscles stimulates activation of the AMP-activated protein kinase (AMPK), which then phosphorylates TBC1D1 and TBC1D4 to promote GLUT4 translocation in an insulin-independent manner (Deshmukh et al. 2006; Chavez et al. 2008; Taylor et al. 2008; An et al. 2010). Moreover, TBC1D1 has been reported to increase the GLUT1 expression levels in adipocytes (Zhou et al. 2008) and mutations in the TBC1D1 gene are linked with obesity (Stone et al. 2006; Chadt et al. 2008; Meyre et al. 2008).

## 1.8 WNK1 and signaling crosstalk in glucose metabolism

Mendes and colleagues (2010) showed that WNK1, although mainly linked to ion transport regulation (see 1.6.5), also has a role in regulating the cell surface expression of GLUT1. WNK1 forms a protein complex with TBC1D4 in human embryonic kidney (HEK293) cells and phosphorylates it *in vitro*. Phosphorylation by WNK1 was found to increase the binding of TBC1D4 to regulatory 14-3-3 proteins and to reduce its interaction with the exocytic small GTPase Rab8A. This novel pathway was able to modulate the cell surface expression of GLUT1 (Figure 1.6).

AKT is the most-studied regulatory protein kinase of TBC1D Rab-GAP proteins, however, two additional protein kinases, WNK1 and SGK1 are also able to participate in the regulation of TBC1D4 and thus may represent pathways to modulate the insulin response. SGK1, upon activation by PI3K, was found to phosphorylate TBC1D4 increasing the cell surface expression of GLUT1 (Palmada et al. 2006). Also, the SGK1 phosphorylation upon TBC1D4 regulates the endocytosis of ENaC (Liang et al. 2010).

Besides sharing TBC1D4 as a common substrate, the three protein kinases AKT, SGK1 and WNK1 were found to share functional interactions. AKT and SGK1 can phosphorylate WNK1 on Thr60 in IGF1-treated cells (Vitari et al. 2004; Xu et al. 2005b) but the resulting phenotypic consequences remain unclear, because they did not affect WNK1 kinase activity or its cellular localization, probably influencing protein-protein interactions (Vitari et al. 2004).

Moreover, AKT1 and SGK1 can phosphorylate WNK1 synergistically inhibiting ROMK by promoting its endocytosis (Cheng and Huang 2011). On the other hand, WNK1 interacts through its N-terminus with, but does not phosphorylate, SGK1 and acts as a scaffold required for efficient SGK1 activation (Xu et al. 2005b; Heise et al. 2010). These examples show an interplay between AKT, SGK and WNK kinases for which a role in GLUT transporter regulation is not understood.

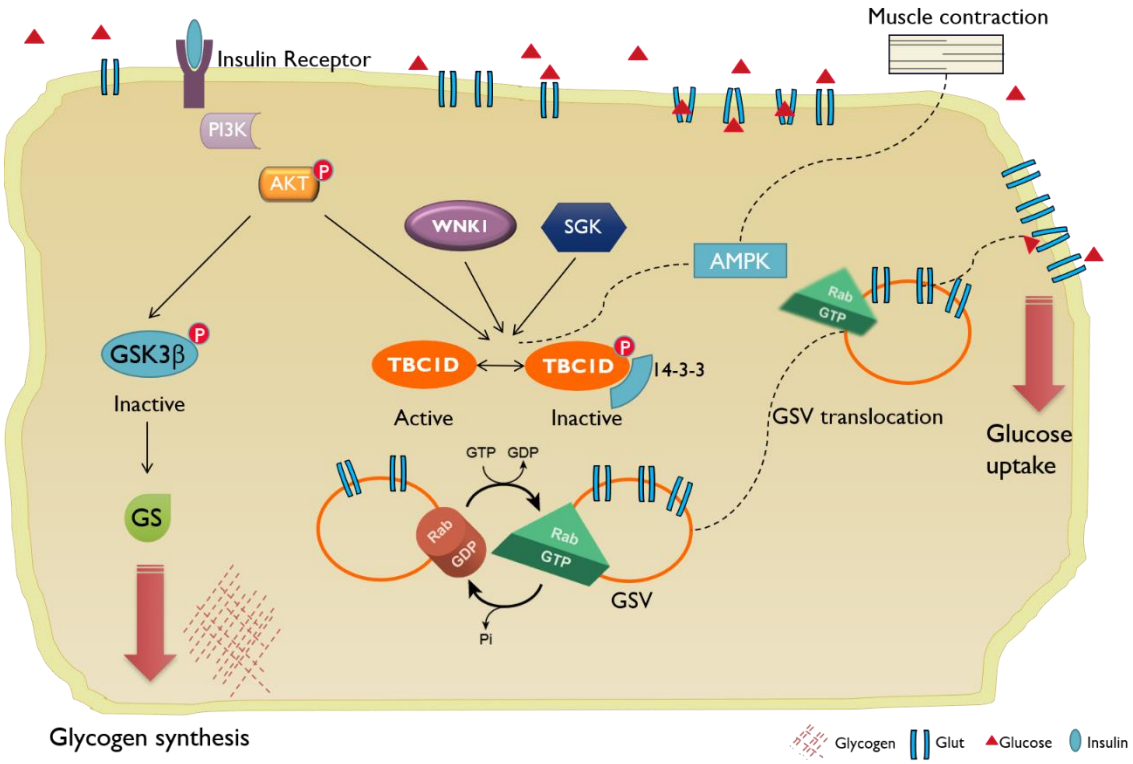


**Figure 1.6 Kinases regulating glucose uptake.** Activation of insulin signaling stimulates PI3K and leads to phosphorylation of AKT. Activated AKT inhibits GSK3β by phosphorylation on Ser9. GSK3β inactivation allows glycogen synthase (GS) dephosphorylation and activation, leading to glycogen synthesis. AKT, WNK1 and SGK1 all phosphorylate the Rab-GAPs TBC1D1 and TBC1D4, inactivating them. TBC1D inhibit Rab-GTPases responsible for vesicle trafficking and their inactivation allows activation of the Rab proteins, GLUT storage vesicle (GSV) translocation and delivery of glucose transporters to the plasma membrane resulting in increased glucose uptake. An alternative insulin-independent signaling pathway regulating glucose transporters is mediated through muscle contraction and AMP-activated protein kinase (AMPK) activation.

## 1.9 Objectives

The work described in this thesis had the following objectives:

1) Determine the effect of WNK1 kinase in GLUT1 PM expression and function, and determine specific phosphosites regulated by WNK1, AKT1 or SGK kinases;

2) Isolate and identify WNK1-interacting proteins

3) Validate hit proteins and determine their role in WNK1-mediated cellular effects

# Chapter 2 Materials and Methods

## 2.1 *In vitro* protein kinase assays

For each condition of the kinase assays, 0.5 µg of the recombinant protein kinase Flag/His-WNK1 (1111-0000-1), GST-AKT1 (0132-0000-1), GST-AKT2 (0276-0000-2), GST-SGK1 (0199-0000-2) or GST-SGK3 (0198-0000-2) (all from ProQuinase) were incubated in 20 µL kinase reaction buffer (30 mM Tris/HCl pH 7.5, 10% glycerol, 1 mM DTT, 1 mM $Na_3VO_4$, 10 mM $MgCl_2$, 100 µM ATP), mixed with their recombinant substrate [0.5 µg of either rMyc-TBC1D1, rMyc-TBC1D4 (Origene Technologies) or recombinant kinase-dead OSR1 (Mendes et al. 2011)], and incubated in the presence of 5 µCi -γ32P ATP at 30˚C for 30 min. Finally, 2x SDS sample buffer (100 mM Tris/HCl pH 6.8, 10% glycerol, 4% SDS, 130 mM DTT, 0.5 mg bromophenol blue) was added, samples boiled and separated by SDS-PAGE followed by Western blot (WB). Membranes were exposed to X-ray films, and subsequently incubated with the indicated antibodies in order to document protein quantities.

## 2.2 TBC1D phosphopeptide identification

The protein kinase assays were repeated under non-radioactive conditions and samples prepared for mass spectrometric determination of the phosphorylation sites as follows (collaboration with Rune Matthiesen, Ana Sofia Carvalho and the CIC bioGUNE center in Derio, Spain).

*In vitro* phosphorylation of 0.5 µg recombinant substrate with 0.5 µg recombinant kinase in duplicate standard 20 µL reactions for 1 h at 30˚C. Then, 20 µl iodoacetamide (IAA) for cysteine alkylation were added for 1 h at 21˚C ( protected from light ), followed by quenching of remaining IAA with 20 µL DTT for 15 min at 21˚C. Duplicates were incubated with either trypsin [cuts after arginin (R) or lysine (K)] or enteropeptidase (also called enterokinase – cuts only after K) and digested overnight at 37˚C. Digested peptides were purified by retention on C12 hydrophobic reverse phase porous resin filled into previously activated and washed small columns. Resin columns were then shipped to the mass spectrometry (MS) center. Peptide separation was performed on a nanoACQUITY UPLC System (Waters) on-line connected to an LTQ Orbitrap XL mass spectrometer (Thermo Electron). An aliquot of each sample was loaded onto a Symmetry 300 C18 UPLC Trap column (180 µm × 20 mm, 5 µm, Waters).

## 2.3 Cell culture, treatment and transfections

HEK293 (human embryonic kidney 293) cells, DLD-1 and SW480 colorectal cells were maintained in Dulbecco's modified minimal essential medium (DMEM), while HT29 colorectal cells were cultured in RPMI (, all supplemented with 10% (v/v) of heat inactivated fetal bovine serum (FBS) (all reagents from Gibco, Life Technologies). Cells were maintained at 37˚C with 5% $CO_2$, and regularly checked for absence of mycoplasm infection.

For ectopic expression of plasmid cDNAs, HEK293 cells were transfected at 80-90% confluence using Metafectene (Biontex) according to the manufacturer's instructions. Transfection efficiencies were found to be around 90%, as determined microscopically using a GFP expression vector. Total amounts of transfected plasmid DNA were kept constant at 6 μg per 60 mm dish or 2 μg per 35 mm dish and adjusted with empty vector, if required. Cells were analyzed after 20 h for biochemical assays.

For gene silencing HEK293 at 30% confluence were transfected with 200 pmol of small interfering RNA oligonucleotides (siRNAs) per 35 mm dish or 400 pmol per 60 mm dish using Metafectene. Cells transfected with siRNAs were analyzed after 48 h, and the determination of target gene expression depletion was determined in each experiment by removing a 40 μL aliquot from the cell lysate prepared for the immunoprecipitation protocol (see below). All results were confirmed in at least three independent experiments.

For gene silencing, HT29, DLD-1 and SW480 cells were used at 30%–40% confluence and transfected with Lipofectamine 2000 (Invitrogen). Transfection of 24-well plates or 35 mm dishes was performed with 100 pmol or 250 pmol respectively, of the indicated siRNAs, using a ratio of 4 μL of Lipofectamine 2000 per 100 pmol of siRNA in a solution of 100 or 250 μL of Optimem (Gibco, Life Technologies) and analyzed after 48 h.

For plasmid transfection, cells were grown in 24-well plates or 35 mm dishes to 60%–80% confluence or transfected 20 to 24 h after siRNA transfection. Cells were transfected using Lipofectamine 2000 (Invitrogen), according to the manufacturer's instructions and analyzed 20–24 h later. Total amounts of transfected DNA were 0.75 μg per well of 24-well plates, or 2.5 μg DNA for 35 mm dishes. If required, the amount of

DNA was adjusted with empty vector. Plasmid transfection efficiencies were judged microscopically by expression of GFP and reached 40%–60%.

For drug treatment assays, cells were seeded in 24- or 6-well plates and treated with either vehicle (DMSO) or 500 µM of ibuprofen (IBU from Sigma-Aldrich), from a 100 mM stock solution prepared in DMSO.

The siRNA oligos were ordered from Eurofins Genomics with the following sequences: control siLuc, 5′-CGU ACG CGG AAU ACU UCG ATT; siRAC1B, 5′-CAG UUG GAG AAA CGU ACG GTT; siSRPK1, 5′-UUA UUC AGC AAG UGU UAC ATT; siWNK1: 5'-GCA GGA GUG UCU AGU UAU A. For AKT1, we used siAKT1 (sc-29195) ordered from Santa Cruz Biotechnology.

## 2.4 Glucose uptake assays

Cells were treated as described and glucose uptake was measured using Glucose Uptake-Glo™ Assay (Promega), according to the manufacturer's instructions. Briefly, this assay is a fluorescence-based method measuring the amount 2-deoxyglucose (2DG) transported into cells for 10 min. 2DG is transported into cells and phosphorylated to produce 2-deoxyglucose-6-phosphate (2DG6P). The addition of Stop Buffer stops 2DG transport, lyses cells, destroys any NADPH within the cells and inactivates proteins. The addition of Neutralization Buffer neutralizes the solution before addition of the 2DG6P Detection Reagent. The glucose-6-phosphate dehydrogenase (G6PDH) within the reagent oxidizes 2DG6P to 6-phosphodeoxygluconate (6PDG) and reduces $NADP^+$ to NADPH. The reductase uses the NADPH to convert the proluciferin to luciferin, which is then used by luciferase to produce light measured in the luminometer – Anthos Lucy-2 (ASYS Hitech). The RLUs (relative light units) were then normalized to the total protein levels measured by PCNA levels through WB.

## 2.5 Expression constructs

TBC1D1 was amplified from pBluescript with the primers KpnTBD1-F and KpnTBD1-R (Table 2.1), cloned into pCR2.1 TOPO-TA vector (Invitrogen) and subcloned as a KpnI fragment into expression plasmid pcDNA$_3$-Myc. This construct will be referred to as Myc-TBC1D1. To introduce the unphosphorylatable alanine (A) or phosphomimetic aspartate (D) codons, the plasmid was mutated at codon 505 from ACA to GCA or GCT to obtain Myc-TBC1D1 T505A/D and at codon 565 and from TCC to GCC or GAC to obtain the constructs Myc-TBC1D1 S565A/D, using the QuickChange Site-Directed Mutagenesis kit (Stratagene) according to the manufacturer's instructions and the primers listed in Table 2.1.

Several previously published constructs were used in this study. pCR3.1/AS160-2myc (Peck et al. 2006) will be from now on referenced as Myc-TBC1D4. To introduce the unphosphorylatable alanine (A) or phosphomimetic aspartate (D) codons, the plasmid was mutated at codon 704 from TCT to GCT or GAT to obtain the constructs Myc-TBC1D4 S704A/D, using the QuickChange Site-Directed Mutagenesis kit (Stratagene) according to the manufacturer's instructions and the primers listed in Table 2.1. pIRES2-EGFP-SGK1 CA and KD, gifts from Florian Lang (University of Tubingen, Germany (Feng et al. 2005), were amplified with Eco-SGK1-F and Kpn-SGK1-R (Table 2.1) cloned into pCR2.1 TOPO-TA and subcloned as EcoRI/KpnI fragments into pEGFP-C2 expression plasmids. Vectors pEGFP-AKT CA and KD were a gift from B. M. Burgering (Utrecht University, The Netherlands) (Burgering and Coffer 1995), recloned as BglII/EcoRI fragments into pEGFP-C1 expression plasmids as described (Gonçalves et al. 2009). HA-GSK3β (S9A) pcDNA3 was a gift from Jim Woodgett (University of Toronto, Canada) (Addgene plasmid # 14754) (Stambolic and Woodgett 1994).

All constructs were verified by automated DNA sequencing.

**Table 2.1 – Table of the primers used for cloning and site directed mutagenesis.**

| | ***Primer*** | ***Sequence*** |
|---|---|---|
| pcDNA3-Myc TBC1D1 | KpnTBD1-F | 5' GGTACCGAACCAATAACATTCACAGCAA |
| | KpnTBD1-R | 5' GGT ACC TCA GTC GCC CGT GGG CT |
| MYC-TBC1D1 site directed mutagenesis | Tbd1 mut T505-A_F | 5' GCAAAGAGATCTTTAGCAGAGTCTTTAG |
| | Tbd1 mut T505-A_R | 5' CTAAAGACTCTGCTAAAGATCTCTTTGC |
| | Tbd1 mut T505-D_F | 5' GCAAAGAGATCTTTAGCTGAGTCTTTAG |
| | Tbd1 mut T505-D_R | 5' CTAAAGACTCAGCTAAAGATCTCTTTGC |
| | Tbd1 mut S565-A_F | 5' CTTTAAGCTCCTCGGCGCCTCGGAGGAC |
| | Tbd1 mut S565-A_R | 5' GTCCTCCGAGGCGCCGAGGAGCTTAAAG |
| | Tbd1 mut S565-D_F | 5' CTTTAAGCTCCTCGGCGACTCGGAGGAC |
| | Tbd1 mut S565-D_R | 5' GTCCTCCGAGTCGCCGAGGAGCTTAAAG |
| MYC-TBC1D4 site directed mutagenesis | Tbd4 mut S704-A_F | 5' GTCTTCACACTTCCTTCGCTGCCCCTTCCTTCAC |
| | Tbd4 mut S704-A_R | 5' GTGAAGGAAGGGGCAGCGAAGGAAGTGTGAAGAC |
| | Tbd4 mut S704-D_F | 5' GTCTTCACACTTCCTTCGATGCCCCTTCCTTCACTG |
| | Tbd4 mut S704-D_R | 5' CAGTGAAGGAAGGGGCATCGAAGGAAGTGTGAAGAC |
| pEGFP SGK1 CA / KD | Eco-SGK1-F | 5' GAA TTC ACG GTG AAA ACT GAG GCT G |
| | Kpn-SGK1-R | 5' GGT ACC TCA GAG GAA AGA GTC CGT G) |

## 2.6 Biotinylation of cell surface proteins

HEK293 cells were first transfected with either siWNK1 or siLuc and incubated for 24 h. In a second transfection, the Myc-TBC1D1/4 A mutants described above were transfected into the control (siLuc) dishes, whereas the Myc-TBC1D1/4 D mutants into the siWNK1 dishes. For all conditions, cells were placed on ice, washed three times with ice cold PBS-CM (PBS pH 8.0 containing 1 mM $CaCl_2$ and 1 mM $MgCl_2$) and left 5 min in cold PBS-CM. Cells were then incubated for 45 min with 0.5 mg of EZ-Link Sulfo-NHS-SS-Biotin (Santa Cruz Biotechnology) to label all cell surface proteins. Cells were rinsed twice and left for 15 min on ice with ice-cold Tris-Q [100 mM Tris/HCl pH 8.0, 150 mM NaCl, 0.1 mM $CaCl_2$, 1 mM $MgCl_2$, 10 mM glycine, 1% (w/v) BSA] to quench the reaction. Cells were again washed three times with cold PBS-CM and lysed in 250 µL

of pull-down buffer [50 mM Tris/HCl pH 7.5, 100 mM NaCl, 10% (v/v) glycerol, 1% (v/v) NP40, supplemented with a protease inhibitor cocktail composed of 1 mM PMSF, 1 mM 1,10-phenanthroline, 1 mM EGTA, 10 µM E64, and 10 µg/mL of each aprotinin, leupeptin, and pepstatin A (all from Sigma-Aldrich)]. Cell lysates were cleared at 9000x g for 5 min at 4˚C. An aliquot of 40 µL, representing total protein levels, was removed and added to 2x SDS modified sample buffer (62.5 mM Tris/HCl pH 6.8, 3% SDS, 10% glycerol, 0.02% bromophenol blue, 196.4 mM DTT), while 200 µL lysate were added to 15 µL of G-protein agarose beads (Roche), rotated for 1 h at 4˚C and centrifuged for 1 min at 3000x g, to perform a pre-clearing of the lysates. The pre-cleared lysates were recovered, added to 20 µL streptavidin-agarose beads (Sigma-Aldrich), previously incubated for 1 h in 1 mL cold pull-down buffer containing 2% (w/v) milk, and washed three times in pull-down buffer. Lysate and beads were rotated for 1 h at 4˚C, centrifuged for 1 min at 3000x g, and washed five times in cold wash buffer (100 mM Tris/HCl pH 7.5, 300 mM NaCl, 1% (v/v) Triton X-100). Captured proteins were recovered in 20 µL of 2x SDS modified sample buffer with 100 mM DTT and analyzed by WB with specific antibodies, as described below.

## 2.7 Immunoprecipitation (IP) and mass spectrometry preparation

HEK293 or HT29 cells were seeded and incubated for 48 h. For each condition cells near 100% confluence in 100 mm culture dishes were placed on ice and washed three times with ice cold PBS-CM (PBS pH 8.0 containing 1 mM $CaCl_2$ and 1 mM $MgCl_2$). Except if otherwise referred, cells were then incubated with the crosslink solution DSP+SPSP (1:1 0,2 mM; Thermo Scientific) for 2 h. To quench the reaction 50 mM Tris/HCl pH 8.0 was added to the dishes and incubated for 15 min. In all IP procedures, cells were again washed 3x with cold PBS-CM and lysed in 750 µL lysis buffer (50 mM Tris/HCl pH 7.5, 2 mM $MgCl_2$, 100 mM NaCl, 10% (v/v) glycerol, 1% (v/v) NP40), supplemented with a protease inhibitor cocktail composed of 1 mM PMSF, 1 mM 1,10-phenanthroline, 1 mM EGTA, 10 µM E64, and 10 µg/mL of each aprotinin, leupeptin, and pepstatin A (all from Sigma-Aldrich). Cell lysates were cleared at 3000x g for 5 min at 4˚C. To perform a pre-clearing of the lysates, the lysate was added to 45 µL streptavidin-agarose beads (Sigma-Aldrich), rotated for 1 h at 4˚C and centrifuged for 1 min at 3000x g. About 700 µL of the pre-cleared lysates were recovered and added to the beads prepared as described in the following section (see 2.8) and rotated overnight at

4˚C. After incubation, the tubes were centrifuged for 1 min at 3000x g and washed 6x in cold wash buffer [50 mM Tris/HCl pH 7.5, 2 mM $MgCl_2$, 150 mM NaCl, 10% (v/v) glycerol, 1% (v/v) NP40]. Captured proteins were recovered in 50 µL 2x SDS modified sample buffer with extra DTT (100 mM). For MS analysis captured proteins were separated on 9% (w/v) 1.5 mm SDS-PAGE gels with 1% (v/v) glycerol and were run at 4˚C for 1 cm. The obtained gel was silver-stained as described below (see 2.11) and the entire stained area was excised as one sample and sent to nano-LC MS analysis using SCIEX TripleTOF 6000 system ITQB institute, Oeiras, Portugal (UniMs). For validation of MS results, co-immunoprecipitate samples were analyzed by WB as described in 2.9.

## 2.8 Beads preparation

60 µl of dry G-protein agarose beads (Roche) were incubated with 1.5 µg of sheep anti-WNK1 antibody (Dundee University) diluted in PBS for 1 h at 4˚C. Beads were washed 3x with PBS and crosslinked to the antibody with 4% (v/v) formaldehyde in PBS for 1 h at 4˚C. After crosslink, beads were washed 3x with PBS and blocked with 2% BSA in PBS solution rotating for 1 h at 4˚C, washed 3x with PBS and added to the pre-cleared lysate recovered (see 2.7).

## 2.9 Western blot (WB) procedures

Membrane protein lysates and IP lysates were separated on 9% (w/v) SDS-PAGE with 1% (v/v) glycerol gels and were run at 4˚C. Total lysates from depletion experiments in HT29 cells were separated in 10 or 12% (w/v) SDS-PAGE gels. For detection of specific proteins, SDS-PAGE gels were transferred onto PVDF membranes (Bio-Rad). WB membranes were blocked in 5% (w/v) milk powder in TBS with 0.1% (v/v) Triton X-100 and probed using the indicated primary antibodies (Table 2.2) followed by a secondary peroxidase-conjugated antibody. For densitometric analysis of WB bands, X-rays films were digitalized, and images analyzed with ImageJ software (NIH).

**Table 2.2 – Table of the used antibodies.**

| ***Primary antibody*** | ***Clone/Catalog Number*** | ***Brand/Supplier*** | ***Secondary antibody*** |
|---|---|---|---|
| mouse α-p21 | C-19; sc-397 | Santa Cruz Biotechnology | Goat α-mouse IgG horseradish peroxidase (HRP) conjugate (Bio-Rad) |
| mouse α-PTBP1 | SH54; sc-56701 | Santa Cruz Biotechnology | |
| mouse α-Shc | PG-797; sc-967 | Santa Cruz Biotechnology | |
| mouse α-Ezrin | 610602 | BD Transduction Laboratories | |
| mouse α-HIS | 37-2900 | Invitrogen | |
| mouse α-MYC | 9E10; M5546 | Sigma-Aldrich | |
| mouse α-NCK | 108; 610099 | BD Transduction Laboratories | |
| mouse α-PCNA | PC10; NA03 | MerckBiosciences | |
| mouse α-RAC1 | 23A8; #05-389 | Millipore | |
| mouse α-SRPK1 | 12; 611072 | BD Transduction Laboratories | |
| mouse α-SRSF1 | 96; sc-33652 | Santa Cruz Biotechnology | |
| mouse α-Transferrin | H68.4; #13-6800 | Invitrogen | |
| mouse α-Tubulin | B-5-1-2; T5168 | Sigma-Aldrich | |
| mouse α-β-catenin | 14; 610154 | BD Transduction Laboratories | |
| rabbit α-Cyclin-D1 | M20; sc-718 | Santa Cruz Biotechnology | Goat α-rabbit IgG horseradish peroxidase (HRP) conjugate (Bio-Rad) |
| rabbit α-GLUT1 | ab652 | Abcam | |
| rabbit α-GSK3β | 27C10; #9315 | Cell Signaling | |
| rabbir α-GFP | ab290 | Abcam | |
| rabbit α-GST | AB3282 | Chemicon | |
| rabbit α-HA | H6908 | Sigma-Aldrich | |
| rabbit a-Ki67 | sc-15402 | Santa Cruz Biotechnology | |
| rabbit α-AKT | #9272 | Cell Signaling | |
| rabbit α-p-GSK3β (S9) | D3A4; #9322 | Cell Signaling | |
| rabbit α-pan 14-3-3 | (K-19); sc-629 | Santa Cruz Biotechnology | |
| rabbit α-PARP | #9542 | Cell Signaling | |
| rabbit α-RAC1B | #09-271 | Millipore | |
| rabbit α-ZO-1 | H-300; sc-10804 | Santa Cruz Biotechnology | |

| *Primary antibody* | *Clone/Catalog Number* | *Brand/Supplier* | *Secondary antibody* |
|---|---|---|---|
| sheep α-p-TBC1D4 (T642) | | Dundee University | Rabbit α-sheep IgG HRP Conjugate (Invitrogen) |
| sheep α-WNK1 | S062B | Dundee University | |

## 2.10 Bioinformatic analysis of MS data

Qualitative nanoLC MS/MS analysis of IP samples generated a set of data in which each MS spectra protein hit was characterized by a protein confidence score (PCS) given by the SCIEX proprietary ProteinPilot™ Software. For PCS>1.3, the confidence in the identification of that particular peptide is equal or higher than 95%. Given that all the experiments were performed in triplicate, we created an algorithm to generate a combined confidence score (CCS), producing five additional integrated confidence levels for the proteins detected among the different replicates: level 5 are proteins detected with PCS ≥ 1.3 in more than one replicate and not in the controls; level 4 are proteins detected in one replicate with an PCS ≥ 1.3 and not in the controls; level 3 are proteins detected in more replicates than in controls, and with an average PCS higher than their respective the controls; level 2 are proteins detected in more replicates than in controls, and with an average PCS lower than their respective the controls; and level 1 are proteins detected in the same number of replicates and controls, with a replicate average PCS higher than the corresponding controls. Additionally, distance to WNK (d2WNK) was calculated for candidate proteins by the search in public databases for described interactions with WNK1.

Gene ontology-based functional annotation analysis of hit proteins was performed using DAVID (Database for Annotation, Visualization and Integrated Discovery at "https://david.ncifcrf.gov/").

## 2.11 Silver staining of SDS-PAGE gels

SDS-PAGE gels intended for MS analysis were silver stained as described (Mortz et al. 2001). Gels were transferred to a glass tray and fixed for 1 h at room temperature in fixer solution [40% ethanol, 10% acetic acid (glacial), 50% dd$H_2O$], and washed overnight in dd$H_2O$. Gels were sensitized in 0.02% sodium thiosulfate (0.04 g $Na_2S_2O_3$,

200 mL $ddH_2O$) for 1 min and washed tree times with $ddH_2O$. Gels were then incubated in cold 0.1% silver nitrate solution (0.2 g $AgNO_3$, 200 mL $ddH_2O$, 0.02% formaldehyde) for 20 min and washed twice with $ddH_2O$. Gels were transferred to a new tray and washed for 1 min before developing in 3% sodium carbonate solution (7.5 g $Na_2CO_3$ in 250 mL $ddH_2O$, 0.05% formaldehyde) until distinct bands were visible. After $ddH_2O$ washing, staining was completed in 5% acetic acid (glacial) for 5 min and gels were stored at 4˚C in 1% acetic acid (glacial) until MS analysis.

### 2.12 Confocal immunofluorescence microscopy

Cells were grown on 10 mm glass coverslips, transfected, and incubated as indicated above, then washed twice in PBS, immediately fixed with 4% (v/v) formaldehyde in PBS for 20 min at room temperature, and subsequently permeabilized with 0.5% (v/v) Triton X-100 in PBS for 30 min at room temperature. Cells were then labeled for 60 min with either mouse α-SRPK1 antibody (1:500) or mouse α-SRSF1 (1:100), combined with rabbit α-HA (1:250) for HA-EV/HA-GSK3β (S9A) transfected cells, washed 3× in PBS-T (PBS + 0.01% Tween) for 5 min with gentle shaking, followed by 30 min incubation with a 1:250 dilution of mouse Alexa Fluor 488 and rabbit Alexa Fluor 546 (both from Invitrogen). Coverslips were washed 3× in PBS, briefly stained with 1.25 µg/mL DAPI (Sigma-Aldrich), washed again, post-fixed with 4% (v/v) formaldehyde in PBS for 10 min at room temperature and then mounted in VectaShield (Vector Laboratories) and sealed with nail polish. Images were recorded with the 405 nm, 488 nm, and 546 nm laser lines of a Leica TCS-SPE confocal microscope and processed with Adobe Photoshop software.

### 2.13 ROI analysis

A region of interest (ROI) was analyzed along optical sections across several cells crossing nucleus and cytoplasm in the confocal microscopy images. The section was analyzed by pixel intensity measurement of the three fluorescent signals (green: SRSF1/SRPK1; blue: nucleus; red: HA) with ImageJ software (NIH).

## 2.14 Statistical analysis

Data were analyzed using Student's *t*-tests, with $P < 0.05$ accepted as the statistical significance level. Shown data reflect the mean ± SEM from at least three independent experiments.

# Chapter 3 Results

## 3.1 WNK1 modulates glucose uptake in HEK293 cells

WNK1 regulates the retention or insertion of various transmembrane transporter proteins at the PM and this can involve different downstream effector mechanisms (Hadchouel et al. 2016). Mendes et al. (2010) described a role for WNK1 in regulating glucose transporter GLUT1 (*SLC2A1* gene) expression at the PM in HEK293 cells. The mechanism occurs through WNK1-mediated phosphorylation of TBC1D4, a Rab GTPase-activating protein (Rab-GAP) that is also involved in insulin-regulated exocytosis of glucose transporter GLUT4. WNK1 expression promoted GLUT1 surface expression while depletion of WNK1 led to a decrease in PM expression of GLUT1.

In order to determine whether the expression of GLUT1 at the PM would indeed lead to an increase in glucose uptake, we used siRNA-mediated depletion of WNK1 in HEK293 cells followed by a glucose uptake assay. Cells were transfected with siWNK1 and incubated for 48 h, after which the glucose uptake was measured using Glucose Uptake-Glo™ Assay (Promega). The efficiency of depletion was confirmed by WB (Figure 3.1A) and determined to be around 80% (Figure 3.1B). Considering the glucose uptake, we experimentally determined a significant reduction of 40% (Figure 3.1C) in glucose uptake levels associated with the depletion of WNK1 in HEK293 cells. Thus, we were able to confirm that WNK1 expression affects glucose uptake, consistent with previous results for GLUT1 PM expression.

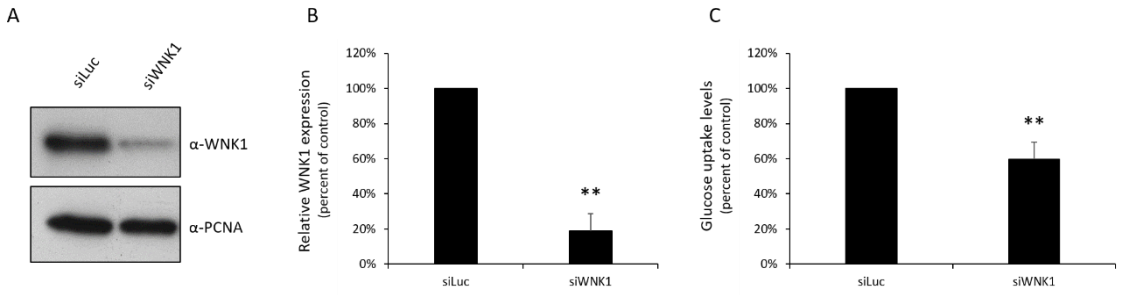


**Figure 3.1 – WNK1 modulates glucose uptake in HEK293 cells.** Cells were transfected with either siLuc (control) or siWNK1 and incubated for 48 h. **(A-B)** Analysis and quantification of WNK1 depletion. Part of the lysate was denatured, separated by SDS-PAGE and transferred to PVDF blotting membranes. Membranes were then analyzed by WB and WNK1 depletion and total protein amount were determined using anti-WNK1 and anti-PCNA antibodies (loading control). **(C)** Quantification of glucose uptake levels. The glucose uptake assay was performed using the Glucose Uptake-Glo™ Assay (Promega) following the manufacturer's instructions and glucose values determined by relative light units (RLUs) normalized to total protein values. Normalization to total protein was performed through

analysis of relative intensities of PCNA bands using ImageJ (NIH). All shown data represent means ± SEM, $^{**}P < 0.01$.

## 3.2 Identification of regulatory protein kinases involved in the phosphorylation of TBC1D proteins *in vitro* – WNK1, AKT1, AKT2, SGK1 and SGK3

Phosphorylation of either the TBC1D1 or TBC1D4 homologs is a key regulatory step in the kinase cascades leading to changes in glucose uptake (Sakamoto and Holman 2008; Zaid et al. 2008). AKT was the first protein kinase described to phosphorylate the Rab-GAPs TBC1D1 and TBC1D4 in response to insulin stimulation (Kane et al. 2002; Zaid et al. 2008). The resulting phosphorylated TBC1D proteins are inactivated, allowing the translocation of GLUT to the PM (Eguez et al. 2005). Nonetheless, multiple kinases were reported to phosphorylate TBC1D proteins, indicating a complex network of regulator kinases in this process, including SGK1 (Palmada et al. 2006) and WNK1, previously described by the host lab (Mendes et al. 2010).

We selected the kinases WNK1, AKT1, AKT2, SGK1 and SGK3 and compared their capability to phosphorylate the Rab-GAP proteins TBC1D1 and TBC1D4 in *in vitro* protein kinase assays. Each recombinant kinase was incubated in the presence of γ32P-ATP alone, or together with purified human Myc-tagged TBC1D1 or TBC1D4. The kinase assay was followed by electrophoretic protein separation and transfer to PVDF membranes. Posterior WB analysis of the radioactive membranes were performed to confirm protein quantities in the different assays.

As shown in Figure 3.2A and B, both AKT kinases autophosphorylated and phosphorylated TBC1D1 and TBC1D4. The results also indicated that both TBC1D proteins were not radioactively labelled in the presence of γ32P-ATP alone. For specific validation of AKT1 activity a phospho-specific antibody for TBC1D4 threonine 642 (Thr 642) was used, one of the first phosphosites described for AKT phosphorylation of TBC1D4 (Kane et al. 2002). Using this antibody, we were able to confirm that the *in vitro* kinase assay reproduced the specific phosphorylation of TBC1D4 by AKT1 at an already described phosphosite (Figure 3.2A).

For the *in vitro* WNK1 kinase assay (Figure 3.2C), recombinant OSR1 (oxidative stress-responsive kinase 1) was included as a well-known positive control (Zagórska et al. 2007). Again, we were able to observe autophosphorylation of the FLAG/HIS-tagged

WNK1 in the presence of γ32P-ATP alone and phosphorylation of both TBC1D proteins *in vitro*.

Based on the previously described role of SGK1 in regulating GLUT translocation to the PM (Palmada et al. 2006), we tested GST-SGK1 and GST-SGK3 for their ability to phosphorylate TBC1Ds *in vitro*. As shown in Figure 3.2D both isoforms of SGK autophosphorylated and phosphorylated TBC1D1 and TBC1D4 *in vitro*.

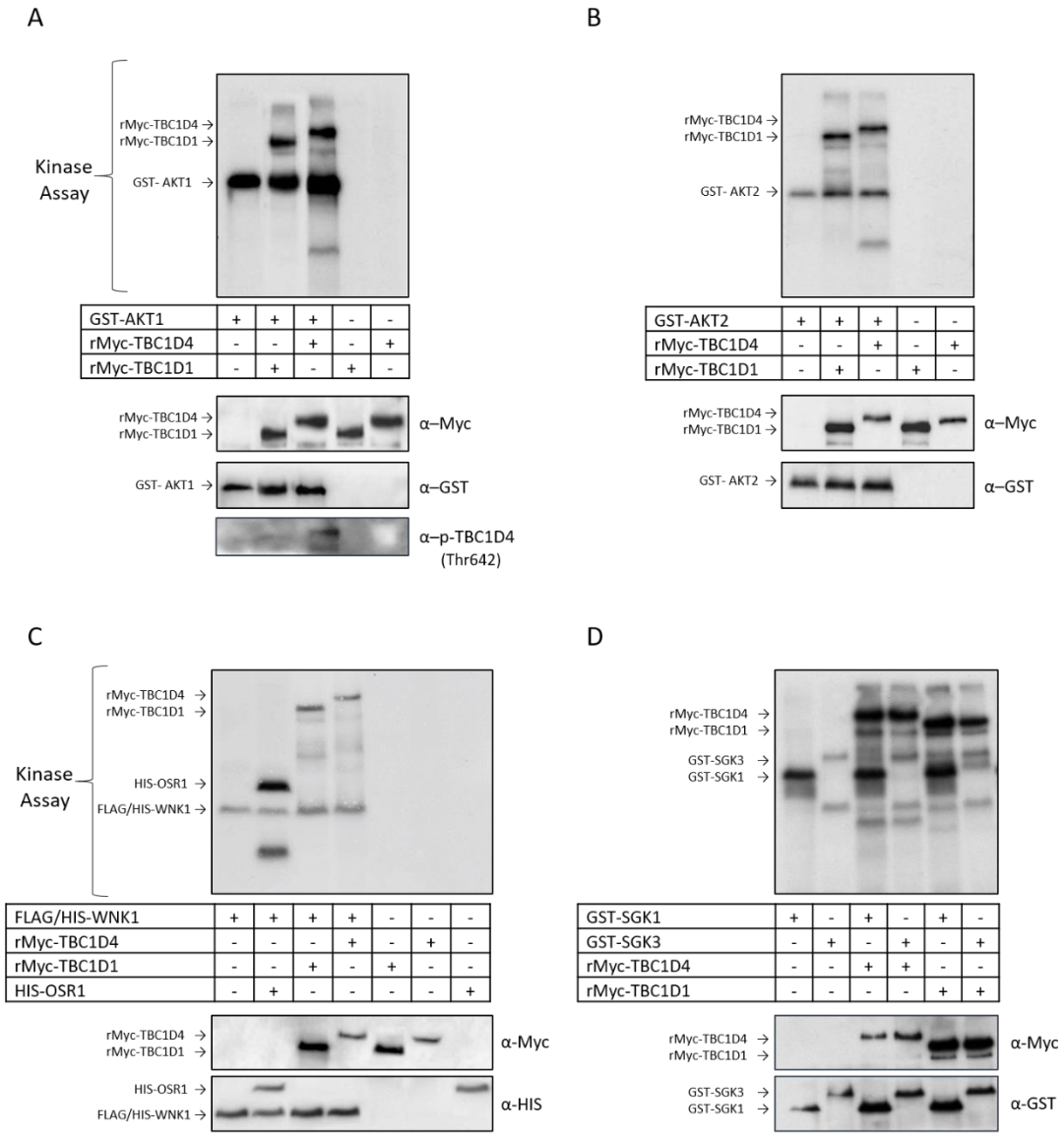


**Figure 3.2 – WNK1, AKT1, AKT2, SGK1 and SGK3 phosphorylate TBC1D1 and TBC1D4 *in vitro***. (**A-B**) AKT1 and AKT2 kinase assays. (**C**) WNK1 kinase assay. (**D**) SGK1 and SGK3 kinase assays. Recombinant tagged kinases were incubated in kinase buffer containing γ32P-ATP, for 30 min at 30˚C, alone or with the indicated Myc-tagged recombinant TBC1D1 and TBC1D4 substrates. For the WNK1 kinase assay, recombinant OSR1 (HIS-OSR1), a

previously described physiological substrate (Zagórska et al. 2007), was used as a positive control. After incubation with the radiolabeled ATP, the samples were separated by SDS-PAGE and transferred to PVDF blotting membranes. Incorporated radioactive γ32P-phosphate was detected by exposing the membranes for 8 or 24 h to X-ray films (Kinase assay). Subsequently, the amounts of recombinant proteins were documented by WB using anti-GST, anti-Myc and anti-HIS, and then reprobed with anti-p-TBC1D4(Thr642) for the WNK1 assay. Note that all studied kinases autophosphorylate and phosphorylated the substrates TBC1D1 and TBC1D4, whereas the Rab-GAPs alone did not autophosphorylate.

## 3.3 Determination of the specific phosphosites of each kinase in TBC1D1 and TBC1D4

Having established the *in vitro* phosphorylation of both TBC1D1 and TBC1D4 proteins by the above studied kinases, we next determined the specific phosphorylated residues in either of these Rab-GAPs. For AKT, several sites of phosphorylation of these TBC1Ds were already known (Kane et al. 2002; Kramer et al. 2006; Zaid et al. 2008), however the less studied kinases WNK1, SGK1 and SGK3 could act either on the same or on unique phosphosites. Phosphorylation sites were determined by mass spectrometry (MS) of the kinase assays (see 3.2) repeated under non-radioactive conditions (see materials and methods) and the obtained results are summarized in the following tables.

Table 3.1 – Summary table of the *in vitro* phosphorylation sites in human TBC1D1 obtained through MS analysis of the *in vitro* kinase assays (S = serine; T = threonine)

| | ***Human TBC1D1 identified phosphosites*** | | | | |
|---|---|---|---|---|---|
| ***AKT1*** | S237 | | | S585 | T596 |
| ***WNK1*** | S237 | | S565 | S585 | |
| ***SGK1*** | S237 | T505 | | | T596 |
| ***SGK3*** | | | | | T596 |

Table 3.2 – Summary table of the *in vitro* phosphorylation sites in human TBC1D4 obtained through MS analysis of the *in vitro* kinase assays.

| | ***Human TBC1D4 identified phosphosites*** | | | | | | | |
|---|---|---|---|---|---|---|---|---|
| ***AKT1*** | T568 | S588 | S609 | | | S725 | S750 | T752 |
| ***WNK1*** | | S588 | | | S704 | | | |
| ***SGK1*** | | S588 | | S673 | S704 | | | T752 |
| ***SGK3*** | T568 | S588 | | | S704 | | | |

The data shown in Tables 3.1 and 3.2 presents some already identified phosphosites for AKT1, such as serine 237 (S237) and threonine 596 (T596) from TBC1D1 (Cheng et al. 2014), and serine 588 (S588) from TBC1D4 (Kane et al. 2002). However, threonine 642, which is a known AKT-specific TBC1D4 phosphosite that we detected by WB in Figure 3.2 was not identified. Interestingly, two new TBC1D1 phosphosites were identified: threonine 505 (T505) as a SGK1-specific phosphosite, and serine 565 (S565) as a WNK1-specific phosphosite (Table 3.1). In the case of TBC1D4 (Table 3.2), we were able to identify serine 704 (S704) as a new non-AKT regulated phosphosite, which can be phosphorylated by kinases WNK1, SGK1 and SGK3. Additional new unique phosphosites were identified: serine 609 (S609) and serine 725 (S725), both specifically phosphorylated by AKT1, and serine 673 (S673) only phosphorylated by SGK1.

In order to study unique and previously unrecognized phosphosites for their relevance in the activity of these Rab-GAPs, we selected for further studies threonine 505 (T505) and serine 565 (S565) in TBC1D1, and serine 704 (S704) in TBC1D4.

## 3.4 Study of SGK1-specific phosphosite Thr505 in TBC1D1 as a GLUT1 PM expression modulator

The specific SGK1 phosphorylated TBC1D1 residue Thr505 was mutated by site-directed mutagenesis into a phosphomimetic aspartate (D) or an unphosphorylatable alanine (A) residue. The resulting constructs were transfected into HEK293 cells and the cell surface proteins labelled by biotinylation. Cells were lysed and the amount of GLUT1 present in whole-cell lysates or at the PM quantified by WB.

The constructs were transfected as depicted in Figure 3.3 and neither the unphosphorylatable TBC1D1 mutant (T505A) nor the phosphomimetic mutant T505D did not cause any significant change in the expression of GLUT1 at PM. According to these results, although TBC1D1 Thr505 residue is specifically phosphorylated *in vitro* by SGK1 in kinase assays (as demonstrated in 3.2 and 3.3), does not seem to play a role in GLUT1 PM regulation.

Considering that SGK1 was described to regulate GLUT1 by Palmada and colleagues (2006), we complemented these studies by testing the effect of a constitutively active (SGK1 CA) and kinase-dead (SGK1 KD) mutants of this kinase. The results depicted in Figure 3.3 revealed that SGK1 KD did not cause a decrease in the amount of GLUT1 present at PM, however, the constitutively active mutant of SGK1 caused an increase in GLUT1. The results confirm published data that SGK1 plays a role in GLUT1 PM expression. The fact that expression of the kinase-dead mutant did not cause any decrease in PM GLUT1 expression suggests a compensation by other kinases when SGK1 is inactive and unable to phosphorylate the TBC1Ds. For comparison, we also used kinase-dead and constitutively active mutants of AKT1, since AKT is the main regulator of these TBC1Ds (Kane et al. 2002; Sano et al. 2003). As expected, both mutants of AKT modulated the expression of GLUT1: AKT KD led to a decrease in GLUT1 PM expression, whereas constitutively active AKT promoted the PM localization.

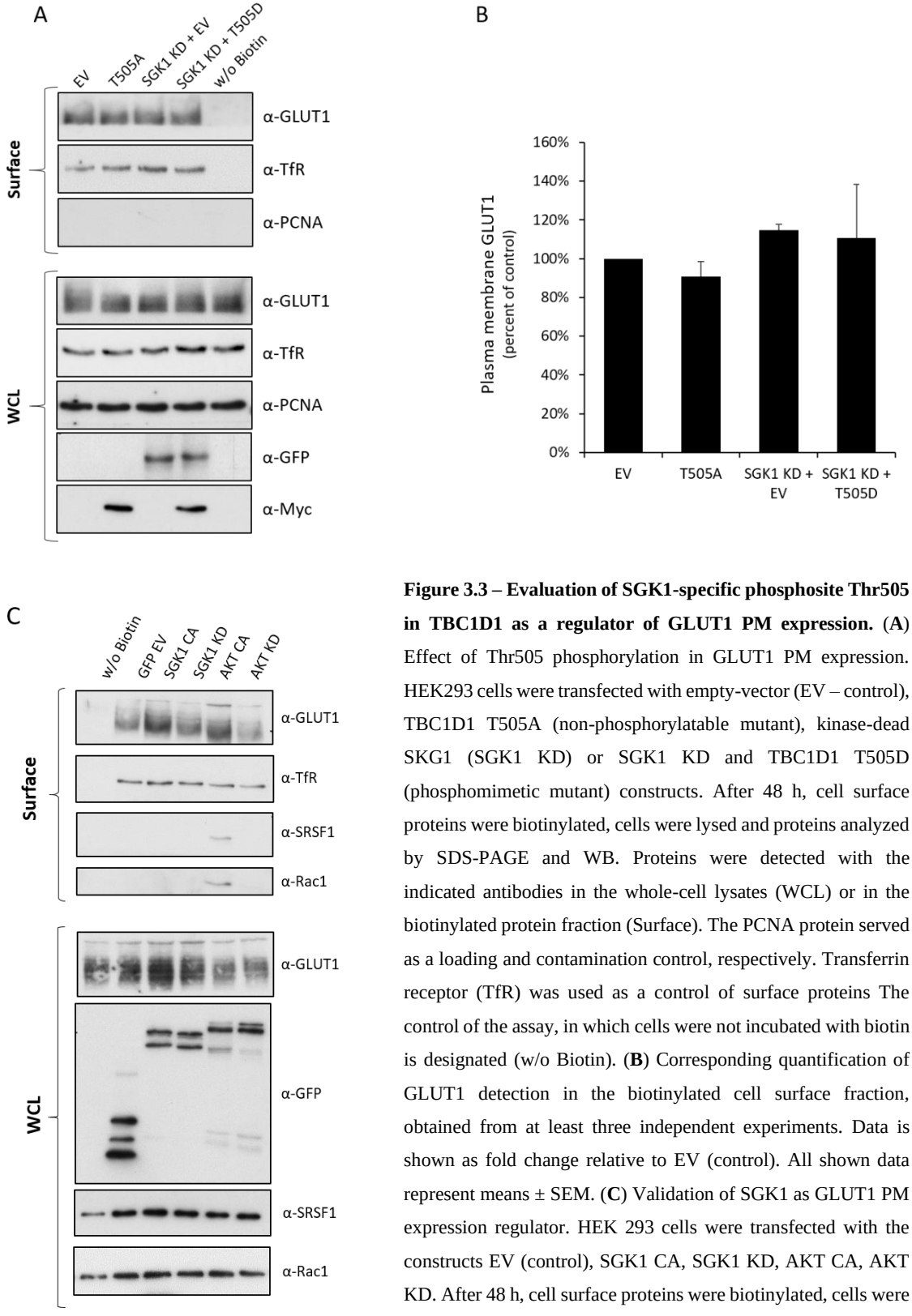


**Figure 3.3 – Evaluation of SGK1-specific phosphosite Thr505 in TBC1D1 as a regulator of GLUT1 PM expression.** (**A**) Effect of Thr505 phosphorylation in GLUT1 PM expression. HEK293 cells were transfected with empty-vector (EV – control), TBC1D1 T505A (non-phosphorylatable mutant), kinase-dead SKG1 (SGK1 KD) or SGK1 KD and TBC1D1 T505D (phosphomimetic mutant) constructs. After 48 h, cell surface proteins were biotinylated, cells were lysed and proteins analyzed by SDS-PAGE and WB. Proteins were detected with the indicated antibodies in the whole-cell lysates (WCL) or in the biotinylated protein fraction (Surface). The PCNA protein served as a loading and contamination control, respectively. Transferrin receptor (TfR) was used as a control of surface proteins The control of the assay, in which cells were not incubated with biotin is designated (w/o Biotin). (**B**) Corresponding quantification of GLUT1 detection in the biotinylated cell surface fraction, obtained from at least three independent experiments. Data is shown as fold change relative to EV (control). All shown data represent means ± SEM. (**C**) Validation of SGK1 as GLUT1 PM expression regulator. HEK 293 cells were transfected with the constructs EV (control), SGK1 CA, SGK1 KD, AKT CA, AKT KD. After 48 h, cell surface proteins were biotinylated, cells were lysed and proteins analyzed by SDS-PAGE and WB. Proteins were detected with the indicated antibodies in the whole-cell lysates (WCL) or in the biotinylated protein fraction (Surface). The nuclear SRSF1 and cytoplasmic RAC1 proteins served as contamination controls.

## 3.5 Validation of the WNK1-regulated phosphosites as modulators of PM expression of GLUT1

Following identification of the WNK1-specific phosphosites TBC1D1-Ser565 and TBC1D4-Ser704, site-directed mutagenesis was used to introduce the respective phosphomimetic aspartate (D) or unphosphorylatable alanine (A) codons. As described above, constructs were transfected into HEK293 cells, followed by biotinylation of cell surface proteins and WB. The mutants for both residues were analyzed under the following conditions: unphosphorylatable mutant (A) alone (expected to decrease the amount of PM GLUT1 expression), WNK1 depletion (positive control for decreased PM GLUT1 expression, see Figure 3.1), and double transfection with siWNK1 and the phosphomimetic mutant (expected to rescue the loss PM GLUT1 expression induced by WNK1 depletion alone).

### 3.5.1 Validation of the TBC1D1 Ser565 phosphosite

When HEK293 cells were transfected with a non-phosphorylatable TBC1D1 mutant S565A, a decrease in GLUT1 PM expression was observed (Figure 3.4). This effect was comparable to the one caused by the depletion of WNK1, used as a positive control. Importantly, the inhibitory effect of siWNK1 on GLUT1 PM expression was abrogated by the transfection of the phosphomimetic mutant TBC1D1 S565D. Thus, TBC1D1 Ser565 was clearly identified as an important phosphosite in the regulation of this Rab-GAP protein and in the consequent GLUT1 PM expression regulation.

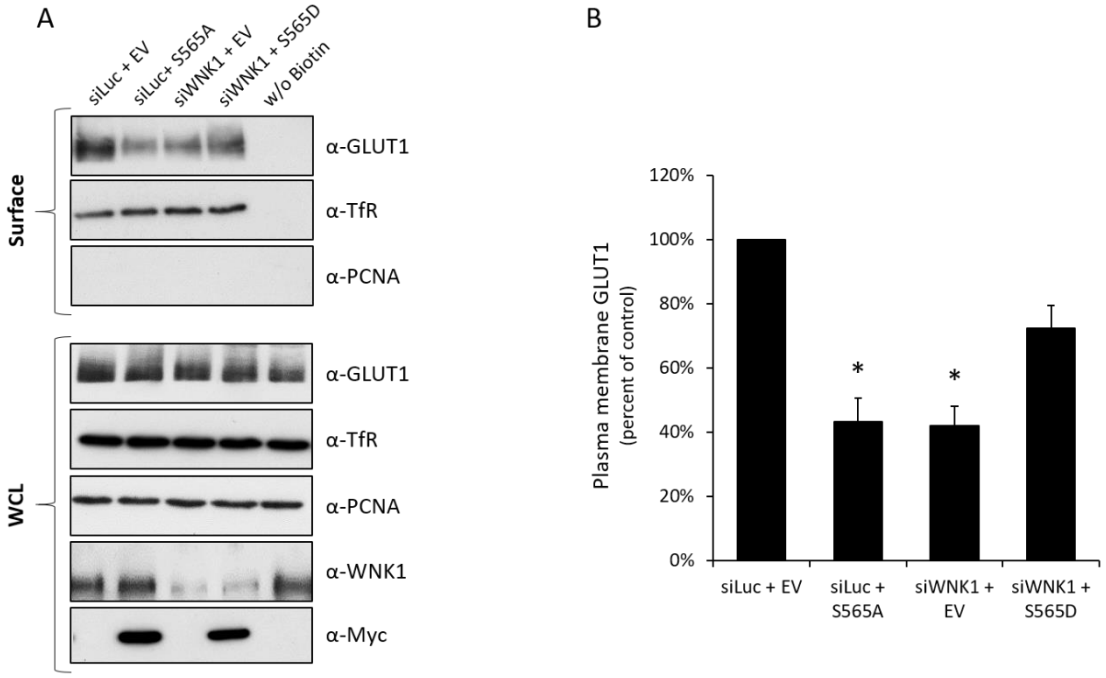


**Figure 3.4 – Validation of WNK1 phosphosite Ser565 in TBC1D1 as a regulator of GLUT1 PM expression.** HEK 293 cells were transfected with siLuc and empty-vector (EV) as control, siLuc and TBC1D1 S565A (non-phosphorylatable mutant), siWNK1 and EV or siWNK1 and TBC1D1 S565D (phosphomimetic mutant). After 48 h, cell surface proteins were biotinylated, cells were lysed and proteins analyzed by SDS-PAGE and WB. (**A**) Detection of the indicated proteins in the whole-cell lysates (WCL) or in the biotinylated protein fraction (Surface). The control of the assay, in which cells were not incubated with biotin is designated (w/o biotin). The PCNA protein served as a loading and contamination control, respectively. Transferrin receptor (TfR) was used as a surface protein control. (**B**) Corresponding quantification of GLUT1 detection in the biotinylated cell surface fraction, obtained from at least three independent experiments. Data is shown as fold change relative to siLuc + EV (control). All shown data represent means ± SEM * $P < 0.05$ compared to control.

### 3.5.2 Validation of the TBC1D4 Ser704 phosphosite

Under the same experimental conditions as above, TBC1D4 Ser704 mutants were transfected. As shown in Figure 3.5 the S704A (non-phosphorylatable) mutant decreased PM GLUT1 expression, whereas the phosphomimetic mutant TBC1D4 S704D was able to counteract the effect of WNK1 depletion by restoring and even increasing the levels of GLUT1 at the PM. Therefore, TBC1D4 Ser704 was also validated as a relevant phosphosite of this Rab-GAP, playing a role in regulation of GLUT1 PM expression levels.

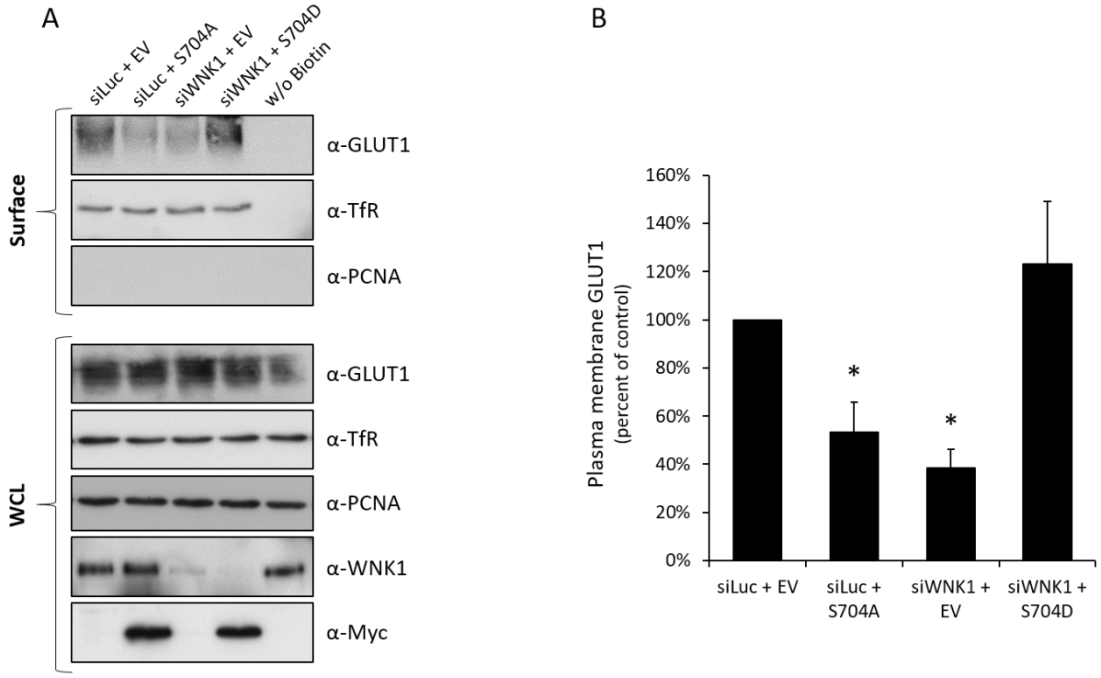


**Figure 3.5 – Validation of WNK1 phosphosite Ser704 in TBC1D4 as a regulator of GLUT1 PM expression.** HEK 293 cells were transfected with the constructs siLuc and empty-vector (EV – control), siLuc and TBC1D4 S704A (non-phosphorylatable mutant), siWNK1 and EV or siWNK1 and TBC1D4 S704D (phosphomimetic mutant). After the treatments described above, cell surface proteins were biotinylated, cells were lysed and proteins analyzed by SDS-PAGE and WB. (**A**) Detection of the indicated proteins in the whole-cell lysates (WCL) or in the biotinylated protein fraction (Surface). Note the successful downregulation of WNK1 expression. The lysate corresponding to without biotin (w/o Biotin) is a control of the assay, in which cells were not incubated with biotin. The PCNA protein served as a loading and contamination control, respectively. Transferrin receptor (TfR) was used as a control of surface proteins. (**B**) Corresponding quantification of GLUT1 detection in the biotinylated cell surface fraction, obtained from at least three independent experiments. Data is shown as fold change relative to siLuc (control). All shown data represent means ± SEM, ***** $P < 0.05$ compared to control.

## 3.6 Determination of WNK1 interactome

Following the validation of WNK1 as a modulator of GLUT1 localization by phosphorylation of TBC1Ds, we set-out to identify WNK1-interacting proteins which participate in this process. To do so, we isolated the WNK1 interactome by co-immunoprecipitation in the presence of crosslinkers in order to stabilize proteins associated with WNK1. For this, HEK293 cells were incubated with DSP (short spacer) and SPDP (long spacer), lysed and incubated with a specific antibody against WNK1 previously crosslinked to agarose beads (see Material and Methods). The recovered proteins were first analyzed by SDS-PAGE followed by MS-compatible silver staining

(Mortz et al. 2001). Noticeably, a particular band profile was observed for each condition. These profiles were reproducible between experimental replicates (Figure 3.6) and therefore, the whole samples from each of the three individual assays were run in gels for 1 cm, excised as one gel slice and then sent to MS analysis.

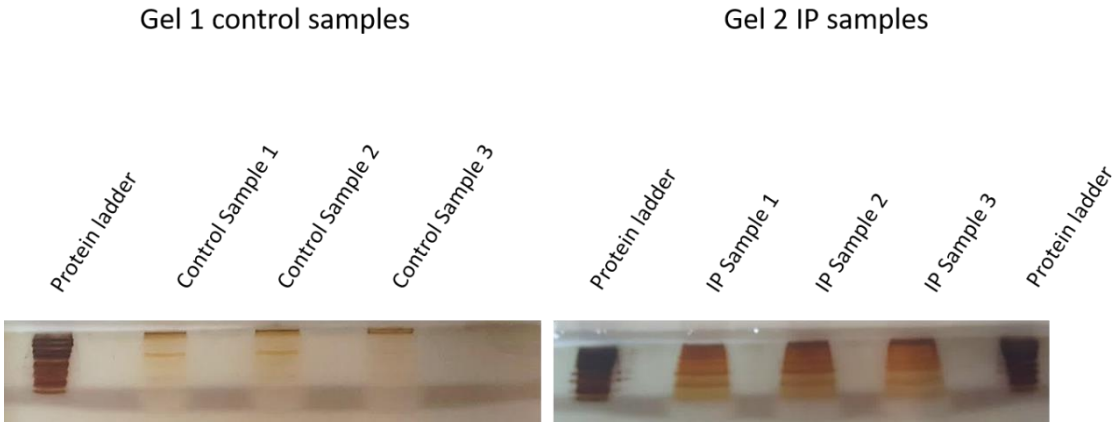


**Figure 3.6 – Protein patterns detected in WNK1 co-immunoprecipitation.** Band profiles of the WNK1 co-precipitates from each experimental condition from three different assays. HEK293 cells were crosslinked with DSP and SPDP lysed and WNK1 was specifically pulled-down with anti-WNK1 antibody crosslinked to agarose beads with PFA 4%. Pulled-down lysates were de-crosslinked with 100 mM DTT, separated on a 9% (w/v) SDS-PAGE gel, and silver stained before sending for MS analysis. Left panel: Control samples. Right panel: Co-immunoprecipitation (IP) samples.

## 3.7 Bioinformatic analysis of MS data highlighted candidate interactors

Qualitative nanoLC MS/MS analysis of our samples generated a set of data in which each MS spectra protein hit was characterized by a protein confidence score (PCS) given by the SCIEX proprietary ProteinPilot™ Software. For PCS >1.3, the confidence in the identification of that particular peptide is equal or higher than 95%. Given that all the experiments were performed in triplicate, we created an algorithm to generate a combined confidence score (CCS), producing five additional integrated confidence levels for the proteins detected among the different replicates: level 5 are proteins detected with PCS ≥ 1.3 in more than one replicate and not in the controls; level 4 are proteins detected in one replicate with an PCS ≥ 1.3 and not in the controls; level 3 are proteins detected in more replicates than in controls, and with an average PCS higher than their respective controls; level 2 are proteins detected in more replicates than in controls, and with an average PCS lower than their respective controls; and level 1 are proteins detected in the same number of replicates and controls, with a replicate average PCS higher than the

corresponding controls. Altogether, we found 825 WNK1 putative interactors (Figure 3.7A), which were sorted through CCS and resulted in 391 proteins with a CCS of 5, 15 of those proteins had already protein-protein interactions described in public databases (Figure 3.7C), 262 were considered to be CCS level 4, 130 protein in CCS level 3, 18 in level 2 and 24 in the lowest confidence level 1 (Figure 3.7B) (see also Supplemental Table).

Gene ontology (GO)-based functional annotation analysis of these 825 hit proteins using DAVID (Database for Annotation, Visualization and Integrated Discovery at https://david.ncifcrf.gov/) revealed 155 annotation clusters and the top three GO-term clusters were cell adhesion, ribosomal protein and splicing/mRNA processing. Although we were interested in hits related with glucose metabolism, the first cluster related with this function was in position 46, associated with low significance of the hits. Considering that the low confidence proteins included in this analysis could introduce a bias, we performed a second analysis restricted to the 391 proteins classified with CCS level 5. The functional clustering revealed that cell adhesion and splicing/mRNA processing were maintained as the first and third clusters, respectively. Moreover, this analysis removed the ribosome related proteins from the second position of relevant clustering groups, which was substituted by actin-binding proteins, suggesting that ribosomal proteins were mainly associated with low CCS and thus were not further considered in this study. Again, the glucose metabolism-related proteins represented the $54^{th}$ cluster with no significant hit proteins from the corrected Benjamini adjusted *p*-value ($P < 0,05$). Hence, we started by analyzing hit proteins from the top three clustering groups cell adhesion, actin binding and splicing/mRNA processing, selecting targets for which suitable commercial antibodies were available.

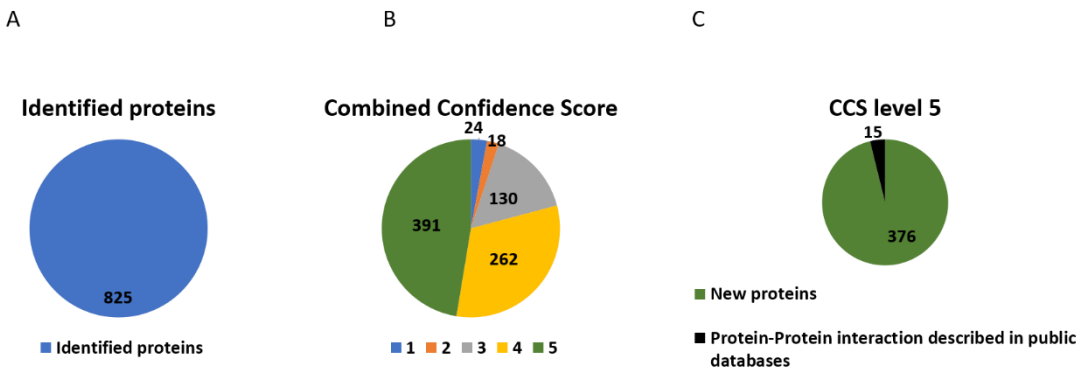


**Figure 3.7 – Proteins detected in WNK1 interactome** (**A**) Graph representing the number of WNK1 interactors detected by Qualitative nanoLC MS/MS analysis. (**B**) Graph representing the distribution of WNK1 interactors detected by combined confidence score (CCS). (**C**) Graph representing the number of WNK1 interactors detected with a high confidence score (CCS=5) and the number of already described protein-protein interactions in public databases.

## 3.8 Validation of candidate WNK1-interacting proteins

To proceed with the validation of putative WNK1 interactors, we selected proteins from the target list associated with the top three clustering groups cell adhesion, actin binding and splicing/mRNA processing (Table 3.3). To assess the robustness of the interaction between WNK1 and the selected targets, we prepared a pool of immunoprecipitated WNK1 and used specific antibodies to detect the target proteins by WB (Figure 3.8).

**Table 3.3 – Summary table of the tested candidate proteins and obtained bioinformatic CCS of MS identified WNK1 interactors.** UNIPROT is the accession number in the UniProt database (https://www.uniprot.org); name of the identified protein; cscore is the PCS in the control triplicates if applicable; tscore is the PCS of the IP triplicates if applicable; CCS is the confidence level conferred by the bioinformatic analysis described above (see 3.7); d2wnk is the calculated distance to WNK1 from protein-protein interactions described in public databases. Bioinformatic analysis performed by Francisco Pinto Faculty of Sciences, University of Lisbon.

| ***UNIPROT*** | ***NAME*** | ***cscore*** | ***tscore*** | ***CCS*** | ***d2wnk*** |
|---|---|---|---|---|---|
| Q9H4A3 | Serine/threonine-protein kinase WNK1 (WNK1) | | 43.79\|41.74\|22.93 | 5 | 0 |
| P63104 | 14-3-3 protein zeta/delta (YWHAZ) | | 10.77\|15.49\|10.05 | 5 | 1 |
| P62258 | 14-3-3 protein épsilon (YWHAE) | | 8.2\|9.94\|14.11 | 5 | 1 |
| P27348 | 14-3-3 protein theta (YWHAQ) | | 6.36\|10.27\|8 | 5 | 1 |
| P35222 | Catenin beta-1 (CTNNB1) | | 5.67\|2.17 | 5 | 1 |
| P31946 | 14-3-3 protein beta/alfa (YWHAB) | | 2.01\|6\|8.28 | 5 | 1 |
| Q07157 | Tight junction protein ZO-1 (TJP1) | | 34.83\|10.84 | 5 | 2 |
| P15311 | Ezrin (EZR) | | 14.67\|2.94\|2.9 | 5 | 2 |
| P26599 | Polypyrimidine tract-binding protein 1 (PTBP1) | | 7.33\|10.19\|8.89 | 5 | 2 |
| P12004 | Proliferating cell nuclear antigen (PCNA) | | 4.17\|7.93 | 5 | 2 |
| P63000 | Ras-related C3 botulinum toxin substrate 1 (RAC1) | | 2.36 | 4 | 2 |
| P29353 | REVERSED SHC-transforming protein 1 (SHC1) | | 1.59 | 4 | 2 |
| Q96SB4 | SRSF protein kinase 1 (SRPK1) | | 2 | 4 | 2 |
| Q07955 | Serine/arginine-rich splicing factor 1 (SRSF1) | 8.42 | 1.9\|7.79\|5.14 | 2 | 2 |

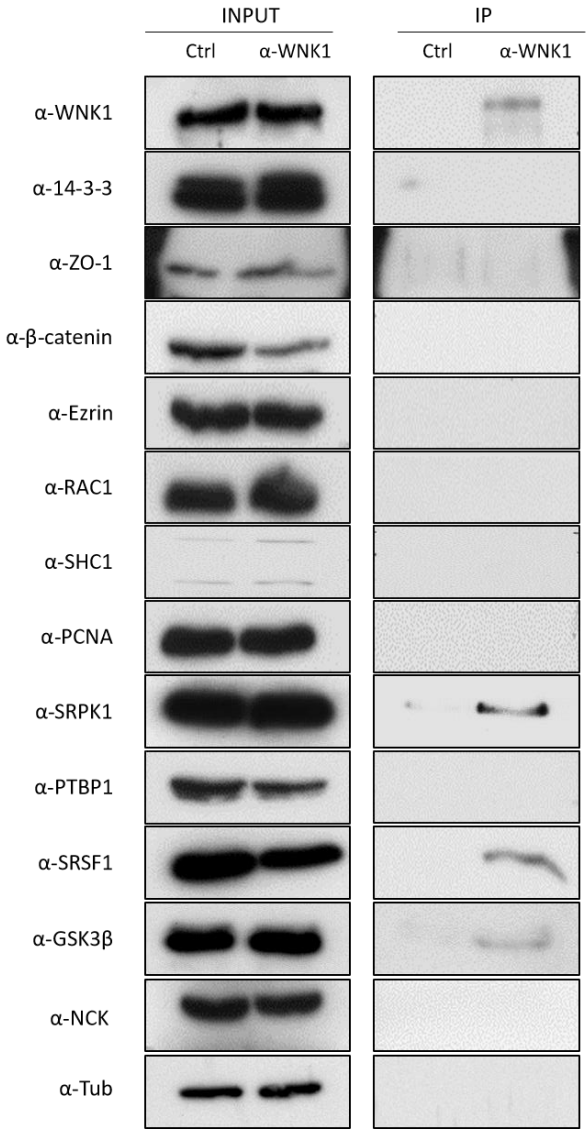


**Figure 3.8 – Validation of hit proteins interacting with WNK1 in HEK293 cells.** WB analysis of proteins co-immunoprecipitating with WNK1. HEK293 cells were seeded and after 48 h were incubated with a solution of the crosslinkers DSP (short spacer) and SPDP (long spacer) for 2 h in order to bind the network of proteins interacting with each other. After crosslink, WNK1 was immunoprecipitated with anti-WNK1 antibody crosslinked to agarose beads with PFA 4%. Pulled-down lysates were de-crosslinked with 100 mM DTT, separated on a 9% (w/v) SDS-PAGE gel and transferred to PVDF membranes followed by WB with the indicated antibodies. Note that GSK3β, SRPK1 and SRSF1 co-immunoprecipitated with WNK1 suggesting an interaction between these proteins in HEK293 cells. INPUT: whole-cell lysates; IP: Immunoprecipitation; Ctrl: without antibody.

According to the availability of specific antibodies we tested ZO-1 (Q07157) and β-catenin (P35222) from the cell adhesion cluster, ezrin (P15311), RAC1 (P63000) and SHC1 (P29353) from the actin binding group. Furthermore, we tested 14-3-3 proteins identified in multiple isoforms in the MS analysis (P63104, P62258, P27348 and P31946), which were described in one report to interact directly with WNK1 (Jin et al.

2004). In this case, a pan-14-3-3 antibody was used. Also, we used PCNA (P12004), a general signaling protein identified in the MS but not related to the selected clusters. None of the above-mentioned candidate proteins co-immunoprecipitated with WNK1 in HEK293 cells in the conditions tested. The fact that we have used crosslinking agents to stabilize the interactions of all the proteins with short and long spacers might have interfered with some interactions, this can explain why we did not identify previously described WNK1 interactors such as 14-3-3. Moreover, we used two proteins as negative controls, NCK (P16333) and tubulin (Q71U36), proteins that were not identified by MS. As expected, the proteins NCK and tubulin were not detected in the co-IP.

Considering the mRNA processing-related proteins, we tested SRPK1 (Q96SB4), SRSF1 (Q07955) and PTBP1 (P26599). Moreover, we decided to include as a positive control, the glycogen synthase kinase-3 beta (GSK3β) protein (P49841), an already described interactor of WNK1 (Sato and Shibuya 2018) that is related with both metabolism and mRNA processing (Gonçalves et al. 2014). As we can perceive in Figure 3.8, we confirmed that GSK3β, SRPK1 and SRSF1 co-immunoprecipitated with WNK1, in HEK293 cells.

## 3.9 Validation of a role for WNK1 in cell viability and proliferation of colon cancer cells

Together, the three WNK1-validated interactors, GSK3β, SRPK1 and SRSF1 are at first sight not related with glucose metabolism. However, these mRNA processing related proteins are profusely studied in the host lab and are known to be involved in the regulation of the expression of the splicing variant RAC1B that is required for survival and cell cycle progression in some colorectal cancer (CRC) cells (Matos and Jordan 2008; Gonçalves et al. 2009, 2014). So far, no evidence has been reported that WNK1 knockdown would have an effect on CRC cell viability and proliferation. We thus tested the effect of WNK1 depletion in several CRC models available in the host lab – SW480, DLD-1 and HT29 cell lines. To do so, we analyzed proliferation and cell viability markers such as Ki-67, cyclin-D1 and p21 by WB (Figure 3.9) and observed that HT29 was the cell line were WNK1 depletion had more pronounced effects after 48 h. In this cell line, WNK1 depletion promoted a decrease in Ki-67 and cyclin-D1 expression, which is associated with decreased cell-cycle progression, accompanied by an increase in p21 expression, related with cell-cycle arrest. Considering these results, we were able to select

HT29 as the CRC cell model to proceed our studies and identify in which way WNK1 is relevant for the proliferation and survival of this cell line.

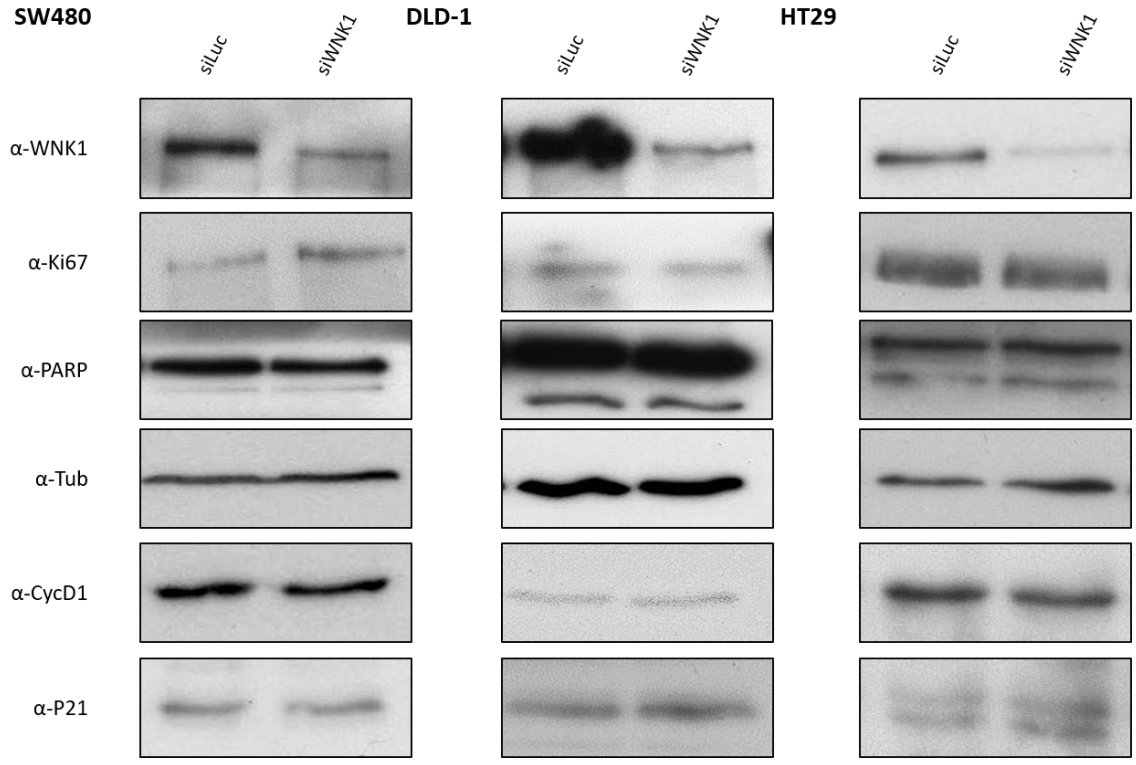


**Figure 3.9 – CRC cell model screening for cell viability and proliferation markers upon WNK1 depletion.** SW480, DLD-1 and HT29 cells were transfected with either siLuc (control) or siWNK1 for 48 h. WB analysis of cell-cycle markers after WNK1 depletion. Note the efficient downregulation of WNK1.

## 3.10 WNK1 depletion leads to a decrease in RAC1B expression in HT29 cells

Previous studies from the host lab have shown that HT29 cells rely on RAC1B expression to sustain cell-cycle progression, survival and proliferation (Matos and Jordan 2008; Matos et al. 2008). Considering the observed decrease in cell-cycle progression and survival upon WNK1 depletion in HT29 cells, we hypothesized a relationship between WNK1 and RAC1B expression. To test this hypothesis, we performed WNK1 depletion in HT29 cells and studied its effect on RAC1B expression levels.

In Figure 3.10, a significant decrease in RAC1B expression (around 40% – Figure 3.10C) can be observed in HT29 cells upon WNK1 depletion, the efficacy of which reached about 85% when compared to control cells (siLuc) (Figure 3.10B). Considering that WNK1 affected expression levels of RAC1B and of typical cell-cycle arrest and cell

death markers, and that WNK1 interacted with RAC1B expression regulators, we intend to understand in which way, these events are related.

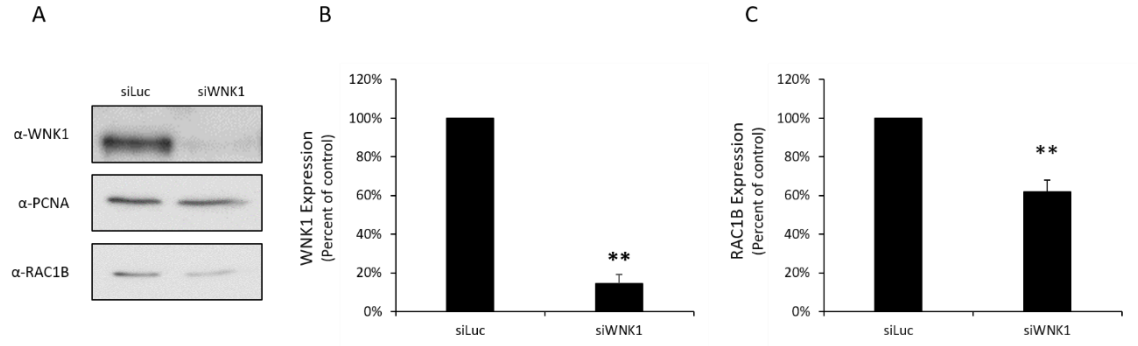


**Figure 3.10 – WNK1 depletion leads to a decrease in RAC1B expression in HT29 cells.** (**A**) WB of a representative WNK1 depletion experiment and associated RAC1B downregulation. (**B**) Assessment of WNK1 siRNA-mediated knockdown efficiency. (**C**) RAC1B expression upon WNK1 depletion in HT29 cells. Data is shown as fold change relative to siLuc (control). All shown data represent means ± SEM, $**P < 0.01$.

## 3.11 Validation of interaction between WNK1 and mRNA splicing-related protein hits in HT29 cells

After identifying the effect of WNK1 on RAC1B levels in HT29 cells, we intended to validate the WNK1-interacting proteins GSK3β, SRPK1 and SRSF1 in this cell line because they were previously shown to regulate RAC1B levels. In particular, Gonçalves et al. (2014) reported that the two protein kinases GSK3β and SRPK1 act upstream of the splicing factor SRSF1 and are required to sustain RAC1B levels in HT29 cells (Gonçalves et al. 2014). We performed the WNK1 IP protocol in HT29 cells using crosslinkers as described above (see 3.6) and used protein-specific antibodies to detect their presence in the co-precipitates by WB. As depicted in Figure 3.11, we were able to validate that the three candidate interacting proteins, GSK3β, SRPK1 and SRSF1, co-immunoprecipitated with WNK1.

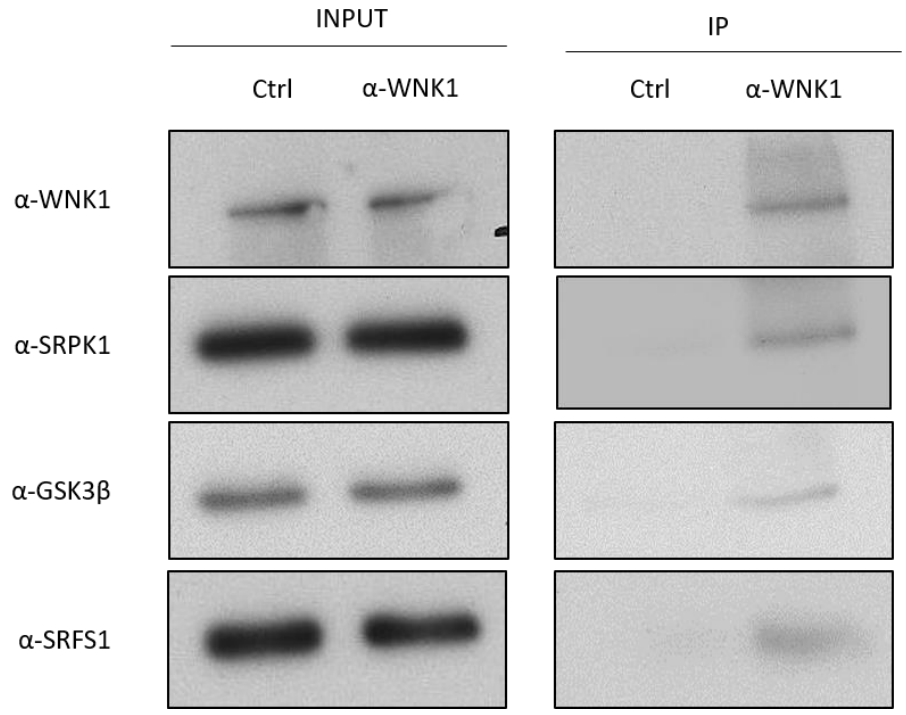


**Figure 3.11 – Validation of hit proteins interacting with WNK1 in HT29 cells.** WB analysis of proteins co-immunoprecipitating with WNK1. HT29 cells were seeded and after 48 h were incubated with a solution of the crosslinkers DSP (short spacer) and SPDP (long spacer) for 2 h, in order to bind the network of proteins interacting with each other. After crosslink, WNK1 was immunoprecipitated with anti-WNK1 antibody crosslinked to agarose beads with PFA 4%. Pulled-down lysates were de-crosslinked with 100 mM DTT, proteins then separated on a 9% (w/v) SDS-PAGE gel and transferred to PVDF membranes followed by WB with the indicated antibodies. Note that GSK3β, SRPK1 and SRSF1 co-immunoprecipitated with WNK1 suggesting an interaction between these proteins in colorectal cancer HT29 cells. INPUT: whole-cell lysates; IP: Immunoprecipitation; Ctrl: without antibody.

## 3.12 Ibuprofen treatment prevents the interaction of WNK1 with GSK3β and SRPK1

Previous studies from the host lab had shown that the non-steroidal, anti-inflammatory drug ibuprofen (IBU), causes a decrease in RAC1B expression in cultured HT29 colorectal tumor cells and in an *in vivo* mouse model (Matos et al. 2013).

To understand if IBU has any effect on the interaction between WNK1 and GSK3β, SRPK1 or SRSF1, we performed a co-immunoprecipitation experiment of endogenous WNK1, without crosslinking agents, in HT29 cells cultured for 48 h in the presence of IBU (500 µM) or DMSO (vehicle). The results presented in Figure 3.12 show that IBU treatment caused a decrease of around 65% and 50%, for co-immunoprecipitated SRPK1 and GSK3β, respectively, although we observed it had no effect on the amount

of WNK1 captured in the IP. The fact that we were able to detect GSK3β and SRPK1 co-immunoprecipitating with WNK1 even in the absence of crosslinking agents, supports the strength and specificity of this interaction. Whereas for SRSF1, it was not possible to detect co-precipitation, in agreement with the CCS classification (see table 3.3 and section 3.7), indicating that the interaction is weaker or the protein merely associated to a WNK1-multi-protein complex.

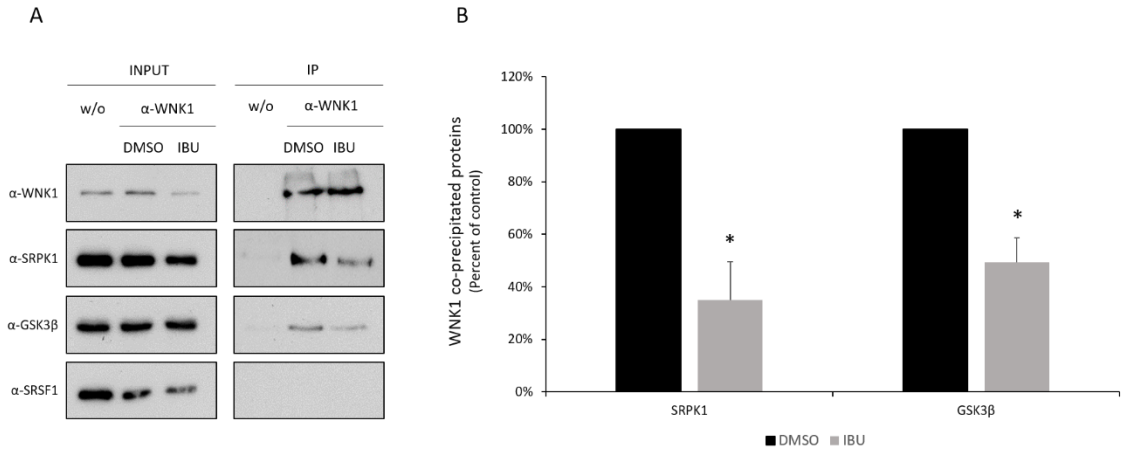


**Figure 3.12 – Ibuprofen treatment interferes with the interaction of WNK1 with GSK3β and SRPK1.** HT29 cells were incubated for 48 h with either DMSO (control) or 500 µM IBU. WNK1 was immunoprecipitated with anti-WNK1 antibody crosslinked to agarose beads with PFA 4%. Pulled-down lysates were separated on a 9% (w/v) SDS-PAGE gel and transferred to PVDF membranes. (**A**) WB analysis of proteins co-immunoprecipitating with WNK1. Co-precipitated proteins were identified with the indicated antibodies. Note that in the absence of crosslinkers SRSF1 no longer co-immunoprecipitated with WNK1. (**B**) Quantitative analysis of the WB shown in (A) of the amount of GSK3β and SRPK1 co-immunoprecipitated with WNK1 in three independent experiments. Note that GSK3β and SRPK1 co-immunoprecipitated with WNK1 in control conditions and that the amount of co-precipitated GSK3β and SPRK1 decreased in IBU-treated cells. All shown data represent means ± SEM.: $*P < 0.05$. INPUT: whole-cell lysates; IP: Immunoprecipitation; w/o: without antibody.

## 3.13 The effect of WNK1 on RAC1B levels involves GSK3β inhibition by Ser9 phosphorylation

In addition to identifying that the two protein kinases GSK3β and SRPK1 were required to sustain RAC1B levels (Gonçalves et al. 2014), work from the host lab revealed that IBU treatment of HT29 cells led to an increase in the inhibitory phosphorylation of GSK3β that occurs at the N-terminal Ser9 (unpublished data). When phosphorylated

GSK3β N-terminus acts as a pseudo-substrate, occupying the same phosphate binding site used by primed substrates, blocking GSK3β kinase activity (Frame et al. 2001).

Considering the results described above on the role of WNK1 depletion in RAC1B downregulation (see 3.10) and in the formation of a complex with GSK3β (see 3.12), we tested if the presence of WNK1 might protect GSK3β from being phosphorylated at Ser9. For this, we compared three parallel conditions known to decrease RAC1B expression (IBU treatment, WNK1 depletion, and SRPK1 depletion) and tested for their association with Ser9 phosphorylation in GSK3β. For this, HT29 cells were transfected with siLuc, siWNK1 or siSRPK1 and treated with DMSO. As a positive control, cells were transfected with siLuc and treated with IBU (500 µM). After 48 h, WB analysis of whole-cell lysates was performed to document siRNA efficacies and the effects on RAC1B expression and GSK3β Ser9 phosphorylation (Figure 3.13A). In Figure 3.13B we can observe that all three conditions led to a significant RAC1B downregulation: 40% for IBU treatment, 46% reduction for WNK1 depletion, and 44% for SRPK1 depletion. When evaluating Ser9 phosphorylation, we observed a significant 80% and 98% increase for IBU treatment and WNK1 depletion, respectively. In contrast, for SRPK1 depletion we observed a slight but statistically not significant increase, which is in agreement with previous data suggesting that SRPK1 acts downstream of GSK3β in this signaling pathway (Gonçalves et al. 2014).

Considering these results, we can suggest that in the presence of WNK1, a protein complex is formed with GSK3β, which prevents GSK3β Ser9 phosphorylation. Upon depletion of WNK1 or complex disruption by ibuprofen treatment, this inhibitory phosphorylation increases and correlates with reduced RAC1B expression.

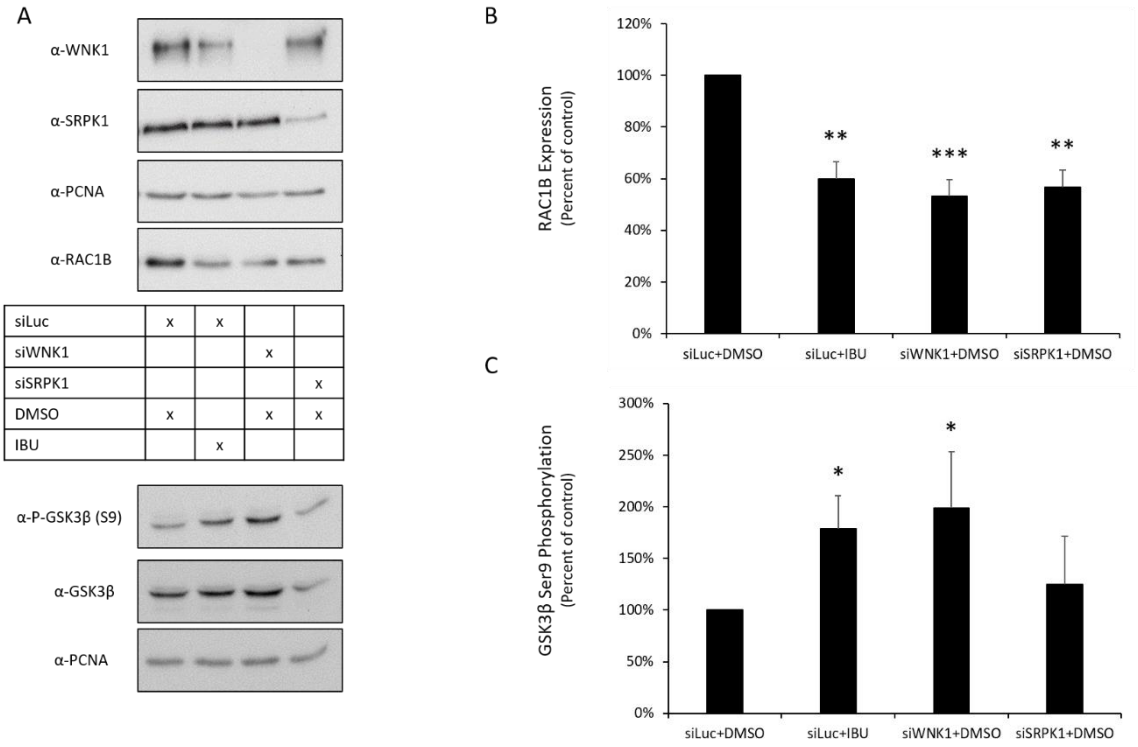


**Figure 3.13 – WNK1 depletion or IBU treatment lead to RAC1B downregulation and are associated with GSK3β Ser9 phosphorylation.** HT29 cells were transfected with a control siLuc, treated with either DMSO (control) or IBU (500 μM), siWNK1 or siSRPK1 both treated with DMSO for 48h. As a positive control for RAC1B downregulation and GSK3β Ser9 phosphorylation siLuc-transfected cells were treated with 500 μM IBU. (**A**) Representative WB of whole-cell lysates with the indicated antibodies. Note the effective depletion of WNK1 and SRPK1 and the effectiveness of IBU positive control. (**B-C**) Quantification of the WB analysis of RAC1B (**B**) and p-GSK3β Ser9 (**C**) shown in (**A**). Bar plots represent protein band intensity quantification, normalized to siLuc+DMSO. Shown is data from at least three independent experiments. All shown data represent means ± SEM, **P* < 0.05, ***P* < 0.01, ****P* < 0.001.

## 3.14 AKT1 depletion abolishes the WNK1 depleted and IBU treatment induced Ser9 phosphorylation in GSK3β

One of the kinases known to inactivate GSK3β through phosphorylation of Ser9 is AKT1 (Cross et al., 1995). In order to understand if the increment in Ser9 phosphorylation observed above (see 3.13) was dependent on AKT1 activity, we cultured HT29 cells and performed WNK1 depletion or IBU treatment in the absence or presence of siRNA-mediated depletion of AKT1.

The results depicted in Figure 3.14 show that Ser9 phosphorylation increases significantly with IBU treatment (Figure 3.14A) and WNK1 depletion (Figure 3.14C) but this increase is lost in both conditions upon AKT1 depletion. This result indicates AKT1

as an important regulator of GSK3β phosphorylation at Ser9 whenever it is not in a protein complex with WNK1.

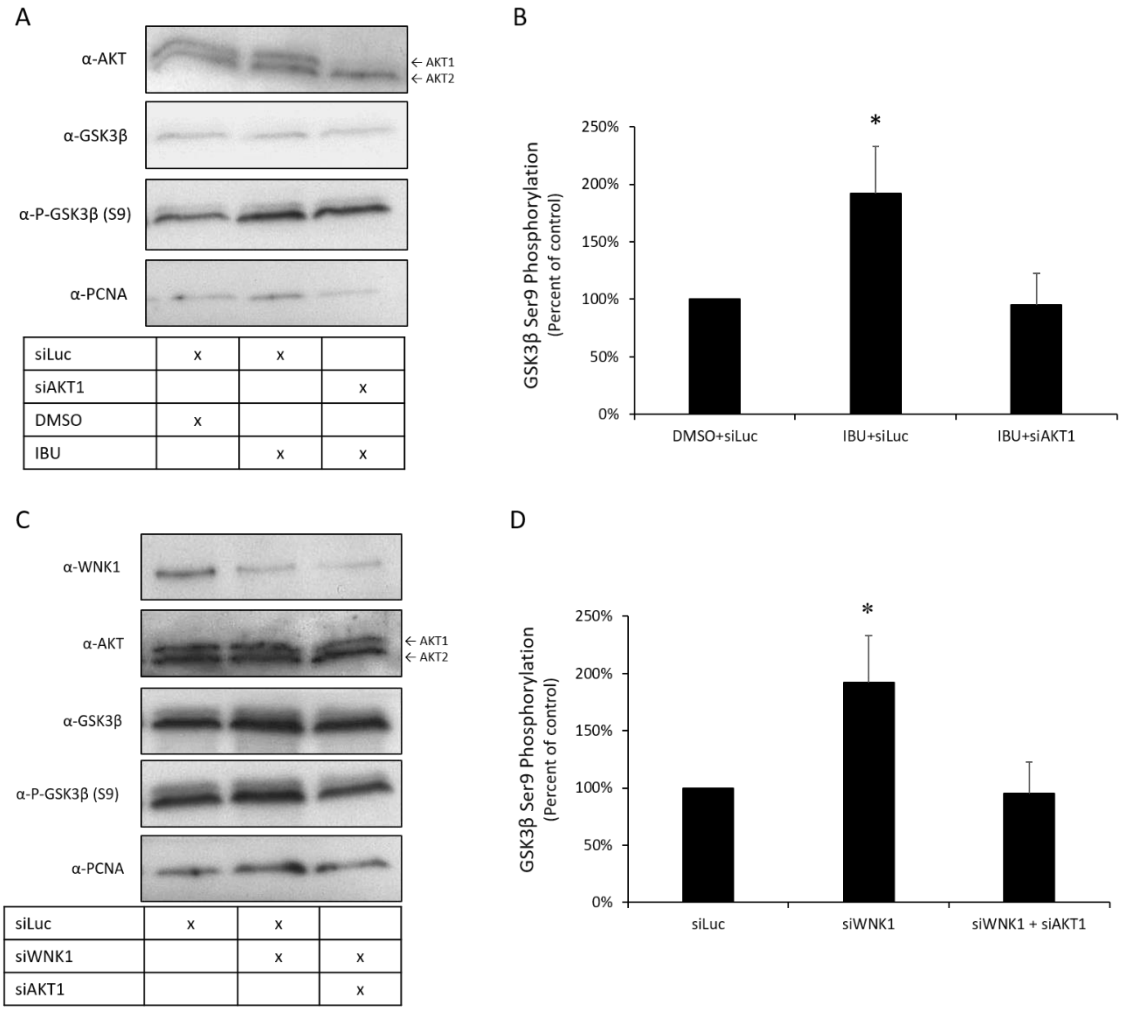


**Figure 3.14 – AKT1 depletion abolishes GSK3β phosphorylation at Ser9 induced by either WNK1 depletion or IBU treatment** (**A-B**) HT29 cells were transfected with siLuc or siAKT1 and treated with either DMSO (control) or IBU (500 µM) for 48 h. (**C-D**) HT29 cells were transfected with siLuc (control), siWNK1 + siLuc and siWNK1+siAKT1 for 48h. (**A**) and (**C**) show representative WB of whole-cell lysates and (**B**) and (**D**) the corresponding bar plots of band intensity quantification, normalized to control conditions. Shown is data from at least three independent experiments. All shown data represent means ± SEM.: $*P < 0.05$.

## 3.15 WNK1 depletion and IBU treatment prevents SRPK1 and SRSF1 translocation to the nucleus in a GSK3β-dependent pathway

Previous studies on RAC1B expression regulation indicated SRSF1 as an enhancer, stimulating inclusion of exon 3b in the RAC1 pre-mRNA, during the splicing process (Gonçalves et al. 2009). Additionally, it is known that SRPK1 knockdown or

inhibition of its catalytic activity reduced phosphorylation and subsequent translocation of SRSF1 to the nucleus, causing a decrease in RAC1B expression (Gonçalves et al. 2014).

Considering our previous results and the observed downregulation of RAC1B expression upon IBU treatment or siRNA-mediated depletion of WNK1 (see 3.10 and 3.13), we hypothesized that GSK3β inhibition through Ser9 phosphorylation could be involved in SRPK1 activation, consequent SRSF1 phosphorylation and RAC1B expression. To test this hypothesis, we started by evaluating the effect of WNK1 depletion and IBU treatment on the subcellular localization of SRPK1 and SRSF1 by confocal immunofluorescence microscopy.

In Figure 3.15 we can observe that both SRSF1 and SRPK1 are present in the nucleus in control conditions and undergo a decrease in nuclear localization, when HT29 cells are treated with IBU. Region of interest (ROI) graphical analysis of the microscopic images clearly shows the co-localization of SRSF1 or SRPK1 (both labelled in green) with nuclei (blue DAPI signal) in control conditions (DMSO + EV). Upon IBU treatment the pixel intensities of ROI indicate the loss of green signal for both SRSF1 and SRPK1, that co-localizes with blue signal. The same loss of co-localization of green (SRSF1 or SRPK1) and blue (DAPI) pixel intensities is observed upon WNK1 depletion in HT29 cells (Figure 3.16). To understand if these effects are dependent on GSK3β inhibition, we repeated the above experiments with cells co-transfected with a non-phosphorylatable mutant of GSK3β [HA-GSK3β (S9A)], that is not subjected to inhibition by phosphorylation, performing as a constitutively active variant (Stambolic and Woodgett 1994). Interestingly, the co-transfection of HA-GSK3β (S9A) reverted the effect observed in both treatments, as we can perceive in ROI graphical analysis (Figure 3.15 and 3.16). Thus, cells presenting HA (red) signal show co-localization of green (SRSF1 or SRPK1) and blue (DAPI), while in cells without HA-GSK3β (S9A) expression, SRSF1 orSRPK1 do not co-localize with the nucleus.

These data indicates GSK3β as a key protein required upstream of SRPK1 and SRSF1 localization and function. Thus, we conclude that WNK1 protects GSK3β from being inactivated by phosphorylation, allowing for increased RAC1B splicing and consequent cancer cell survival.

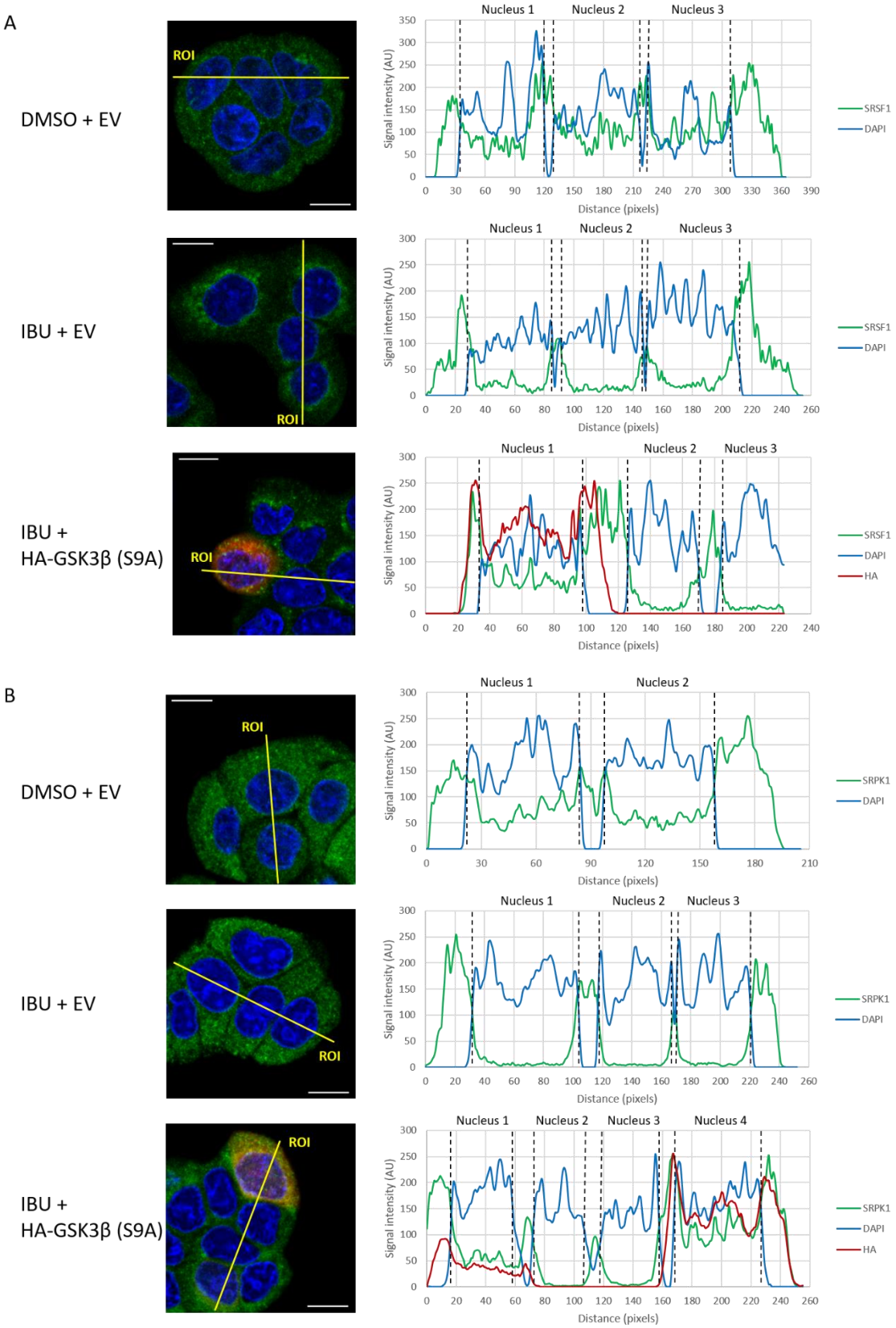


**Figure 3.15 – Effect of IBU treatment on SRSF1 and SRPK1 subcellular localization in HT29 cells.** HT29 cells were treated with DMSO (control) or IBU (500 µM) and 24 h later co-transfected with the indicated constructs [empty-vector (EV) or HA-GSK3β (S9A)]. 48 h after the initial transfection, cells were analyzed by confocal immunofluorescence microscopy. (**A-B**) Shown is the colored overlay of three confocal immunofluorescence images (left), which detected cell nuclei in blue (DAPI), the localization of endogenous SRSF1 (**A**) or SRPK1 (**B**) protein in green, and the tagged-HA in red. The nucleus and cytoplasm distribution of the three fluorescent signals was analyzed

along optical sections (yellow lines) across several cells by plotting pixel intensities along the traced path (right graphs). In control cells, SRSF1/SRPK1 signals (green) were localized both to the cytosol and the cell nucleus (blue); however, in IBU-treated cells, nuclear signals for SRSF1/SRPK1 are nearly absent. Moreover, note the reversion effect observed upon transfection of HA-GSK3β (S9A), SRSF1/SRPK1 nuclear signals are observed in HA-GSK3β (S9A) transfected cells.

### 3.16 WNK1 depletion in HT29 cells led to a decrease in glucose uptake levels

The work described above established two roles for WNK1: as a kinase involved in the regulation of glucose uptake in HEK293 cells (see 3.1) and as a protein complex partner forGSK3β that affects SRPK1, SRSF1 and splicing of RAC1B (see 3.10-15). In order to understand if both roles are related, as part of the same signaling pathway, HT29 cells were transfected with siRAC1B, siWNK1 or siLuc (used as control) for 48 h followed by a glucose uptake assay. The efficiency of depletion was confirmed by WB (Figure 3.17A) and determined to be 80% for WNK1 (Figure 3.17C) and 90% for RAC1B (Figure 3.17B). In addition, these WB analyses allowed to confirm that WNK1 depletion caused a significant concomitant decrease in RAC1B expression (~50% – Figure 3.17B). Considering the glucose uptake, the depletion of WNK1 in HT29 cells revealed a significant reduction of 40% (Figure 3.17D) in glucose uptake levels, however, RAC1B depletion did not significantly affect the uptake in these cells. Together, these data indicate that the decrease in RAC1B and the reduction in glucose uptake are parallel, independent effects caused by WNK1 depletion. Thus, we were able to confirm the role of WNK1 on glucose uptake in cancer cell models and uncover a new role in the complex signaling pathway regulating RAC1B expression.

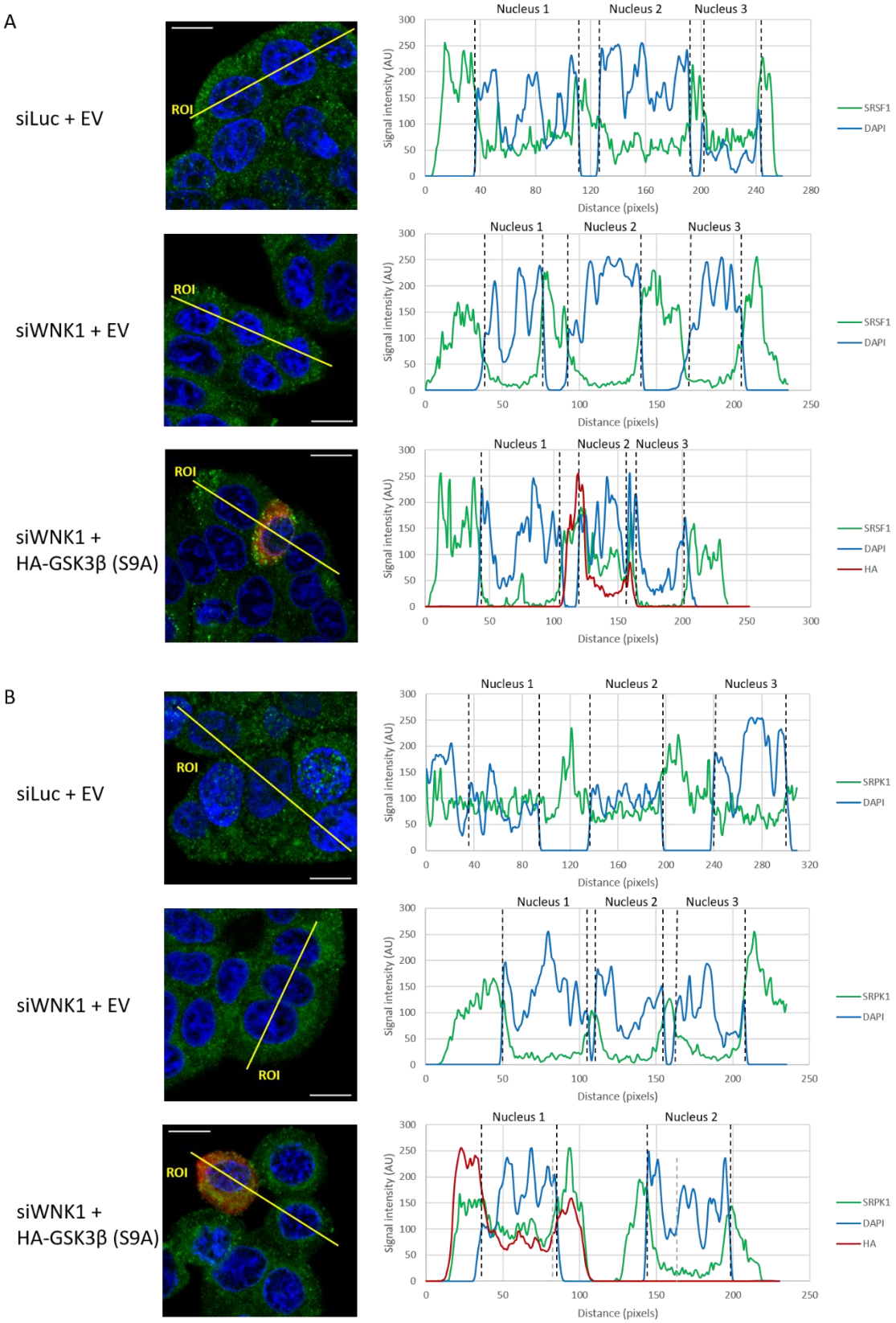


**Figure 3.16 – Effect of WNK1 depletion on SRSF1 and SRPK1 subcellular localization in HT29 cells.** HT29 cells were transfected with siLuc or siWNK1 and 24 h later co-transfected with the indicated constructs [empty-vector (EV) or HA-GSK3β (S9A)]. 48 h after the initial transfection, cells were analysed by confocal immunofluorescence microscopy. (**A-B)** Shown is the colored overlay of three confocal immunofluorescence images (left), which detected

cell nuclei in blue (DAPI), the localization of endogenous SRSF1 (**A**) or SRPK1 (**B**) protein in green, and the tagged-HA in red. The nucleus and cytoplasm distribution of the three fluorescent signals was analyzed along optical sections (yellow lines) across several cells by plotting pixel intensities along the traced path (right graphs). In control cells, SRSF1/SRPK1 signals (green) were localized both to the cytosol and the cell nucleus (blue); however, in WNK1 depleted cells, nuclear signals for SRSF1/SRPK1 are nearly absent. Moreover, note the reversion effect observed upon co-transfection of HA-GSK3β (S9A), SRSF1/SRPK1 nuclear signals are observed in HA-GSK3β (S9A) transfected cells.

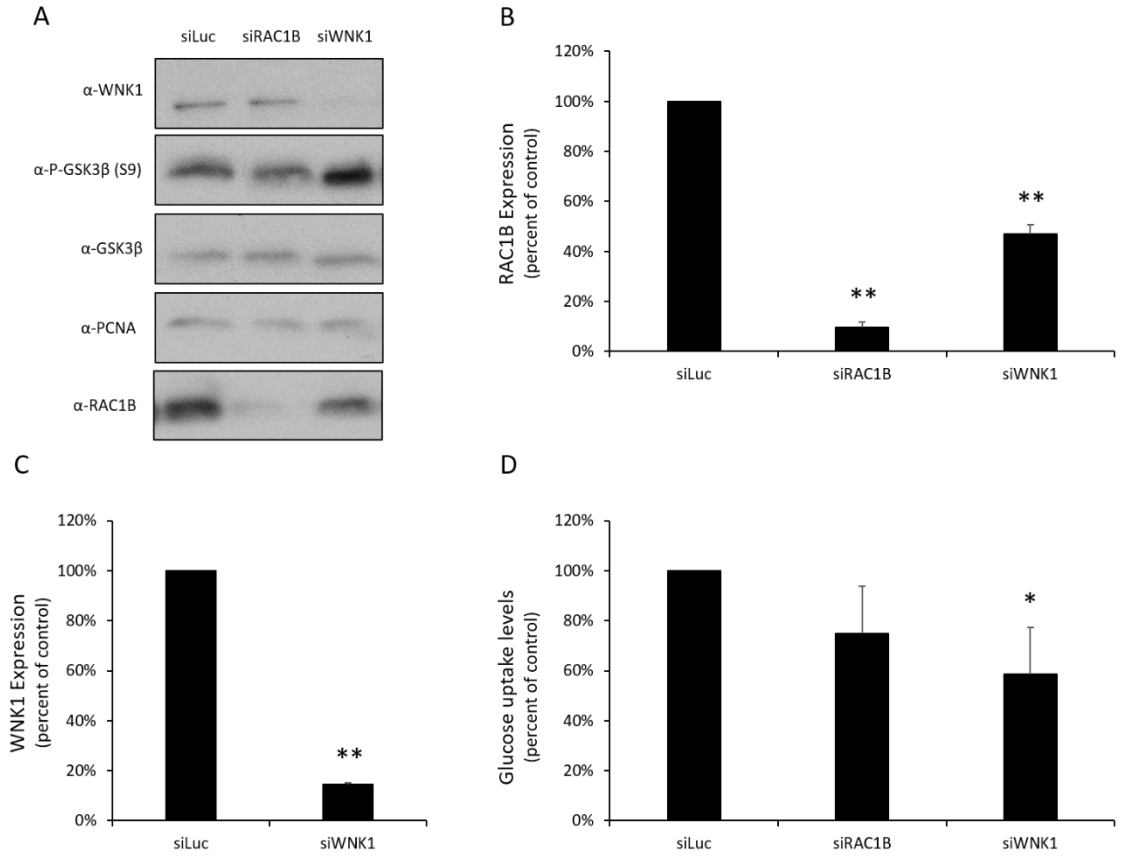


**Figure 3.17 – WNK1 modulates glucose uptake in HT29 cells.** Cells were transfected with either siLuc (control), siRAC1B or siWNK1 for 48 h. A part of the lysate was denatured by adding SDS modified sample buffer, then separated by SDS-PAGE and transferred to PVDF blotting membranes, whereas the remaining lysate used for glucose uptake measurements. (**A**) Representative WB of whole-cell lysates with the indicated antibodies. (**B**) Quantification of RAC1B or (**C**) WNK1 protein levels following transfection with either siLuc (control), siRAC1B or siWNK1. (**D**) Determination of glucose uptake levels. The glucose uptake was measured using Glucose Uptake-Glo™ Assay (Promega) following the manufacturer's instructions and glucose values determined by relative light units (RLUs) normalized to total protein values. Total protein was calculated measuring the relative intensities of PCNA bands using ImageJ (NIH). Shown is data from at least three independent experiments. All shown data represent means ± SEM, $*P < 0.05$, $**P < 0.01$.

# Chapter 4 General Discussion and Conclusions

In agreement with the three objectives formulated for this doctoral thesis, the following section on general discussion and conclusions is divided into three parts. In the first part, the identification and validation of novel phosphosites regulating GLUT1 by serine/threonine kinases phosphorylation is discussed. Discussion is performed in view of the current paradigms on signaling transduction mechanisms and importance of the study for cellular metabolism. The second part of this chapter discusses the advantages and limitations of the biochemical method used for the identification of the WNK1 interactome. Finally, in the last part of this chapter the cellular and biomedical implications that result from the identified WNK1 interactors in cancer development and survival are discussed.

## 4.1 Part 1

### 4.1.1 WNK1 affects GLUT1 PM expression and glucose uptake

In this work, we intended to further investigate the role of WNK1 in GLUT1 regulation, as this kinase was previously identified as a new player in the regulation of glucose transporter translocation to the PM (Mendes et al. 2010). WNK1 was found to regulate the PM expression of GLUT1 through TBC1D4 phosphorylation, associated with Rab8A activation and consequent delivery of GLUT1 channels at the PM.

The results presented in this dissertation demonstrated for the first time that WNK1 signaling regulates glucose uptake in both HEK293 cells (Figure 3.1C) and CRC tumor cell model HT29 (Figure 3.17D), confirming WNK1 as a modulator of cell metabolism in both normal and cancer cell lines.

### 4.1.2 WNK1 phosphorylates TBC1D proteins at both specific and shared residues

Regarding the phosphosite MS results (Tables 3.1 and 3.2), we were able to detect several already described AKT-regulated phosphosites. However, we were not able to detect the well-established Thr642 phosphorylation. This might be related to issues about the sensitivity of the method, because the identification of phosphorylated peptides has three major pitfalls, as reviewed by Dephoure et al., 2013. First, the method includes a digestion and a peptide fragmentation step (see materials and methods), which may cause loss of the phosphate group or generate peptides too short to be efficiently detected. In addition, a relative low phosphorylation rate of the region in the protein may lead to low

occupancy of the phosphosite that therefore will not be confidently detected by MS. Many factors, including peptide length, hydrophobicity, and charge affect the chromatographic properties and ionization efficiencies and consequently the efficiency of detection of different peptides. Lastly, due to peptide similarity it may not be possible to identify the precise site of the modification (Dephoure et al. 2013). Therefore, the main problems associated with this technique are related to false-negative results, whereas the identified phosphosites are of high confidence.

Likewise, the *in vivo* phosphorylation of Thr642 was detected by MS (Kane et al. 2002), not however, in our *in vitro* assays, although we were able to detect specific Thr642 TBC1D4 phosphorylation by WB upon AKT1 *in vitro* kinase assay (Figure 3.2A). This discrepancy remains unanswered and it could be that efficient phosphorylation at Thr642 needs the interaction of other cellular proteins.

### 4.1.3 SGK1 phosphorylates TBC1D proteins at specific residues without regulating GLUT1

Interestingly, the transfection of the mutants SGK1 KD, TBC1D1 T505A (non-phosphorylatable mutant) and TBC1D1 T505D (phosphomimetic mutant) did not cause a significant change in the PM expression of GLUT1. Therefore, we were not able to validate Thr 505 as a determinant phosphosite for GLUT1 localization. Nevertheless, our results showed that SGK1 and SGK3 are able to phosphorylate TBC1D proteins in *in vitro* kinase assays (Figure 3.2D) and the transfection of SGK1 CA increased GLUT1 PM expression, concordant with previous results on SGK1 regulating GLUT1 (Palmada et al. 2006). Thus, Thr 505 is a phosphosite in TBC1D1, which is phosphorylated by SGK1, but might be involved in the regulation of other cellular functions not related to GLUT1 PM expression. Interestingly, proteogenomic studies revealed a TBC1D1 T505 phosphosite enrichment in breast cancer samples (Mertins et al. 2016). Indeed, recent studies have proposed different perspectives on the role of SGK1 in cancer development. For example, SGK1 was defined as essential for proliferation and survival of thyroid cancer cells with PI3K-activating mutations (Orlacchio et al. 2017). Also, SGK1 was related with CRC cell proliferation, migration and survival (Liang et al. 2017). Additionally, SGK1 was involved in cancer chemotherapy resistance development associated with poor survival prognosis in non-small cell lung cancer (NSCLC) patients (Tang et al. 2018). Curiously, in breast cancer it has been reported that SGK1 activation

is important for progesterone treatment effect leading to a significant reduction in cell migration and cell invasion (Godbole et al. 2018).

Consequentially, further studies are needed to understand the importance of TBC1D1 Thr505 phosphorylation by SGK1 for signaling pathways and how the respective cellular processes are dysregulated in cancer phenotypes.

### 4.1.4 The identified WNK1-phosphorylated TBC1D sites are functionally relevant

In this work, we validated new phosphosites involved in GLUT1 PM expression regulated by WNK1, namely Ser565 in TBC1D1 (Figure 3.4) and Ser704 in TBC1D4 (Figure 3.5). Phosphorylation on serine/threonine residues on TBC1D is important for the inactivation of its Rab-GAPs activity (Roach et al. 2007; Chavez et al. 2008; Sakamoto and Holman 2008) and the subsequent modulation of the cell surface levels of GLUT glucose transporters.

TBC1D4 phosphorylation is commonly assessed using the phospho-AKT substrate (PAS) antibody, which recognizes phosphorylated AKT substrates in an (R/K)X(R/K)XXS*/T* recognition motif (Kane et al. 2002). Considering the well-known role of AKT in TBC1D regulation, we searched for non-AKT regulated phosphosites. None of the phosphosites studied, TBC1D1 T505 (AKRSLT*) and S565 (FKLLGS*) or TBC1D4 S704 (LHTSFS*) fit the AKT recognition motif. Whereas TBC1D1 T505 and S565 phosphosites where exclusively detected when the assays were performed with SGK1 and WNK1, respectively (see Table 3.1), the phosphorylation of TBC1D4 phosphosite S704 was detected in the presence of SGK1, SGK3 and WNK1 (see Table 3.2).

Chen and colleagues (2008) detected Ser565 phosphorylation in MS data from HA-TBC1D1 transfected in serum supplemented cultured HEK293 cells. In this thesis work, we associated WNK1 protein kinase to the TBC1D1 phosphosite Ser565. Our results show that S565A mutant transfection caused a significant decrease in GLUT1 PM expression, comparable with the effect observed in WNK1-depleted cells. Remarkably, the transfection of S565D mutant after WNK1 depletion was not enough to restore the levels of PM GLUT1 expression obtained in control conditions. Accordingly, we might infer that S565 phosphorylation in TBC1D1 is necessary but not sufficient for the inactivation of the Rab-GAP and that WNK1 phosphorylation on other residues might be

required for full TBC1D1 inhibition. However, it cannot be excluded that the S565D mutant is only partially phosphomimetic, for example if the phosphorylation site serves as a recognition motif for adaptor proteins. Then, the S-D alteration might change the binding pocket causing an inability of the mutant to bind the adaptor protein (Dephoure et al. 2013). Additionally, it is possible that in the WNK1-depleted cells used, the endogenous TBC1D1 cannot be inactivated efficiently for requiring interaction with the WNK1 protein to become inhibited.

Phosphorylation of TBC1D4 in Ser704 residue has been associated with physical exercise stimulating AMPK regulated Rab-GAP inactivation in skeletal muscle (Treebak et al. 2009, 2014; Kjøbsted et al. 2016). However, regarding non-exercise related phosphorylation little was known about this phosphosite, despite the fact that it is phosphorylated following insulin stimulation (Treebak et al. 2009). In the present work we related the phosphorylation of Ser704 in TBC1D4 with the protein kinases WNK1, SGK1 and SGK3 but not AKT (see 3.3 and 3.5.2). Interestingly, our results indicate that transfection of mutant TBC1D4 S704D reverts the decrease of GLUT1 PM expression caused by WNK1 depletion, confirming the importance of WNK1-regulation to PM expression of GLUT1 and metabolism control. SGK1 and SGK3 were also identified as Ser704 TBC1D4 phosphorylating kinases in our MS data, but were not further analyzed.

Together, these data provide additional insights into WNK1 function in glucose uptake regulation and cell metabolism, acting upon TBC1D1 and TBC1D4, two key regulators of glucose transporters.

Dysregulation of glucose uptake in humans is of high importance in two major illnesses, type 2 diabetes and cancer. The molecular responses to insulin (see 1.7.2.2) are lost in type 2 diabetes, a leading health problem worldwide. According to the International Diabetes Federation, the total number of patients with diabetes is predicted to rise to 628.6 million by the year 2045 (International Diabetes Federation 2017). Thus, knowledge of how signaling and trafficking pathways are coordinated is essential to understand the pathogenesis of diabetes and this may be used to generate new therapeutic options for the restoration of insulin response in the growing population of type 2 diabetes patients.

Additionally, reprogramming energy metabolism is one of the hallmarks of cancer cells, which adjust their energy metabolism in order to fuel their rapid cell growth and division (Hanahan and Weinberg 2011). This adjustment in metabolism was first postulated by Otto Warburg, who observed that cancer cells use the less energy-efficient

glycolysis despite the presence of oxygen (Warburg 1956). In this process, cancer cells compensate for the lower yield in ATP production by upregulating glucose transporters, markedly GLUT1, which substantially increases import of extracellular glucose into the cytoplasm (Jones and Thompson 2009). In fact, alterations on several proteins involved in GLUT1 PM expression regulation are altered in cancer phenotypes. For instance, Ser565 in TBC1D1, a phosphosite described in this work as a GLUT1 PM expression regulator was found to be phosphorylated in samples from NSCLC cell models (Klammer et al. 2012). Also, deregulation of SGK1 (Lang et al. 2006), together with SGK3 (Bruhn et al. 2010) has been observed in several types of cancer. Furthermore, AKT is one of the most frequently hyperactivated kinases in human cancers (Altomare and Testa 2005) and is a target for several cancer therapies (Song et al. 2019). Finally, WNK1, a kinase shown to have a role in GLUT1 PM expression and with a signaling cascade which affects several cancer signaling pathways (Kankanamalage et al. 2018) has also been recently shown to regulate GLUT4 PM expression in skeletal muscle cells (Kim et al. 2018). Thus, WNK1 has the potential to control tumor cell metabolism and serve as a therapeutic target. Accordingly, WNK-specific inhibitors are being developed based on the distinct catalytic domain features(Yamada et al. 2016; Zhang et al. 2016).

Moreover, overexpression of GLUT1 is correlated with poor survival in most solid tumors and the evaluation of GLUT1 expression might be used as a prognostic tool in cancer patients (Wang et al. 2017). This fact suggests that GLUT1 is a promising therapeutic target in tumors, from the expression levels to the regulation of the channel localization and activity. Consequently, increasing the knowledge about the signaling pathways involved in the regulation of glucose uptake might be helpful to define therapeutic targets and fight cancer development.

## 4.2 Part 2

### 4.2.1 Proteomic approach to identify WNK1-interacting proteins

In order to define biological pathways regulated by WNK1, binding partners were identified by a proteomic approach using crosslinking agents and MS, followed by exploring protein-protein interactions (PPI) networks.

Regarding the MS results, we were able to detect some already described WNK1-interacting proteins (see Table 3.3) such as 14-3-3 (Mendes et al. 2010), whereas others

such as TBC1D4 were not retrieved. However, the validation experiments did not confirm most interactions and raised some questions about the robustness of the method. In fact, the major weaknesses about the use of cross-linking agents in MS experiments are the complexity of MS/MS fragmentation of cross-linked peptides, the relative low abundance of cross-linked peptides in highly complex peptide mixtures, and finally, the cross-linked products' heterogeneity (Yu and Huang 2018). In future experiments, different cross-linking agents, possibly using cleavable reagents, which can reduce the fragmentation together with a better enrichment feature to reduce the complexity of peptide mixtures (Yu and Huang 2018). This feature together with a bioinformatic analysis should provide a better snapshot of protein interaction networks in living cells.

To increase the confidence of our results, we performed a bioinformatic analysis, diluting the heterogeneity effect of crosslinked products by introducing the CCS of proteins identified in three samples. In fact, the validation experiments in HT29 cells with crosslinking agents (Figure 3.11) versus without crosslinking agents (Figure 3.12A), show that the hit with high CCS (SRPK1) was co-immunoprecipitated in both conditions, whereas SRSF1, a protein with a CCS of 2, was lost from the interaction complex without the use of cross-linking agents (Figure 3.12A).

Since proteins do not act independently but in a network of complex molecular interactions, networks of PPI may provide new sources of information about biological pathways. This was the case of this work and the following part describes a new role identified for WNK1.

## 4.3 Part 3

### 4.3.1 WNK1-interacting proteins reveal a novel role for WNK1 in alternative pre-mRNA splicing

Although the interactome of WNK1 was expected to yield targets related to metabolism, our gene ontology analysis pointed towards a function related with mRNA processing. Indeed, the validated WNK1-interacting proteins, SRPK1 and SRSF1, together with GSK3β [used as a previously described positive control (Sato and Shibuya 2018)] were identified in two cell lines HEK293 (Figure 3.8) and HT29 (Figure 3.11). Actually, all proteins are described to modulate pre-mRNA splicing events (Gonçalves et

al. 2009, 2014). We thus reasoned that WNK1 might have a role in regulating alternative splicing.

Accordingly, the main finding of this work is a novel function of WNK1 as a scaffolding protein interacting with GSK3β, SRPK1 and SRSF1, which promotes changes in alternative splicing of RAC1B in colorectal HT29 cells (Figure 3.10 and 3.12). WNK1 interaction protects GSK3β from the inhibitory phosphorylation at Ser9 (Figure 3.13). This phosphorylation is at least in part mediated by AKT1 (Figure 3.14). In consequence, the active, unphosphorylated GSK3β allows the translocation of SRPK1/SRSF1 to the nucleus (Figures 3.15 and 3.16), which is an important regulatory step for the generation of RAC1B, as demonstrated by previous studies (Gonçalves et al. 2009, 2014; Jordan et al. 2019). Moreover, this work has provided a new component for the signaling pathway affected by IBU, a non-steroidal anti-inflammatory drug known to repress the expression of RAC1B in colon cancer cells (Matos et al. 2013). Herein, we showed that IBU treatment of HT29 cells decreased complex formation between WNK1 and GSK3β (Figure 3.12), leading to a decrease in RAC1B expression. Both IBU treatment and depletion of endogenous WNK1 kinase led to the observed decrease in RAC1B expression and affected GSK3β phosphorylation at Ser9 and subcellular SRPK1 localization. The increase in Ser9 phosphorylation in GSK3β observed after IBU treatment and WNK1 depletion (Figure 3.13) is in agreement with the results from Greenspan and colleagues (2011) and compatible with data suggesting it operates downstream of WNK1 (Sato and Shibuya 2018).

Expression of RAC1B has been shown to be essential for the survival (Matos and Jordan 2005; Matos et al. 2008) and malignant progression by overcoming BRAF-induced senescence in colorectal cells (Henriques et al. 2015). Besides the role in CRC, RAC1B contributes to cellular transformation by promoting proliferation, survival and EMT in lung, breast, liver and thyroid carcinomas (Melzer et al. 2019). Moreover, RAC1B overexpression has been associated with chemotherapy resistance development, the major obstacle in treating CRC. Therefore, in this work, the role of WNK1 in RAC1B expression provides new insights into how the regulation of alternative splicing events by protein kinases can contribute to tumor development. Also, we identify a new role of WNK kinases in tumorigenesis and provide new targets for pharmacological modulation of RAC1B expression and possible cancer treatment.

### 4.3.2 The role of WNK1 in alternative splicing or glucose metabolism rely on a different molecular mechanism

Altogether, this thesis contributes new insights on WNK1 signaling pathways involved in cell glucose metabolism and mRNA alternative splicing regulation. In the case of metabolism, WNK1 activity is important for modulating the Rab-GAP activity of TBC1D proteins by phosphorylating specific residues, which has also been described for AKT and SGK (Kane et al. 2002; Palmada et al. 2006). The regulatory crosstalk between WNK1, AKT and SGK kinases remains, however, to be established and thus is an interesting subject for future investigations. In contrast, in the case of mRNA splicing regulation, the mechanism underlying WNK1 function depends on PPI with GSK3β and thus, clearly differs from its role in glucose uptake.

In conclusion, our results provided more molecular details for the role of WNK1 in regulating glucose uptake but also identify a new and independent role in regulating the expression of RAC1B, a GTPase important for the survival, proliferation and mobility of colorectal cancer cells (Figure 4.1). It is possible that both functions constitute a pro-tumorigenic role of WNK1 in CRC, by coordinating changes in cell metabolism and tumor cell survival. Actually, as mentioned before, specific WNK kinase inhibitors are already being developed (Yamada et al. 2016; Zhang et al. 2016) and their use can be valuable for the treatment of cancer (Ardito et al. 2017), targeting not only GLUT1 traffic but also tumor-cell specific changes in alternative splicing, of which RAC1B might only be one example.

In the future, it will be important to find physiological stimuli or conditions that promote the activity of WNK1 towards TBC1D proteins and regulation of GLUT PM expression. It will also be essential to understand in more detail the underlying molecular mechanisms of WNK1 signaling, find new interactors, and elucidate possible crosstalk between WNK1 and AKT or SGK signaling pathways, in different cellular and tissue contexts. This knowledge will be important to prevent unexpected side effects in using WNK inhibitors and also provide new targets to explore with potential benefit for tumorigenesis and type 2 diabetes treatment.

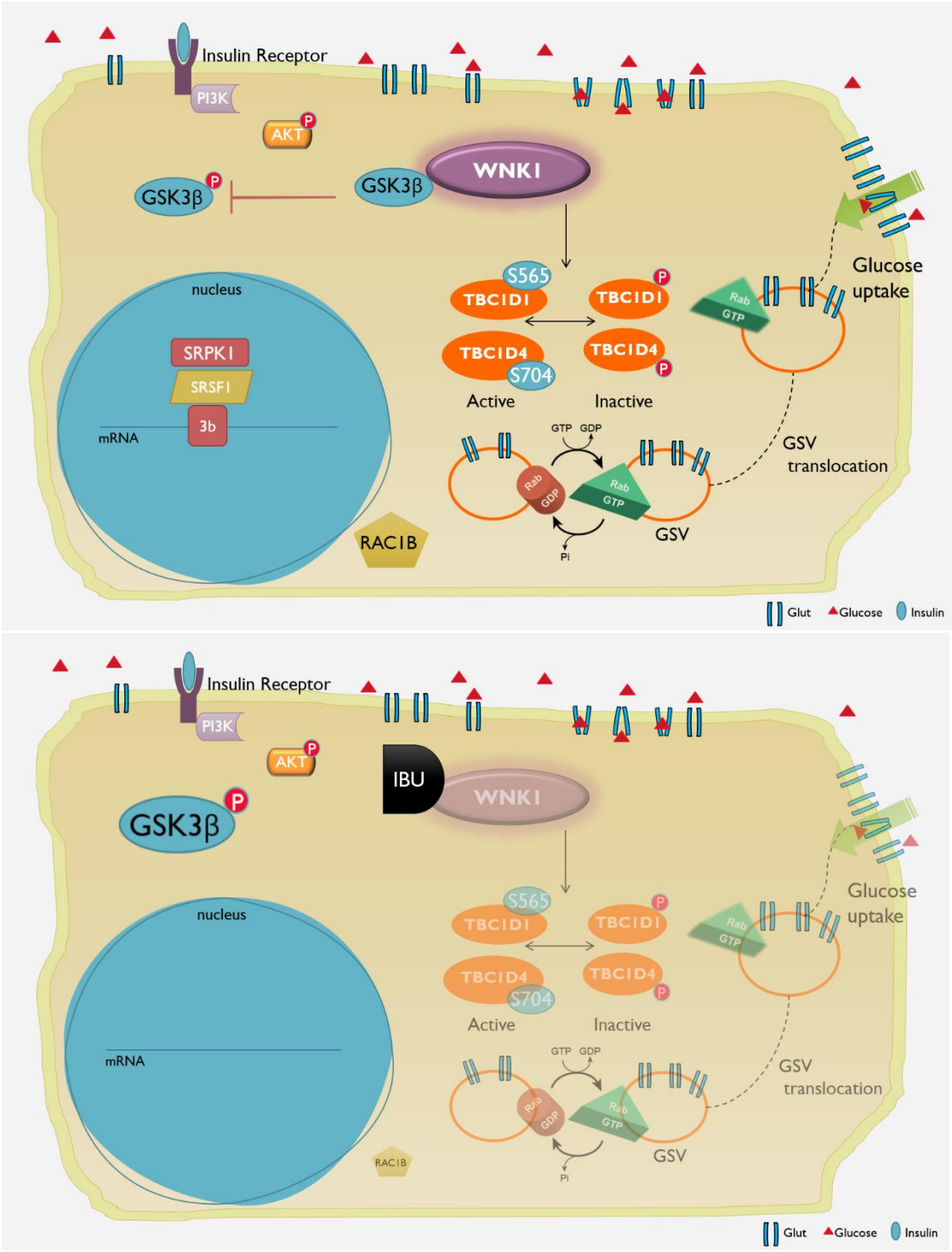


**Figure 4.1 Summary of WNK1 effects in cellular signaling.** Upper panel: WNK1 regulates glucose uptake by phosphorylation of two Ser residues in TBC1D1 (Ser 565) and TBC1D4 (Ser 704). By protein interaction with WNK1, the phosphorylation of GSK3β is prevented, there is nuclear localization of SRPK1 and SRSF1 leading RAC1B expression. Lower Panel: WNK1 depletion causes a decrease in glucose uptake. Both WNK1 depletion and IBU treatment cause RAC1B downregulation and are corelated with an increase of GSK3β phosphorylation at Ser9. This inhibitory phosphorylation is at least in part dependent on AKT1 and leads to a decrease in the nuclear expression of both SRPK1 and SRSF1.

# Chapter 5 Bibliography

Alessi DR, James SR, Downes CP, Holmes AB, Gaffney PR, Reese CB, Cohen P. 1997. Characterization of a 3-phosphoinositide-dependent protein kinase which phosphorylates and activates protein kinase B alpha. *Current Biology* **7**: 261–269.

Altomare DA, Testa JR. 2005. Perturbations of the AKT signaling pathway in human cancer. *Oncogene* **24**: 7455–7464.

An D, Toyoda T, Taylor EB, Yu H, Fujii N, Hirshman MF, Goodyear LJ. 2010. TBC1D1 regulates insulin- and contraction-induced glucose transport in mouse skeletal muscle. *Diabetes* **59**: 1358–1365.

Ardito F, Giuliani M, Perrone D, Troiano G, Muzio L Lo. 2017. The crucial role of protein phosphorylation in cell signaling and its use as targeted therapy (Review). *International Journal of Molecular Medicine* **40**: 271–280.

Arencibia JM, Pastor-Flores D, Bauer AF, Schulze JO, Biondi RM. 2013. AGC protein kinases: From structural mechanism of regulation to allosteric drug development for the treatment of human diseases. *Biochimica et Biophysica Acta - Proteins and Proteomics* **1834**: 1302–1321.

Barford D, Das AK, Egloff M-P. 2002. The structure and mechanism of protein phosphatases: Insights into Catalysis and Regulation. *Annual Review of Biophysics and Biomolecular Structure* **27**: 133–164.

Bazúa-Valenti S, Chávez-Canales M, Rojas-Vega L, González-Rodríguez X, Vázquez N, Rodríguez-Gama A, Argaiz ER, Melo Z, Plata C, Ellison DH, et al. 2014. The Effect of WNK4 on the Na + –Cl − Cotransporter Is Modulated by Intracellular Chloride . *Journal of the American Society of Nephrology* **26**: 1781–1786.

Beenstock J, Mooshayef N, Engelberg D. 2016. How Do Protein Kinases Take a Selfie (Autophosphorylate)? *Trends in Biochemical Sciences* **41**: 938–953.

Bogan JS. 2012. Regulation of Glucose Transporter Translocation in Health and Diabetes. *Annual Review of Biochemistry* **81**: 507–532.

Brazil DP, Hemmings BA. 2001. Ten years of protein kinase B signalling: A hard Akt to follow. *Trends in Biochemical Sciences* **26**: 657–664.

Bruhn MA, Pearson RB, Hannan RD, Sheppard KE. 2010. Second AKT: The rise of SGK in cancer signalling. *Growth Factors* **28**: 394–408.

Brunet A, Park J, Tran H, Hu LS, Hemmings BA, Greenberg ME. 2002. Protein Kinase SGK Mediates Survival Signals by Phosphorylating the Forkhead Transcription Factor FKHRL1 (FOXO3a). *Molecular and Cellular Biology* **21**: 952–965.

Burgering BMT, Coffer PJ. 1995. Protein kinase B (c-Akt) in phosphatidylinositol-3-OH kinase signal transduction. *Nature* **376**: 599–602.

Cartee GD. 2015. Roles of TBC1D1 and TBC1D4 in insulin- and exercise-stimulated glucose transport of skeletal muscle. *Diabetologia* **58**: 19–30.

Chadt A, Leicht K, Deshmukh A, Jiang LQ, Scherneck S, Bernhardt U, Dreja T, Vogel H, Schmolz K, Kluge R, et al. 2008. Tbc1d1 mutation in lean mouse strain confers leanness and protects from diet-induced obesity. *Nature Genetics* **40**: 1354–1359.

Chávez-Canales M, Zhang C, Soukaseum C, Moreno E, Pacheco-Alvarez D, Vidal-Petiot E, Castañeda-Bueno M, Vázquez N, Rojas-Vega L, Meermier NP, et al. 2014. The WNK-SPAK-NCC cascade revisited: WNK1 stimulates the activity of the NaCl cotransporter via SPAK, an effect antagonized by WNK4. *Hypertension* **64**: 1047–1053.

Chavez JA, Roach WG, Keller SR, Lane WS, Lienhard GE. 2008. Inhibition of GLUT4 translocation by Tbc1d1, a Rab GTPase-activating protein abundant in skeletal muscle, is partially relieved by AMP-activated protein kinase activation. *Journal of Biological Chemistry* **283**: 9187–9195.

Chen M, Manley JL. 2009. Mechanisms of alternative splicing regulation: insights from molecular and genomics approaches. *Nature Reviews Molecular Cell Biology* **10**: 741–754.

Chen S, Murphy J, Toth R, Campbell DG, Morrice NA, Mackintosh C. 2008. Complementary regulation of TBC1D1 and AS160 by growth factors, insulin and AMPK activators. *Biochemical Journal* **409**: 449–459.

Chen Y, Lippincott-Schwartz J. 2013. Rab10 delivers GLUT4 storage vesicles to the plasma membrane. *Communicative and Integrative Biology* **6**: 3–5.

Cheng C-J, Huang C-L. 2011. Activation of PI3-Kinase Stimulates Endocytosis of ROMK via Akt1/SGK1-Dependent Phosphorylation of WNK1. *Journal of the American Society of Nephrology* **22**: 460–471.

Cheng KKY, Zhu W, Chen B, Wang Y, Wu D, Sweeney G, Wang B, Lam KSL, Xu A.

2014. The adaptor protein APPL2 inhibits insulin-stimulated glucose uptake by interacting with TBC1D1 in skeletal muscle. *Diabetes* **63**: 3748–3758.

Chu N, Salguero AL, Liu AZ, Chen Z, Dempsey DR, Ficarro SB, Alexander WM, Marto JA, Li Y, Amzel LM, et al. 2018. Akt Kinase Activation Mechanisms Revealed Using Protein Semisynthesis. *Cell* **174**: 897-907.e14.

Ciaraldi TP, Carter L, Mudaliar S, Henry RR. 2010. GSK-3ß and Control of Glucose Metabolism and Insulin Action in Human Skeletal Muscle. *Molecular Cell Endocrinology* **315**: 153–158.

Cohen P. 2002. The origins of protein phosphorylation. *Nature Cell Biology* **4**: 127–130.

Cohen P, Frame S. 2001. Timeline: The renaissance of GSK3. *Nature Reviews Molecular Cell Biology* **2**: 769–776.

Cross DAE, Alessi DR, Cohen P, Andjelkovich M, Hemmings BA. 1995. Inhibition of glycogen synthase kinase-3 by insulin mediated by protein kinase B. *Nature* **378**: 785–789.

Datta SR, Brunet A, Greenberg ME. 1999. Cellular survival: A play in three akts. *Genes and Development* **13**: 2905–2927.

Davies H, Hunter C, Smith R, Stephens P, Greenman C, Bignell G, Teague J, Butler A, Edkins S, Stevens C, et al. 2005. Somatic mutations of the protein kinase gene family in human lung cancer. *Cancer Research* **65**: 7591–7595.

Day EK, Sosale NG, Lazzara MJ. 2016. Cell signaling regulation by protein phosphorylation: A multivariate, heterogeneous, and context-dependent process. *Current Opinion in Biotechnology* **40**: 185–192.

de los Heros P, Kahle KT, Rinehart J, Bobadilla NA, Vázquez N, San Cristobal P, Mount DB, Lifton RP, Hebert SC, Gamba G. 2006. WNK3 bypasses the tonicity requirement for K-Cl cotransporter activation via a phosphatase-dependent pathway. *Proceedings of the National Academy of Sciences* **103**: 1976–1981.

Delaloy C, Lu J, Houot A, Disse-nicodeme S, Gasc J, Corvol P, Jeunemaitre X. 2003. Multiple Promoters in the WNK1 Gene : One Controls Expression of a kidney-specific kinase-defective isoform. *Molecular and Cellular Biology* **23**: 9208–9221.

Dephoure N, Gould KL, Gygi SP, Kellogg DR. 2013. Mapping and analysis of

phosphorylation sites: a quick guide for cell biologists. *Molecular Biology of the Cell* **24**: 535–542.

Deshmukh A, Coffey VG, Zhong Z, Chibalin A V., Hawley JA, Zierath JR. 2006. Exercise-induced phosphorylation of the novel Akt substrates AS160 and filamin A in human skeletal muscle. *Diabetes* **55**: 1776–1782.

Ding JH, Zhong X-Y, Hagopian JC, Cruz MM, Ghosh G, Feramisco J, Adams JA, Fu X-D. 2006. Regulated Cellular Partitioning of SR Protein-specific Kinases in Mammalian Cells. *Molecular Biology of the Cell* **17**: 876–885.

Doble BW, Woodgett JR. 2003. GSK-3: tricks of the trade for a multi-tasking kinase. *Journal of Cell Science* **116**: 1175–1186.

Eguez L, Lee A, Chavez JA, Miinea CP, Kane S, Lienhard GE, McGraw TE. 2005. Full intracellular retention of GLUT4 requires AS160 Rab GTPase activating protein. *Cell Metabolism* **2**: 263–272.

Embi N, Rylatt DB, Cohen P. 1980. Glycogen Synthase Kinase-3 from Rabbit Skeletal Muscle. *European Journal of Biochemistry* **107**: 519–527.

Feng Y, Wang Q, Wang Y, Yard B, Lang F. 2005. SGK1-mediated Fibronectin Formation in Diabetic Nephropathy. *Cellular Physiology and Biochemistry* **16**: 237–245.

Ferrer JC, Favre C, Gomis RR, Fernández-Novell JM, García-Rocha M, De La Iglesia N, Cid E, Guinovart JJ. 2003. Control of glycogen deposition. *FEBS Letters* **546**: 127–132.

Frame S, Cohen P, Biondi RM. 2001. A Common Phosphate Binding Site Explains the Unique Substrate Specificity of GSK3 and Its Inactivation by Phosphorylation. *Molecular Cell* **7**: 1321–1327.

Gamba G. 2005. Role of WNK kinases in regulating tubular salt and potassium transport and in the development of hypertension. *AJP: Renal Physiology* **288**: F245–F252.

Giannakouros T, Nikolakaki E, Mylonis I, Georgatsou E. 2011. Serine-arginine protein kinases: A small protein kinase family with a large cellular presence. *FEBS Journal* **278**: 570–586.

Godbole M, Togar T, Patel K, Dharavath B, Yadav N, Janjuha S, Gardi N, Tiwary K, Terwadkar P, Desai S, et al. 2018. Up-regulation of the kinase gene SGK1 by

progesterone activates the AP-1–NDRG1 axis in both PR-positive and -negative breast cancer cells. *Journal of Biological Chemistry* **293**: 19263–19276.

Gonçalves V, Henriques A, Pereira J, Costa AN, Moyer MP, Moita LF, Gama-Carvalho M, Matos P, Jordan P. 2014. Phosphorylation of SRSF1 by SRPK1 regulates alternative splicing of tumor-related Rac1b in colorectal cells. *RNA* **20**: 474–482.

Gonçalves V, Matos P, Jordan P. 2009. Antagonistic SR proteins regulate alternative splicing of tumor-related Rac1b downstream of the PI3-kinase and Wnt pathways. *Human Molecular Genetics* **18**: 3696–3707.

Gonçalves V, Pereira JFS, Jordan P. 2018. Signaling pathways driving aberrant splicing in cancer cells. *Genes* **9**.

Greenman C, Stephens PJ, Smith R, Dalgliesh GL, Hunter C, Bignell GR, Davies H, Teague J, Butler AP, Edkins S, et al. 2007. Patterns of somatic mutation in human cancer genomes. *Nature* **446**: 153–158.

Greenspan E, Madigan J, Broadman L, Rosenberg D. 2011. Ibuprofen inhibits activation of nuclear β-catenin in human colon adenomas and induces the phosphorylation of GSK-3β. *Cancer Prevention Research* **4**: 161–171.

Gui JF, Lane WS, Fu XD. 1994. A serine kinase regulates intracellular localization of splicing factors in the cell cycle. *Nature* **369**: 678–682.

Hadchouel J, Ellison DH, Gamba G. 2016. Regulation of Renal Electrolyte Transport by WNK and SPAK-OSR1 Kinases. *Annual Review of Physiology* **78**: 367–389.

Hall JE. 2015. *Guyton and Hall Textbook of Medical Physiology*. 13th ed. Elsevier Health Sciences.

Halse R, Rochford JJ, McCormack JG, Vandenheede JR, Hemmings BA, Yeaman SJ. 1999. Control of Glycogen Synthesis by Glucose, Glycogen, and Insulin in Cultured Human Muscle Cells. *Diabetes* **242**: 776–780.

Hanahan D, Weinberg RA. 2011. Hallmarks of cancer: the next generation. *Cell* **144**: 646–74.

Hanks SK. 2003. Genomic analysis of the eukaryotic protein kinase superfamily: A perspective. *Genome Biology* **4**: 111.

Hanks SK, Hunter T. 1995. The eukaryotic protein kinase superfamily : kinase (catalytic)

domain structure and classification. *FASEB Journal* **9**: 576–596.

Heise CJ, Xu BE, Deaton SL, Cha SK, Cheng CJ, Earnest S, Sengupta S, Juang YC, Stippec S, Xu Y, et al. 2010. Serum and Glucocorticoid-induced Kinase (SGK) 1 and the epithelial sodium channel are regulated by multiple with no lysine (WNK) family members. *Journal of Biological Chemistry* **285**: 25161–25167.

Henriques AFA, Barros P, Moyer MP, Matos P, Jordan P. 2015. Expression of tumor-related Rac1b antagonizes B-Raf-induced senescence in colorectal cells. *Cancer Letters* **369**: 368–375.

Hernández F, Barreda EG de, Fuster-Matanzo A, Goñi-Oliver P, Lucas JJ, Avila J. 2009. The role of GSK3 in Alzheimer disease. *Brain Research Bulletin* **80**: 248–250.

Hernández F, Pérez M, Lucas JJ, Mata AM, Bhat R, Avila J. 2004. Glycogen Synthase Kinase-3 Plays a Crucial Role in Tau Exon 10 Splicing and Intranuclear Distribution of SC35. *The Journal of Biological Chemestry* **279**: 3801–3806.

Hoorn EJ, Nelson JH, McCormick JA, Ellison DH. 2011. The WNK Kinase Network Regulating Sodium, Potassium, and Blood Pressure. *Journal of the American Society of Nephrology* **22**: 605–614.

Huang S, Czech MP. 2007. The GLUT4 Glucose Transporter. *Cell Metabolism* **5**: 237–252.

Hubbard SR, Wei L, Ellis L, Hendrickson WA. 1994. Crystal structure of the tyrosine kinase domain of the human insulin receptor. *Nature* **372**: 746–754.

Humphrey SJ, James DE, Mann M. 2015. Protein Phosphorylation: A Major Switch Mechanism for Metabolic Regulation. *Trends in Endocrinology and Metabolism* **26**: 676–687.

Hunter T. 2009. Tyrosine phosphorylation: thirty years and counting. *Current Opinion in Cell Biology* **21**: 140–146.

Hunter T, Karin M. 1992. The regulation of transcription by phosphorylation. *Cell* **70**: 375–387.

Hunter T, Sefton BM, Holley RW. 1980. Transforming gene product of Rous sarcoma virus phosphorylates tyrosine (phosphotyrosine/protein kinase/src gene/phosphoproteins). *Biochemistry* **77**: 1311–1315.

International Diabetes Federation. 2017. *International Diabetes Federation's Diabetes Atlas*. 8th ed.

Jin J, Smith FD, Stark C, Wells CD, Fawcett JP, Kulkarni S, Metalnikov P, Donnell PO, Taylor L, Taylor P, et al. 2004. Proteomic, Functional, and Domain-Based Analysis of In Vivo 14-3-3 Binding Proteins Involved in Cytoskeletal Regulation and Cellular Organization. *Current Biology* **14**: 1436–1450.

Jones RG, Thompson CB. 2009. Tumor suppressors and cell metabolism. *Genes & Development* **23**: 537–548.

Jope R, Roh M-S. 2012. Glycogen Synthase Kinase-3 (GSK3) in Psychiatric Diseases and Therapeutic Interventions. *Current Drug Targets* **7**: 1421–1434.

Jordan P, Gonçalves V, Matos P. 2019. A New Twist to Ibuprofen : Alternative Action in Alternative Splicing. *European Medical Journal* **4**: 64–71.

Kahle KT, Rinehart J, de los Heros P, Louvi A, Meade P, Vazquez N, Hebert SC, Gamba G, Gimenez I, Lifton RP. 2005a. WNK3 modulates transport of Cl- in and out of cells: Implications for control of cell volume and neuronal excitability. *Proceedings of the National Academy of Sciences* **102**: 16783–16788.

Kahle KT, Rinehart J, Giebisch G, Gamba G, Hebert SC, Lifton RP. 2008a. A novel protein kinase signaling pathway essential for blood pressure regulation in humans. *Trends in Endocrinology and Metabolism* **19**: 91–95.

Kahle KT, Ring AM, Lifton RP. 2008b. Molecular Physiology of the WNK Kinases. *Annual Review of Physiology* **70**: 329–355.

Kahle KT, Wilson FH, Lifton RP. 2005b. Regulation of diverse ion transport pathways by WNK4 kinase: A novel molecular switch. *Trends in Endocrinology and Metabolism* **16**: 98–103.

Kane S, Sano H, C. H. Liu S, Asara JM, William SL, C. Garner C, E. Lienhard G. 2002. A Method to Identify Serine Kinase Substrates AKT phosphorylates a novel adipocyte protein with a Rab GTPase-activating protein (GAP) domain. *Journal of Biological Chemistry* **277**: 22115–22118.

Kankanamalage SG, Karra AS, Cobb MH. 2018. WNK pathways in cancer signaling networks. *Cell Communication and Signaling* **16**: 4–9.

Kim JH, Kim H, Hwang KH, Chang JS, Park KS, Cha SK, Kong ID. 2018. WNK1 kinase is essential for insulin-stimulated GLUT4 trafficking in skeletal muscle. *FEBS Open Bio* **8**: 1866–1874.

Kjøbsted R, Pedersen AJT, Hingst JR, Sabaratnam R, Birk JB, Kristensen JM, Højlund K, Wojtaszewski JFP. 2016. Intact regulation of the AMPK signaling network in response to exercise and insulin in skeletal muscle of male patients with type 2 diabetes: Illumination of AMPK activation in recovery from exercise. *Diabetes* **65**: 1219–1230.

Klammer M, Kaminski M, Zedler A, Oppermann F, Blencke S, Marx S, Müller S, Tebbe A, Godl K, Schaab C. 2012. Phosphosignature Predicts Dasatinib Response in Non-small Cell Lung Cancer. *Molecular & Cellular Proteomics* **11**: 651–668.

Klip A, Sun Y, Chiu TT, Foley KP. 2014. Signal transduction meets vesicle traffic: the software and hardware of GLUT4 translocation. *AJP: Cell Physiology* **306**: C879–C886.

Koizumi J, Okamoto Y, Onogi H, Mayeda A, Krainer AR, Hagiwara M. 1999. The subcellular localization of SF2/ASF is regulated by direct interaction with SR protein kinases (SRPKs). *Journal of Biological Chemistry* **274**: 11125–11131.

Kostich M, English J, Madison V, Gheyas F, Wang L, Qiu P, Greene J, Laz T. 2002. Human members of the eukaryotic protein kinase family. *Genome Biology* **3**: research0043.1.

Kramer HF, Witczak CA, Taylor EB, Fujii N, Hirshman MF, Goodyear LJ. 2006. AS160 regulates insulin- and contraction-stimulated glucose uptake in mouse skeletal muscle. *Journal of Biological Chemistry* **281**: 31478–31485.

Lang F, Böhmer C, Palmada M, Seebohm G, Strutz-Seebohm N, Vallon V. 2006. (Patho)physiological Significance of the Serum- and Glucocorticoid-Inducible Kinase Isoforms. *Physiological Reviews* **86**: 1151–1178.

Lang F, Cohen P. 2001. Regulation and Physiological Roles of Serum- and Glucocorticoid-Induced Protein Kinase Isoforms. *Science Signaling* **2001**: re17.

Lazrak A, Liu Z, Huang C-L. 2006. Antagonistic regulation of ROMK by long and kidney-specific WNK1 isoforms. *Proceedings of the National Academy of Sciences* **103**: 1615–1620.

Lee BH, Chen W, Stippec S, Cobb MH. 2007. Biological cross-talk between WNK1 and the transforming growth factor β-Smad signaling pathway. *Journal of Biological Chemistry* **282**: 17985–17996.

Leroux AE, Schulze JO, Biondi RM. 2018. AGC kinases, mechanisms of regulation and innovative drug development. *Seminars in Cancer Biology* **48**: 1–17.

Liang X, Buttertworth MB, Peters KW, Frizzel RA. 2010. AS160 Modulates Aldosterone-stimulated Epithelial Sodium Channel Forward Traffickin. *Molecular Biology of the Cell* **21**: 2024–2033.

Liang X, Lan C, Jiao G, Fu W, Long X, An Y, Wang K, Zhou J, Chen T, Li Y, et al. 2017. Therapeutic inhibition of SGK1 suppresses colorectal cancer. *Experimental & Molecular Medicine* **49**: e399.

Liu X, Klein PS. 2018. Glycogen synthase kinase-3 and alternative splicing. *Wiley Interdisciplinary Reviews: RNA* **9**: 1–17.

Loh C, Shaw KT, Carew J, Viola JPB, Luo C, Perrino BA, Rao A, Natl PGP, A ASUS. 1996. Calcineurin Binds the Transcription Factor NFAT1 and Reversibly Regulates Its Activity. **271**: 10884–10891.

Luo J. 2009. The Role of Glycogen Synthase Kinase 3β (GSK3β) in Tumorigenesis and Cancer Chemotherapy. *Cancer Letters* **273**: 194–200.

Ma C-T, Ghosh G, Fu X-D, Adams JA. 2010. Mechanism of Dephosphorylation of the SR Protein ASF/SF2 By Protein Phosphatase 1. *Journal of Molecular Biology* **403**: 386–404.

MacAulay K, Woodgett JR. 2008. Targeting glycogen synthase kinase-3 (GSK-3) in the treatment of Type 2 diabetes. *Expert Opinion on Therapeutic Targets* **12**: 1265–1274.

Manning G, Whyte DB, Martinez R, Hunter T. 2002. The Protein Kinase complement of the human genome. *Sience* **298**: 1912–1934.

Matos P, Jordan P. 2005. Expression of Rac1b stimulates NF-κB-mediated cell survival and G1/S progression. *Experimental Cell Research* **305**: 292–299.

Matos P, Jordan P. 2008. Increased Rac1b expression sustains colorectal tumor cell survival. *Molecular Cancer Research* **6**: 1178–84.

Matos P, Kotelevets, Larissa Gonçalves V, Henriques A, Zerbib P, Moyer MP, Chastre E, Jordan P. 2013. Ibuprofen Inhibits Colitis-Induced Overexpression of Tumor-Related Rac1b. *Neoplasia* **15**: 102–111.

Matos P, Oliveira C, Velho S, Gonçalves V, da Costa LT, Moyer MP, Seruca R, Jordan P. 2008. B-Raf(V600E) cooperates with alternative spliced Rac1b to sustain colorectal cancer cell survival. *Gastroenterology* **135**: 899–906.

McCance K, Huether S. 2014. *Pathophysiology: The Biologic Basis for Disease in Adults and Children*. 7th editio. Elsevier.

McManus EJ, Sakamoto K, Armit LJ, Ronaldson L, Shpiro N, Marquez R, Alessi DR. 2005. Role that phosphorylation of GSK3 plays in insulin and Wnt signalling defined by knockin analysis. *EMBO Journal* **24**: 1571–1583.

Medina M, Wandosell F. 2011. Deconstructing GSK-3: The Fine Regulation of Its Activity. *International Journal of Alzheimer's Disease* **2011**: 1–12.

Melzer C, Hass R, Lehnert H, Ungefroren H. 2019. RAC1B: A Rho GTPase with Versatile Functions in Malignant Transformation and Tumor Progression. *Cells* **8**: 21.

Mendes AI, Matos P, Moniz S, Jordan P. 2010. Protein kinase WNK1 promotes cell surface expression of glucose transporter GLUT1 by regulating a Tre-2/USP6-BUB2-Cdc16 domain family member 4 (TBC1D4)-Rab8A complex. *Journal of Biological Chemistry* **285**: 39117–39126.

Mendes AI, Matos P, Moniz S, Luz S, Amaral MD, Farinha CM, Jordan P. 2011. Antagonistic Regulation of Cystic Fibrosis Transmembrane Conductance Regulator Cell Surface Expression by Protein Kinases WNK4 and Spleen Tyrosine Kinase. *Molecular and Cellular Biology* **31**: 4076–4086.

Mertins P, Mani DR, Ruggles K V, Gillette MA, Clauser KR, Wang P, Wang X, Qiao JW, Cao S, Petralia F, et al. 2016. Proteogenomics connects somatic mutations to signaling in breast cancer. *Nature* **534**: 55–62.

Meyre D, Farge M, Lecoeur C, Proenca C, Durand E, Allegaert F, Tichet J, Marre M, Balkau B, Weill J, et al. 2008. R125W coding variant in TBC1D1 confers risk for familial obesity and contributes to linkage on chromosome 4p14 in the French population. *Human Molecular Genetics* **17**: 1798–1802.

Min X, Lee BH, Cobb MH, Goldsmith EJ. 2004. Crystal structure of the kinase domain of WNK1, a kinase that causes a hereditary form of hypertension. *Structure* **12**: 1303–1311.

Moniz S, Jordan P. 2010. Emerging roles for WNK kinases in cancer. *Cellular and Molecular Life Sciences* **67**: 1265–1276.

Moniz S, Martinho O, Pinto F, Sousa B, Loureiro C, Oliveira MJ, Moita LF, Honavar M, Pinheiro C, Pires M, et al. 2013. Loss of WNK2 expression by promoter gene methylation occurs in adult gliomas and triggers Rac1-mediated tumour cell invasiveness. *Human Molecular Genetics* **22**: 84–95.

Moniz S, Matos P, Jordan P. 2008. WNK2 modulates MEK1 activity through the Rho GTPase pathway. *Cellular Signalling* **20**: 1762–1768.

Moniz S, Veríssimo F, Matos P, Brazão R, Silva E, Kotevelets L, Chastre E, Gespach C, Jordan P. 2007. Protein kinase WNK2 inhibits cell proliferation by negatively modulating the activation of MEK1/ERK1/2. *Oncogene* **26**: 6071–6081.

Mortz E, Krogh TN, Vorum H, Görg A. 2001. Improved silver staining protocols for high sensitivity protein identification using matrix-assisted laser desorption/ionization-time of flight analysis. *Proteomics* **1**: 1359–1363.

Muslin AJ, Tanner JW, Allen PM, Shaw AS. 1996. Interaction of 14-3-3 with signaling proteins is mediated by the recognition of phosphoserine. *Cell* **84**: 889–897.

Ngo JCK, Chakrabarti S, Ding JH, Velazquez-Dones A, Nolen B, Aubol BE, Adams JA, Fu XD, Ghosh G. 2005. Interplay between SRPK and Clk/Sty kinases in phosphorylation of the splicing factor ASF/SF2 is regulated by a docking motif in ASF/SF2. *Molecular Cell* **20**: 77–89.

Orlacchio A, Ranieri M, Brave M, Arciuch VA, Forde T, De Martino D, Anderson KE, Hawkins P, Di Cristofano A. 2017. SGK1 is a critical component of an AKT-independent pathway essential for PI3K-mediated tumor development and maintenance. *Cancer Research* **77**: 6914–6926.

Palmada M, Jeyaraj S, Keller K, Akel A, Boehmer C, Rajamanickam J, Lang F. 2006. SGK1 Kinase Upregulates GLUT1 Activity and Plasma Membrane Expression. *Diabetes* **55**: 421–427.

Pawson T, Nash P. 2003. Assembly of cell regulatory systems through protein interaction

domains. *Science* **300**: 445–452.

Pawson T, Scott JD. 2005. Protein phosphorylation in signaling – 50 years and counting. *Trends in Biochemical Sciences* **30**: 286–290.

Pearce LR, Komander D, Alessi DR. 2010. The nuts and bolts of AGC protein kinases. *Nature Reviews Molecular Cell Biology* **11**: 9–22.

Peck GR, Chavez JA, Roach WG, Budnik BA, Lane WS, Karlsson, Håkan K. Zierath JR, Lienhard GE. 2009. Insulin-stimulated Phosphorylation of the Rab GTPase-activating Protein TBC1D1 Regulates GLUT4 Translocation. *Journal of Biological Chemistry* **284**: 30016–30023.

Peck GR, Ye S, Pham V, Fernando RN, Macaulay SL, Chai SY, Albiston AL. 2006. Interaction of the Akt Substrate, AS160, with the Glucose Transporter 4 Vesicle Marker Protein, Insulin-Regulated Aminopeptidase. *Molecular Endocrinology* **20**: 2576–2583.

Piala AT, Moon TM, Akella R, He H, Cobb MH, Goldsmith EJ. 2014. Chloride sensing by WNK1 involves inhibition of autophosphorylation. *Science Signaling* **7**.

Qian W, Liang H, Shi J, Jin N, Grundke-Iqbal I, Iqbal K, Gong CX, Liu F. 2011. Regulation of the alternative splicing of tau exon 10 by SC35 and Dyrk1A. *Nucleic Acids Research* **39**: 6161–6171.

Ragolia L, Begum N. 1998. Protein phosphatase-1 and insulin action. *Molecular and Cellular Biochemistry* **182**: 49–58.

Richardson C, Sakamoto K, de los Heros P, Deak M, Campbell DG, Prescott AR, Alessi DR. 2011. Regulation of the NKCC2 ion cotransporter by SPAK-OSR1-dependent and -independent pathways. *Journal of Cell Science* **124**: 789–800.

Rinehart J, Kahle KT, de los Heros P, Vazquez N, Meade P, Wilson FH, Hebert SC, Gimenez I, Gamba G, Lifton RP. 2005. WNK3 kinase is a positive regulator of NKCC2 and NCC, renal cation-Cl- cotransporters required for normal blood pressure homeostasis. *Proceedings of the National Academy of Sciences* **102**: 16777–16782.

Rinehart J, Vázquez N, Kahle KT, Hodson CA, Ring AM, Gulcicek EE, Louvi A, Bobadilla NA, Gamba G, Lifton RP. 2011. WNK2 kinase is a novel regulator of essential neuronal cation-chloride cotransporters. *Journal of Biological Chemistry*

**286**: 30171–30180.

Ring AM, Cheng SX, Leng Q, Kahle KT, Rinehart J, Lalioti MD, Volkman HM, Wilson FH, Hebert SC, Lifton RP. 2007. WNK4 regulates activity of the epithelial Na+ channel in vitro and in vivo. *Proceedings of the National Academy of Sciences* **104**: 4020–4024.

Roach P. 2002. Glycogen and its Metabolism. *Current Molecular Medicine* **2**: 101–120.

Roach WG, Chavez JA, Mîinea CP, Lienhard GE. 2007. Substrate specificity and effect on GLUT4 translocation of the Rab GTPase-activating protein Tbc1d1. *Biochemical Journal* **403**: 353–358.

Robinson DR, Wu YM, Lin SF. 2000. The protein tyrosine kinase family of the human genome. *Oncogene* **19**: 5548–5557.

Romashkova JA, Makarov SS. 1999. NF-kappaB is a target of AKT in anti-apoptotic PDGF signalling [see comments] 1. *Nature* **401**: 86–90.

Rosenbaek LL, Kortenoeven MLA, Aroankins TS, Fenton RA. 2014. Phosphorylation decreases ubiquitylation of the thiazide-sensitive cotransporter NCC and subsequent clathrin-mediated endocytosis. *Journal of Biological Chemistry* **289**: 13347–13361.

Sakaguchi K, Herrera JE, Saito S, Miki T, Bustin M, Vassilev A, Anderson CW, Appella E. 1998. DNA damage activates p53 through a phosphorylation-acetylation cascade. *Genes and Development* **12**: 2831–2841.

Sakamoto K, Holman GD. 2008. Emerging role for AS160/TBC1D4 and TBC1D1 in the regulation of GLUT4 traffic. *American Journal of Physiology-Endocrinology and Metabolism* **295**: E29–E37.

Sano H, Kane S, Sano E, Mîinea CP, Asara JM, Lane WS, Garner CW, Lienhard GE. 2003. Insulin-stimulated Phosphorylation of a Rab GTPase-activating Protein Regulates GLUT4 Translocation. *Journal of Biological Chemistry* **278**: 14599–14602.

Sato A, Shibuya H. 2018. Glycogen synthase kinase 3ß functions as a positive effector in the WNK signaling pathway. *PLoS ONE* **13**: 1–11.

Schrum JP, Zhu TF, Szostak JW. 2010. The origins of cellular life. *Cold Spring Harbor perspectives in biology* **2**: 1–16.

Sharma K, D'Souza RCJ, Tyanova S, Schaab C, Wiśniewski JR, Cox J, Mann M. 2014. Ultradeep Human Phosphoproteome Reveals a Distinct Regulatory Nature of Tyr and Ser/Thr-Based Signaling. *Cell Reports* **8**: 1583–1594.

Shekarabi M, Zhang J, Khanna AR, Ellison DH, Delpire E, Kahle KT. 2017. WNK Kinase Signaling in Ion Homeostasis and Human Disease. *Cell Metabolism* **25**: 285–299.

Shyamasundar S, Lim JP, Bay BH. 2016. MiR-93 inhibits the invasive potential of triple-negative breast cancer cells in vitro via protein kinase WNK1. *International Journal of Oncology* **49**: 2629–2636.

Sjöblom T, Jones S, Wood LD, Parsons DW, Lin J, Barber TD, Mandelker D, Leary RJ, Ptak J, Silliman N, et al. 2006. The consensus coding sequences of human breast and colorectal cancers. *Science* **314**: 268–274.

Song M, Bode AM, Dong Z, Lee M-H. 2019. AKT as a Therapeutic Target for Cancer. *Cancer Research* **79**: 1019–1031.

Stambolic V, Suzuki A, De la Pompa JL, Brothers GM, Mirtsos C, Sasaki T, Ruland J, Penninger JM, Siderovski DP, Mak TW. 1998. Negative regulation of PKB/Akt-dependent cell survival by the tumor suppressor PTEN. *Cell* **95**: 29–39.

Stambolic V, Woodgett JR. 1994. Mitogen inactivation of glycogen synthase kinase-3 β in intact cells via serine 9 phosphorylation. *Biochemical Journal* **303**: 701–704.

Stephens P, Edkins S, Davies H, Greenman C, Cox C, Hunter C, Bignell G, Teague J, Smith R, Stevens C, et al. 2005. A screen of the complete protein kinase gene family identifies diverse patterns of somatic mutations in human breast cancer. *Nature Genetics* **37**: 590–592.

Stone S, Abkevich V, Russell DL, Riley R, Timms K, Tran T, Trem D, Frank D, Jammulapati S, Neff CD, et al. 2006. TBC1D1 is a candidate for a severe obesity gene and evidence for a gene/ gene interaction in obesity predisposition. *Human Molecular Genetics* **15**: 2709–2720.

Subramanya AR, Liu J, Ellison DH, Wade JB, Welling PA. 2009. WNK4 diverts the thiazide-sensitive NaCl cotransporter to the lysosome and stimulates AP-3 interaction. *Journal of Biological Chemistry* **284**: 18471–18480.

Sun T, Aceto N, Meerbrey KL, Kessler JD, Zhou C, Migliaccio I, Nguyen DX, Pavlova

NN, Botero M, Huang J, et al. 2011. Activation of multiple proto-oncogenic tyrosine kinases in breast cancer via loss of the PTPN12 phosphatase. *Cell* **144**: 703–718.

Sun X, Gao L, Yu RK, Zeng G. 2006. Down-regulation of WNK1 protein kinase in neural progenitor cells suppresses cell proliferation and migration. *Journal of Neurochemistry* **99**: 1114–1121.

Tang B, Tang F, Wang Z, Qi G, Liang X, Li B, Yuan S, Liu J, Yu S, He S. 2016. Upregulation of Akt/Nf-κB-regulated inflammation and Akt/Bad-related apoptosis signaling pathway involved in hepatic carcinoma process: Suppression by carnosic acid nanoparticle. *International Journal of Nanomedicine* **11**: 6401–6420.

Tang Z, Shen Q, Xie H, Zhou Z, Shi G, Zhang C, Mohammed A, Wu Y, Ni S, Zhou X. 2018. Serum and glucocorticoid-regulated kinase 1 (SGK1) is a predictor of poor prognosis in non-small cell lung cancer, and its dynamic pattern following treatment with SGK1 inhibitor and γ-ray irradiation was elucidated. *Oncology Reports* **39**: 1505–1515.

Taylor EB, An D, Kramer HF, Yu H, Fujii NL, Roeckl KSC, Bowles N, Hirshman MF, Xie J, Feener EP, et al. 2008. Discovery of TBC1D1 as an insulin-, AICAR-, and contraction-stimulated signaling nexus in mouse skeletal muscle. *Journal of Biological Chemistry* **283**: 9787–9796.

Taylor SS, Radzio-Andzelm E, Hunter T. 1995. How do protein kinases discriminate between serine/threonine and tyrosine? Structural insights from the insulin receptor protein-tyrosine kinase. *FASEB Journal* **9**: 1255–1266.

Terker AS, Zhang C, Erspamer KJ, Gamba G, Ellison DH, Health O, Hospital X, Unit P. 2016. Unique chloride-sensing properties of WNK4 permit the distal nephron to modulate potassium homeostasis. *Kidney International* **89**: 127–134.

Thong FSL, Bilan PJ, Klip A. 2007. The Rab GTPase-activating protein AS160 integrates Akt, protein kinase C, and AMP-activated protein kinase signals regulating GLUT4 traffic. *Diabetes* **56**: 414–423.

Thorens B, Mueckler M. 2009. Glucose transporters in the 21st Century. *American Journal of Physiology-Endocrinology and Metabolism* **298**: E141–E145.

Treebak JT, Pehmøller C, Kristensen JM, Kjøbsted R, Birk JB, Schjerling P, Richter EA, Goodyear LJ, Wojtaszewski JFP. 2014. Acute exercise and physiological insulin

induce distinct phosphorylation signatures on TBC1D1 and TBC1D4 proteins in human skeletal muscle. *Journal of Physiology* **592**: 351–375.

Treebak JT, Taylor EB, Witczak CA, An D, Toyoda T, Koh H-J, Xie J, Feener EP, Wojtaszewski JFP, Hirshman MF, et al. 2009. Identification of a novel phosphorylation site on TBC1D4 regulated by AMP-activated protein kinase in skeletal muscle. *American Journal of Physiology-Cell Physiology* **298**: C377–C385.

Veríssimo F, Jordan P. 2001. WNK kinases, a novel protein kinase subfamily in multi-cellular organisms. *Oncogene* **20**: 5562–5569.

Veríssimo F, Silva E, Morris JD, Pepperkok R, Jordan P. 2006. Protein kinase WNK3 increases cell survival in a caspase-3-dependent pathway. *Oncogene* **25**: 4172–4182.

Vidal-Petiot E, Cheval L, Faugeroux J, Malard T, Doucet A, Jeunemaitre X, Hadchouel J. 2012. A new methodology for quantification of alternatively spliced exons reveals a highly tissue-specific expression pattern of WNK1 isoforms. *PLoS ONE* **7**: 1–9.

Vitari AC, Deak M, Collins BJ, Morrice N, Prescott AR, Phelan A, Humpreys S, Alessi DR. 2004. WNK1, the kinase mutated in an inherited high-blood-pressure syndrome, is a novel PKB (protein kinase B)/Akt substrate. *Biochemical Journal* **378**: 257–268.

Wang J, Ye C, Chen C, Xiong H, Xie B, Zhou J, Chen Y, Zheng S, Wang L. 2017. Glucose transporter GLUT1 expression and clinical outcome in solid tumors: a systematic review and meta-analysis. *Oncotarget* **8**: 16875–16886.

Warburg O. 1956. On the Origin of Cancer Cells. *Science* **123**: 309–314.

Webster MK, Goya L, Ge Y, Maiyar AC, Firestone GL. 1993. Characterization of sgk, a novel member of the serine/threonine protein kinase gene family which is transcriptionally induced by glucocorticoids and serum. *Molecular and Cellular Biology* **13**: 2031–2040.

Wilson FH, Disse-Nicodème S, Choate KA, Ishikawa K, Nelson-Williams C, Desitter I, Gunel M, Milford D V., Lipkin GW, Achard JM, et al. 2001. Human hypertension caused by mutations in WNK kinases. *Science* **293**: 1107–1112.

Wu D, Pan W. 2010. GSK3: a multifaceted kinase in Wnt signaling. *Trends in Biochemical Sciences* **35**: 161–168.

Xu BE, English JM, Wilsbacher JL, Stippec S, Goldsmith EJ, Cobb MH. 2000. WNK1,

a Novel Mammalian Serine/Threonine Protein Kinase Lacking the Catalytic Lysine in Subdomain II. *Journal of Biological Chemistry* **275**: 16795–16801.

Xu BE, Min X, Stippec S, Lee BH, Goldsmith EJ, Cobb MH. 2002. Regulation of WNK1 by an autoinhibitory domain and autophosphorylation. *Journal of Biological Chemistry* **277**: 48456–48462.

Xu BE, Stippec S, Chu P-Y, Lazrak A, Li X-J, Lee B-H, English JM, Ortega B, Huang C-L, Cobb MH. 2005a. WNK1 activates SGK1 to regulate the epithelial sodium channel. *Proceedings of the National Academy of Sciences* **102**: 10315–10320.

Xu BE, Stippec S, Lazrak A, Huang CL, Cobb MH. 2005b. WNK1 activates SGK1 by a phosphatidylinositol 3-kinase-dependent and non-catalytic mechanism. *Journal of Biological Chemistry* **280**: 34218–34223.

Xu BE, Stippec S, Lenertz L, Lee BH, Zhang W, Lee YK, Cobb MH. 2004. WNK1 Activates ERK5 by an MEKK2/3-dependent Mechanism. *Journal of Biological Chemistry* **279**: 7826–7831.

Yaffe MB, Elia AEH. 2001. Phosphoserine/threonine-binding domains. *Current Opinion in Cell Biology* **13**: 131–138.

Yamada K, Park HM, Rigel DF, DiPetrillo K, Whalen EJ, Anisowicz A, Beil M, Berstler J, Brocklehurst CE, Burdick DA, et al. 2016. Small-molecule WNK inhibition regulates cardiovascular and renal function. *Nature Chemical Biology* **12**: 896–898.

Yang J, Cron P, Thompson V, Good VM, Hess D, Hemmings BA, Barford D. 2002. Molecular mechanism for the regulation of protein kinase B/Akt by hydrophobic motif phosphorylation. *Molecular Cell* **9**: 1227–1240.

Yu C, Huang L. 2018. Cross-Linking Mass Spectrometry (XL-MS): an Emerging Technology for Interactomics and Structural Biology. *Anal Chemestry* **90**: 144–165.

Zagórska A, Pozo-Guisado E, Boudeau J, Vitari AC, Rafiqi FH, Thastrup J, Deak M, Campbell DG, Morrice NA, Prescott AR, et al. 2007. Regulation of activity and localization of the WNK1 protein kinase by hyperosmotic stress. *The Journal of Cell Biology* **176**: 89—100.

Zaid H, Antonescu CN, Randhawa VK, Klip A. 2008. Insulin action on glucose transporters through molecular switches, tracks and tethers. *Biochemical Journal* **413**: 201–215.

Zhang J, Deng X, Kahle KT. 2016. Leveraging unique structural characteristics of WNK kinases to achieve therapeutic inhibition. *Science Signaling* **9**: 1–4.

Zhou QL, Jiang ZY, Holik J, Chawla A, Hagan GN, Leszyk J, Czech MP. 2008. Akt substrate TBC1D1 regulates GLUT1 expression through the mTOR pathway in 3T3-L1 adipocytes. *Biochemical Journal* **411**: 647–655.

Zhou Z, Fu X-D. 2013. Regulation of Splicing by SR proteins and SR Protein-Specific Kinases. *Chromosoma* **122**: 191–207.

Zhou Z, Qiu J, Wen L, Zhou Y, Plocinik RM, Li H, Hu Q, Ghosh G, Adams JA, Rosenfeld MG, et al. 2012. The Akt-SRPK-SR Axis Constitutes a Major Pathway in Transducing EGF Signaling to Regulate Alternative Splicing in the Nucleus. *Molecular cell* **47**: 422–433.